

RADIOBIOLOGY EXPERIMENTAL VERIFICATION USING 3D BIO-  
PHANTOM FOR CARBON ION RADIOTHERAPY



A Thesis Submitted in Partial Fulfillment of the Requirements for the  
Degree of Doctor of Philosophy in Physics  
Suranaree University of Technology  
Academic Year 2021

การตรวจสอบการทดลองทางชีววิทยารังสีโดยใช้หุ่นจำลองทางชีววิทยาแบบ  
สามมิติสำหรับการรักษาด้วยรังสีคาร์บอนไอออน



นางสาวเดอา เอาลีเย คาร์ตินิ

วิทยานิพนธ์นี้เป็นส่วนหนึ่งของการศึกษาตามหลักสูตรปริญญาวิทยาศาสตรดุษฎีบัณฑิต  
สาขาวิชาฟิสิกส์  
มหาวิทยาลัยเทคโนโลยีสุรนารี  
ปีการศึกษา 2564

RADIOBIOLOGY EXPERIMENTAL VERIFICATION USING 3D BIO-  
PHANTOM FOR CARBON ION RADIOTHERAPY


Suranaree University of Technology has approved this thesis submitted in partial fulfillment of the requirements for the Degree of Doctor of Philosophy.

Thesis Examining Committee



(Assoc. Prof. Dr. Panomsak Meemon)

Chairperson



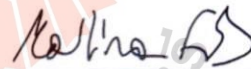
(Asst. Prof. Dr. Chinorat Kobdaj)

Member (Thesis Advisor)



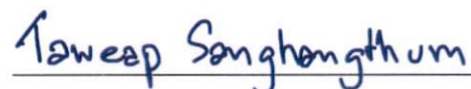
(Asst. Prof. Dr. Chutima Talabnin)

Member (Thesis Co-advisor)



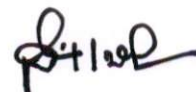
(Dr. Martina Christina Fuss)

Member (Thesis Co-advisor)



(Asst. Prof. Dr. Taweap Sanghangthum)

Member



(Assoc. Prof. Dr. Chatchai Jothiyangkoon)

Vice Rector for Academic Affairs  
and Quality Assurance

(Prof. Dr. Santi Maensiri)

Dean of Institute of Science

เดอา เออาเลีย คาร์ตินิ : การตรวจสอบการทดลองทางชีววิทยารังสีโดยใช้หุ่นจำลองทางชีววิทยาแบบสามมิติสำหรับการรักษาด้วยรังสีคาร์บอนไอออน (RADIOBIOLOGY EXPERIMENTAL VERIFICATION USING 3D BIO-PHANTOM FOR CARBON ION RADIOTHERAPY). อาจารย์ที่ปรึกษา : ผู้ช่วยศาสตราจารย์ ดร.ชินรัตน์ กอบเดช, 96 หน้า.


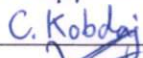


คำสำคัญ: การเพาะเลี้ยงเซลล์แบบสามมิติ/ การตรวจสอบทางกัมมันตภาพรังสี/ การวางแผนการรักษา/ การใช้รังสีรักษาด้วยลำแสงไอออน

การตรวจสอบ 3D bio-phantom ประกอบด้วย การเพาะเลี้ยงเซลล์ใน Matrigel matrix ภายในไมโครเวลเพลทเป็นเครื่องมือทางเลือกสำหรับการตรวจสอบปริมาณทางชีวภาพได้ ถูกดำเนินการในการศึกษานี้ โดยเซลล์ CHO-K1 ที่เลี้ยงใน Matrigel ภายในจานเพาะเลี้ยง 96 หลุมแสดงให้เห็นถึงเซลล์จำนวนมากกว่าซึ่งมีรูปร่างเซลล์เหมือนเซลล์จริงเมื่อเทียบกับการเพาะเลี้ยงเซลล์แบบชั้นเดียว และมีระบบที่สะดวกเป็นอย่างมากสำหรับการศึกษาการอยู่รอดของเซลล์ที่ร้อยละ 1 หรือต่ำกว่าร้อยละ 1 ของเศษส่วนการอยู่รอด การทดลองการวัดปริมาณรังสีของแผ่นฟิล์มถูกดำเนินการเพื่อแยกแยะการมีอยู่ของสนามใดๆ ที่ไม่สม่ำเสมอซึ่งเกิดจากโครงสร้างโพลีไสตรีน ของจานหลุม ความไวต่อรังสีของเซลล์ CHO ใน Matrigel หลังจากการฉายรังสีด้วยรังสีเอกซ์และคาร์บอนไอออนที่มีค่าพลังงานเดียวถูกพบว่ามีค่าความไวต่อรังสีน้อยกว่าการเลี้ยงเซลล์แบบชั้นเดียวมาตรฐาน ในลำดับถัดมา การวางแผนการรักษาได้ถูกปรับให้เหมาะสมกับปริมาณรังสีชีวภาพแบบระนาบในปริมาตรสี่เหลี่ยมใน TRiP98 โดยใช้ตารางใช้ตาราง RBE ของเซลล์ CHO เฉพาะสำหรับ Matrigel การกระจายการอยู่รอดของเซลล์ในสามมิติถูกวิเคราะห์และเปรียบเทียบกับที่อยู่รอดของเซลล์ที่ได้จาก stack phantom มาตรฐาน ซึ่งผลลัพธ์ที่ได้นั้นเป็นที่น่าพึงพอใจและใกล้เคียงตามการทำนายของ TRiP98 เป็นอย่างมาก การปรับแผ่นหลุมให้มีขนาดเล็กลงได้ดำเนินการโดยการเพาะเลี้ยงเซลล์ของสัตว์เลี้ยงลูกด้วยน้ำนมใน Matrigel matrix ภายในจานเพาะเลี้ยง 384 หลุม ชนิด V-bottom เส้นโค้งการตอบสนองปริมาณรังสีของเซลล์ใน Matrigel ต่อการฉายรังสีด้วยรังสีเอกซ์และคาร์บอนไอออนที่มีค่าพลังงานเดียวได้รับการวัดและเซลล์ xrs-5 แสดงความไวต่อรังสีสูงกว่าเมื่อเทียบกับเซลล์ CHO ดังนั้นจึงทำให้เซลล์ xrs-5 เหมาะสำหรับการตรวจสอบการอยู่รอดของเซลล์ในบริเวณที่มีปริมาณรังสีต่ำ ลำดับสุดท้าย การตรวจสอบแผนการรักษาในบริเวณที่มีปริมาณรังสีต่ำจึงได้ดำเนินการโดยใช้ 3D bio-phantom การกระจายการอยู่รอดของเซลล์ในการตัดด้านข้างถูกวิเคราะห์และการอยู่รอดของเซลล์ที่วัดได้เป็นที่น่าพึงพอใจกับผลการอยู่รอดที่คาดหวัง กล่าวโดยสรุปคือ 3D bio-phantom นั้นเป็นเครื่องมือที่ใช้งานได้จริงสำหรับการตรวจสอบผลกระทบทางชีวภาพ

โดยคำนวณจากระบบการวางแผนการรักษาและสามารถใช้เป็นเครื่องมือการตรวจสอบสำหรับการวางแผนการรักษาที่เกี่ยวข้องกับรูปทรงที่ซับซ้อนหรือกลยุทธ์การเพิ่มประสิทธิภาพได้อย่างแปลกใหม่



สาขาวิชาฟิสิกส์  
ปีการศึกษา 2564

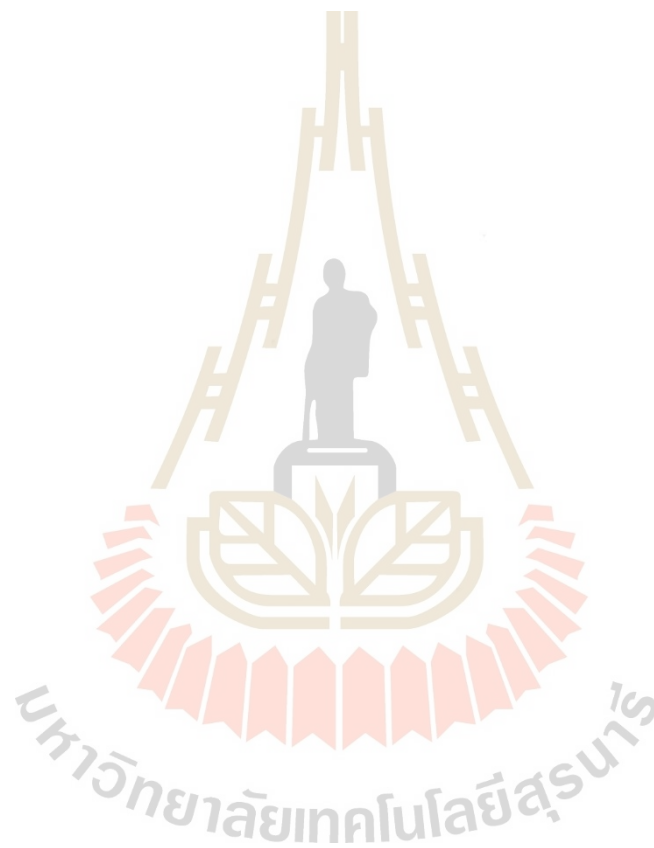
ลายมือชื่อนักศึกษา \_\_\_\_\_   
 ลายมือชื่ออาจารย์ที่ปรึกษา \_\_\_\_\_   
 ลายมือชื่ออาจารย์ที่ปรึกษาร่วม \_\_\_\_\_   
 ลายมือชื่ออาจารย์ที่ปรึกษาร่วม \_\_\_\_\_ 

DEA AULIA KARTINI : RADIOBIOLOGY EXPERIMENTAL VERIFICATION USING  
3D BIO-PHANTOM FOR CARBON ION RADIOTHERAPY. THESIS ADVISOR :  
ASST. PROF. CHINORAT KOBDAJ, Ph.D. 96 PP.

Keyword: 3D cell culture/ Radiobiological verification/ Treatment planning/ Ion  
beam radiotherapy

The investigation of 3D bio-phantom consisting of cells cultured in Matrigel matrix inside micro-well plates as an alternative tool for biological dose verification have been performed in this study. CHO-K1 cells cultured in Matrigel inside 96-well plate yielded a high cell number with a realistic cell shape, compared to cells cultured in monolayer, and present a very convenient system for studying the cell survival at and below 1% of survival fraction. Film dosimetric experiments were conducted to rule out the presence of any field inhomogeneities caused by the well plate polystyrene structure. The radio-sensitivity of CHO cells in Matrigel after irradiation with X-rays and monoenergetic carbon ions was found to be lower than for standard monolayer culture. Next, a treatment plan was optimized for a flat biological dose in a rectangular volume in TRiP98 employing a dedicated CHO RBE table for Matrigel. The cell survival distribution in three dimensions was analyzed and compared to the cell survival obtained from the reference stack phantom. The result showed very good agreement and follow the TRiP98 prediction closely. Adaptation to smaller well plate has been conducted by culturing mammalian cells in Matrigel matrix inside V-bottom 384-well plate. Dose response curves of cells in Matrigel to irradiation with X-rays and monoenergetic carbon ions have been measured and xrs-5 cells show a higher radio-sensitivity compared to CHO cells thus making xrs-5 cells suitable for investigating cell survival at low-dose region. Finally, the treatment plan verification in low-dose region has been performed using refined 3D bio-phantom. Cell survival distribution in lateral cuts was analyzed and the measured cell survivals were in a good agreement with the expected survival.

In conclusion, the 3D bio-phantom is a practical tool for verifying the biological effect calculated by treatment planning systems and could be used as verification tool for treatment planning involving a complex geometries or unconventional optimization strategies.



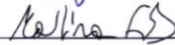
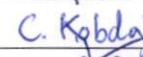
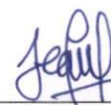
School of Physics  
Academic Year 2021

Student's Signature \_\_\_\_\_

Advisor's Signature \_\_\_\_\_

Co-Advisor's Signature \_\_\_\_\_

Co-Advisor's Signature \_\_\_\_\_



## ACKNOWLEDGEMENTS

I have never imagined that I could finish my PhD study. Many things have happened in the last five years during my study (Covid-19 pandemic is one of them) and without the help from everyone I would never make it until this far or maybe I have already given up before trying my best to finish my study. First of all, I would like to express my deepest gratitude to my thesis advisor Asst. Prof. Dr. Chinorat Kobdaj for his guidance, advice and support since the beginning I start my study in Thailand until I finish my study, thank you for everything Ajarn. I would also like to extend my gratitude to Dr. Martina Fuß for her guidance from the very beginning I start my PhD research at GSI. Thank you for all the discussion that we had and for taking care of me during my research stay at GSI. I also wish to show my gratitude to Asst. Prof. Dr. Chutima Talabnin, who welcomes me in her lab and teaches me many things about cell culture.

I would like to say thank you to Dr. Olga Sokol, Dr. Julia Wiedemann and Gianmarco Camazzola for their great help and assistance during beam time in Marburg. I would never forget all the hectic moment during beam time and how you comfort me whenever I made mistakes. I would also like to extend my sincere thanks to everyone in Treatment Planning and Validation group, Dr. Michael Krämer and Dr. Albana Topi for always welcoming me in the group and giving many valuable advice and suggestion to my work. Many thanks to Dr. Thomas Friedrich for providing the RBE table for CHO cells in Matrigel. I would like to pay my special regards to everyone in the International Office, Dr. Pradeep Ghosh and Jennifer Steitz, for their great assistance and support during my stay at GSI for 3 years. Without your assistance and companion, I would never have been able to adapt to life in Germany and my life in Darmstadt will be miserable.

Next, I would like to acknowledge the financial support from SUT-Ph.D. Scholarship for ASEAN which provides a full scholarship to me and thanks to that I am able to pursue Ph.D. in SUT. I also would like to acknowledge the support from Thailand Center of Excellent in Physics (ThEP) under grant number



TheP-61-PHM-SUT4 and GSI/FAIR GET INvolved Programme which provide financial support for my research at GSI. I believe that I could finish my research work due to the funding supports I have received during my study.

I wish to say thank you to everyone in Nuclear and Particle Physics group: P'Yip, P'Noei, Christoph, Sure, Thiri, Tiw, Pharewa and others for always helping me to adapt the life in Thailand. Also, I would like to say thank you to all my friends at GSI Biophysics for being a good companion and friend during my stay at GSI. I would also express my thanks to my Indonesian friends, especially Rara, Isti, Mia and Windy who always help me and give support to each other whenever we have problems with our life and studies. Last but not least, I wish to express my sincere gratitude to my family, especially my Mom who always believe in me and giving her endless supports and prayers for me. I did it Mom! I love you to the moon and back.

Dea Aulia Kartini



# CONTENTS

	Page
ABSTRACT IN THAI . . . . .	I
ABSTRACT IN ENGLISH . . . . .	III
ACKNOWLEDGEMENTS . . . . .	V
CONTENTS . . . . .	VII
LIST OF TABLES . . . . .	XI
LIST OF FIGURES . . . . .	XII
LIST OF ABBREVIATIONS . . . . .	XV
<b>CHAPTER</b>	
<b>I INTRODUCTION . . . . .</b>	<b>1</b>
<b>II RESEARCH BACKGROUND . . . . .</b>	<b>4</b>
2.1 Physics of ion beam radiotherapy . . . . .	4
2.1.1 Energy loss of particle . . . . .	4
2.1.2 Radiation dose . . . . .	6
2.1.3 Lateral scattering . . . . .	6
2.1.4 Fragmentation tail . . . . .	7
2.2 Relative biological effectiveness . . . . .	8
2.2.1 Cell survival curve . . . . .	8
2.3 TRiP98 treatment planning system . . . . .	10
2.4 Gafchromic EBT3 film . . . . .	10
<b>III CHO CELL CULTURE AND BASIC CELL TESTS . . . . .</b>	<b>12</b>
3.1 Cell culture setups . . . . .	12
3.1.1 Matrigel setup . . . . .	12
Cell seeding . . . . .	13
Cell recovery . . . . .	13
3.1.2 Monolayer setup . . . . .	15
3.1.3 Stack setup . . . . .	15
3.2 Clonogenic assay . . . . .	16
3.3 Cell growth test . . . . .	17
3.3.1 Cell growth curve . . . . .	17

## CONTENTS (Continued)

		Page
3.4	Cell proliferation test . . . . .	19
3.4.1	The shape of cells cultured in Matrigel . . . . .	19
3.4.2	Proliferation of cells cultured in Matrigel . . . . .	20
3.5	Oxygen level measurement inside Matrigel matrix . . . . .	22
3.6	Summary . . . . .	24
<b>IV</b>	<b>RADIOBIOLOGICAL VERIFICATION OF SIMPLE TREATMENT PLAN USING 3D BIO-PHANTOM . . . . .</b>	<b>25</b>
4.1	Survival irradiation setup . . . . .	26
4.1.1	X-rays survival experiment . . . . .	26
4.1.2	Carbon ion survival experiment . . . . .	27
4.2	EBT3 film irradiation setup . . . . .	29
4.3	Treatment planning system . . . . .	30
4.4	Sample preparation . . . . .	30
4.5	In-vitro irradiation setup . . . . .	31
4.6	Results and discussion . . . . .	33
4.6.1	Response of cells cultured in Matrigel-based phantom to irradiations . . . . .	33
4.6.2	Radiation field homogeneity of stacked 96-well plate with Gafchromic EBT3 film . . . . .	36
4.6.3	Treatment plan verification . . . . .	38
4.6.4	Adaptation to 384-well plate . . . . .	40
4.7	Summary . . . . .	42
<b>V</b>	<b>ADAPTATION TO XRS-5 CELLS AND OUT-OF-FIELD RADIOBIOLOGICAL VERIFICATION . . . . .</b>	<b>44</b>
5.1	Matrigel cell culture with xrs-5 cell . . . . .	44
5.1.1	Cell growth curve . . . . .	44
5.1.2	Plating efficiency . . . . .	45
5.1.3	Cell proliferation in Matrigel . . . . .	46
5.2	Response of xrs-5 cells cultured in Matrigel to irradiation . . . . .	49
5.2.1	X-rays survival curve . . . . .	49
5.2.2	Carbon ion survival curve . . . . .	51

## CONTENTS (Continued)

	Page
5.3 Field homogeneity of V-bottom 384-well plate using Gafchromic EBT3 film . . . . .	57
5.3.1 Film dosimetry setup . . . . .	57
5.3.2 Response of Gafchromic EBT3 film . . . . .	58
5.4 Out-of-field radiobiological verification using 3D bio-phantom	59
5.4.1 Treatment planning system . . . . .	59
5.4.2 In-vitro irradiation setup . . . . .	60
5.4.3 Out-of-field treatment plan verification . . . . .	61
5.5 Summary . . . . .	63
<b>VI SUMMARY AND CONCLUSION</b> . . . . .	<b>64</b>
REFERENCES . . . . .	67
APPENDICES	
APPENDIX A CELL CULTURES PROTOCOL . . . . .	76
A.1 Matrigel dilution . . . . .	76
A.2 Matrigel cell seeding protocol in 96-well plate	76
A.3 Matrigel cell recovering protocol in 96-well plate - Dispase protocol . . . . .	77
A.4 Matrigel cell recovering protocol in 96-well plate - Cooling protocol . . . . .	78
A.5 Matrigel cell recovering protocol in 96-well plate - Centrifuge protocol . . . . .	78
A.6 Matrigel cell recovering protocol in 96-well plate - Cooling and centrifuge protocol . .	79
A.7 Matrigel cell seeding protocol in 384-well plate	79
A.8 Matrigel cell recovering protocol in 384-well plate . . . . .	80
A.9 Matrigel cell seeding protocol in V-bottom 384-well PP plate . . . . .	80
A.10 Matrigel cell recovery protocol in V-bottom 384-well PP plate . . . . .	81

## CONTENTS (Continued)

	Page
A.11 Monolayer cell culture protocol in 96-well plate - Cell seeding . . . . .	82
A.12 Monolayer cell culture protocol in 96-well plate - Cell recovering . . . . .	82
A.13 Monolayer cell culture protocol in stack phantom - Cell seeding . . . . .	83
A.14 Monolayer cell culture protocol in stack phantom - Cell recovering . . . . .	83
A.15 Monolayer cell culture protocol in T-25 TCF - Cell seeding . . . . .	83
A.16 Monolayer cell culture protocol in T-25 TCF - Cell recovering . . . . .	84
APPENDIX B TRIP98 TREATMENT PLANS CODE . . . . .	85
B.1 96-well plate plan . . . . .	85
B.2 Stack phantom plan . . . . .	86
B.3 Out-of-field plan for V-bottom 384-well plate . . . . .	88
APPENDIX C MICRO-WELL PLATE DESIGN . . . . .	90
APPENDIX D MIT TECHNICAL DETAILS . . . . .	92
CURRICULUM VITAE . . . . .	96

## LIST OF TABLES

Table		Page
3.1	Number of CHO cells in Matrigel setup in comparison to monolayer setup. . . . .	21
4.1	List of $\alpha$ and $\beta$ parameters of CHO cells cultured in Matrigel and monolayer setups. . . . .	35
4.2	Standard deviations of Gafchromic EBT3 film profile. . . . .	38
4.3	Number of CHO cells in Matrigel setup inside F-bottom 384-well plate. . . . .	41
5.1	Number of colonies obtained after 8 days of incubation. . . . .	47
5.2	Number of xrs-5 cells in Matrigel setup inside 96-well plate. . . . .	47
5.3	Number of CHO cells in Matrigel setup inside V-bottom 384-well PP plate. . . . .	48
5.4	Number of xrs-5 cells recovered from Matrigel in 384-well PP plate following the change of trypsin. . . . .	49
5.5	List of xrs-5 $\alpha$ parameter extracted from X-rays survival curves. . . . .	53
5.6	List of xrs-5 $\alpha$ parameter extracted from carbon ion survival curves. . . . .	55
5.7	Standard deviations of EBT3 films. . . . .	58

## LIST OF FIGURES

Figure		Page
2.1	Depth dose profile of carbon ions and protons. . . . .	5
2.2	Lateral profile of carbon beam in comparison to proton beam.	7
2.3	Survival curves of CHO-K1 cells irradiated by X-ray and carbon ions. . . . .	9
3.1	The final structure of Matrigel layers inside 96-well plate. .	14
3.2	Stack phantom consists of PMMA box and polystyrene slides.	16
3.3	Cell growth curve of CHO cells. . . . .	18
3.4	The doubling time of CHO cells. . . . .	19
3.5	The shape of CHO cells cultured in different setup and incubation time. . . . .	20
3.6	Oxygen spot sensor placed inside the bottom part of 96-well plate. . . . .	22
3.7	Final structure of sensor placed inside Matrigel layers. . . .	23
3.8	Cell oxygenation inside Matrigel matrix within 48 hours of incubation. . . . .	23
4.1	Well plates arrangement for radiobiological verification irradiation.	25
4.2	Cells were cultured in Matrigel in three wells and irradiated by X-ray beams with same dose. . . . .	26
4.3	Experimental setup for X-rays irradiation. . . . .	27
4.4	Cells in Matrigel and monolayer setup were irradiated by monoenergetic carbon ion beams. . . . .	28
4.5	Experimental setup for monoenergetic carbon ion irradiation.	28
4.6	EBT3 film irradiation setup. . . . .	29
4.7	Wells arrangement for radiobiological verification irradiation. .	31
4.8	Irradiation setup for radiobiological verification using Matrigel setup. . . . .	31
4.9	Experimental setup for radiobiological verification using stack phantom. . . . .	32

## LIST OF FIGURES (Continued)

Figure		Page
4.10	Survival curve of CHO cells cultured in Matrigel setup after irradiation with X-ray beams. . . . .	33
4.11	Survival curve of CHO cells cultured in Matrigel and mono-layer setups after irradiation with 180 MeV/u monoenergetic carbon ion beams. . . . .	34
4.12	Excessive number of colonies was obtained after irradiated by monoenergetic carbon ion with dose of 8 Gy in Matrigel setup. . . . .	35
4.13	Comparison of film profiles at the edge and center part of 96-well plate. . . . .	36
4.14	Field homogeneity assessment using Gafchromic EBT3 film. . . . .	37
4.15	Cell survival rate after being irradiated to active scanning carbon ion beam. . . . .	39
4.16	Survival fractions of CHO cells cultured in Matrigel inside 384-well plate after irradiated to active scanning carbon ion beam. . . . .	42
5.1	Cell growth curve of xrs-5 cells. . . . .	45
5.2	The doubling time of xrs-5 cells. . . . .	46
5.3	Measured xrs-5 cell survival curves after irradiation with X-ray beams. . . . .	51
5.4	Measured X-rays survival curves of xrs-5 cells in comparison with existing X-rays survival curves. . . . .	52
5.5	Samples arrangement for survival experiment with carbon ions at MIT. . . . .	52
5.6	The bottom part of 384-well plate was covered by agarose layer. . . . .	53
5.7	Measured xrs-5 cell survival curves after irradiation with monoenergetic carbon ions in comparison to X-ray survival curves. . . . .	54
5.8	Measured carbon ion survival curves of xrs-5 cells in comparison to existing carbon ion survival curves. . . . .	55



## LIST OF FIGURES (Continued)

Figure		Page
5.9	Survival curves of CHO-K1 and xrs-5 cells cultured in Matrigel after irradiation with carbon ions and X-rays. . . . .	56
5.10	Film dosimetry setup using Gafchromic EBT3 film. . . . .	57
5.11	Profiles of EBT3 films after irradiation with active scanning carbon ion beams . . . . .	59
5.12	Sample arrangement for out-of-field radiobiological irradiation.	61
5.13	Survival fraction of xrs-5 cells in lateral cuts at extended target and fragmentation tail regions. . . . .	62
C.1	Design of flat-bottom 96-well PS plate. . . . .	90
C.2	Design of flat-bottom 384-well PS plate. . . . .	91
C.3	Design of V-bottom 384-well PP plate. . . . .	91
D.1	Outline of accelerator at MIT and the position of beam outlets.	92
D.2	Measured absorbed dose in z distribution in water phantom for simple treatment plan. . . . .	94
D.3	Measured absorbed dose in z distribution inside water phantom for out-of-field treatment plan. . . . .	94
D.4	Measured absorbed dose in lateral x-distribution inside water phantom for out-of-field treatment plan. . . . .	95

## LIST OF ABBREVIATIONS

CHO	Chinese Hamster Ovary
DSB	Double-Strand Breaks
ECM	Extracellular Matrix
FBS	Fetal Bovine Serum
GSI	GSI Helmholtz Centre for Heavy Ion Research
IMRT	Intensity-Modulated Radiotherapy
LEM	Local Effect Model
LET	Linear Energy Transfer
MG	Matrigel
MEM	Minimum Essential Medium
MIT	Marburg Ion-Beam Therapy Centre
MO	Monolayer
NIH	National Institutes of Health
OAR	Organ at Risk
OD	Optical Density
PBS	Phosphate Buffered Saline
PE	Plating Efficiency
PMMA	Polymethyl Methacrylate
PP	Polypropylene
PS	Polystyrene
RBE	Relative Biological Effectiveness
ROI	Region of Interest
SOBP	Spread-Out Bragg Peak
TCF	Tissue Culture Flask
TRIP98	Treatment Planning for Particles, 1998 edition
WET	Water Equivalent Thickness

# CHAPTER I

## INTRODUCTION

Cancer is a deadly disease caused by abnormal cells which grow into a lump of cancer cells (Pardee and Stein, 2011). It can spread out to nearby healthy tissue or metastasize to distant locations. There are several modalities to treat cancer and one of them is radiotherapy. Radiotherapy is a treatment utilizing high energy radiation such as photons and electrons to kill the cancer cells. In the late 1990s, ion beam radiotherapy becomes a new modality for treating cancer cells, especially deep-seated cancer such as head and neck cancers. Ion beam radiotherapy treats the cancer patients by irradiating the tumor or cancer cells with ion beams such as carbon ions and protons. The advantage of the ion beam radiotherapy lies in the inverted depth-dose profile where most of the energy is deposited at the end of the beam range formed a peak which is called Bragg-peak. Because of this, the deep-seated cancer cells will receive a maximum dose while sparing the surrounding healthy tissue. In 2021, the first proton radiotherapy facility in Thailand will be operated at King Chulalongkorn Memorial Hospital at Bangkok. The proton beams are produced by cyclotron machine allowing to generate energy beam with range of 70 – 250 MeV. The beams will be delivered using a moving gantry which can rotate in  $360^\circ$  so the irradiation could be delivered from any angle.

Due to the high linear energy transfer (LET) or mass stopping power of ion beam radiotherapy, the relative biological effectiveness (RBE) is increasing towards to the Bragg-peak (Krämer, 2001). RBE is defined as the ratio between two different radiation doses that yield the same biological effects (Hall and Giaccia, 2012). This is the reason why radiobiological effectiveness is essential in treatment planning of ion beam radiotherapy. However, there is a challenging in performing biological verification because it is not easy to do direct measurement on biological effects (Krämer et al., 2003). Measuring the cell survival is the easiest method to observe the biological effects after irradiation. Different verification tools or "phantoms" have been used for conducting RBE-weighted treatment plan verification at GSI Helmholtz Centre for Heavy Ion Research (GSI)

(Krämer et al., 2003; Gemmel et al., 2008; Krämer and Durante, 2010; Krämer et al., 2014; Sokol et al., 2017) for different purposes. Therefore, phantom that could observe the cell inactivation in different areas of treatment plan with high spatial resolution is needed for performing biological measurement.

Recently, multi-well plates have been used to culture cells in radiobiology experiment by different research groups (Gemmel et al., 2010; Gemmel et al., 2011; Klein et al., 2017; Patel et al., 2017; Mein et al., 2019). However, the field homogeneity has never been investigated despite the well plate were not completely filled (Buglewicz et al., 2019). An experiment on radiobiological verification utilizing multi-well plates has been conducted at GSI by obtaining the survival curve of CHO cells cultured in monolayers inside the 24-well plates. Since verification method using the 24-well plates with monolayers cell culture has limited spatial resolution in x- and y-plane, another attempt has been made by culturing the CHO cells in Matrigel matrix inside the 24-well plates (Peroni, 2018) which works quite well. To ensure there are no reflection or other border effects from the wall of well plates, Gafchromic films were irradiated in- and outside of the 24-well plates in monoenergetic oxygen beam with energy of 30 MeV/u (Kartini, 2018).

A new radiobiological verification setup utilizing micro-well plate with Matrigel matrix to achieve higher spatial resolution is investigated in this study. The feasibility study of Matrigel cell culture has been performed by observing the shape and cell proliferation in Matrigel matrix which is presented in Chapter III. The response of cells cultured in Matrigel to different type of irradiation are also investigated in this study. In addition, the investigation on radiation field homogeneity will be carried out by irradiating Gafchromic EBT3 films placed following stacked micro-well plates to ensure there is no artefact caused by the structure of micro-well plate. After that, the verification of RBE-weighted treatment plan is performed using 3D bio-phantom which allows to observe the experimental data in specific location which is a convenient system for observing the spatial distribution of cell survival in three dimension. The dose response curve, EBT3 film measurement, and treatment plan verification are reported in Chapter IV.

Next, the technique has been extended to radio-sensitive cell line and higher spatial resolution by culturing xrs-5 cells in Matrigel inside V-bottom

384-well polypropylene (PP) plate. The cell growth as well as the response of cells in Matrigel inside 384-well PP plate to irradiation have been investigated and presented in Chapter V. Finally, the radiobiological verification in out-of-field region has been performed using 3D bio-phantom that has been adapted to xrs-5 cell and 384-well PP plate in order to observe the cell survival at low dose region which could not be observed using CHO cells.



## CHAPTER II

### RESEARCH BACKGROUND

#### 2.1 Physics of ion beam radiotherapy

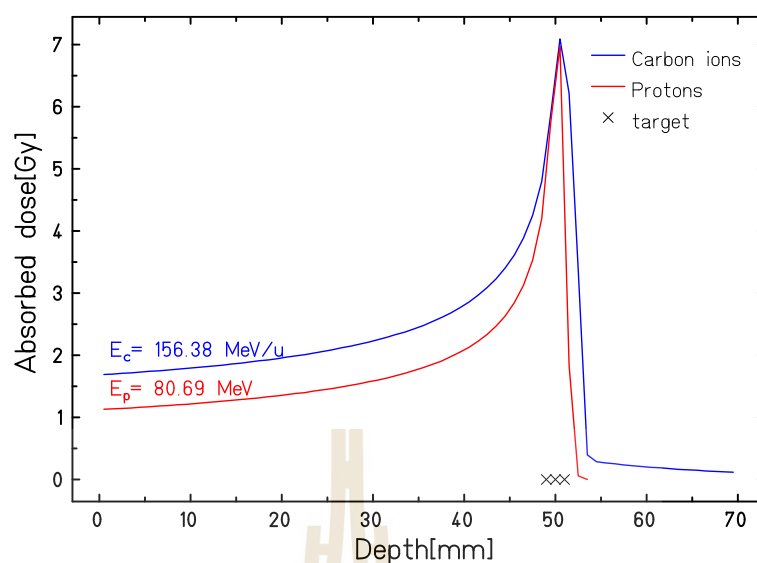
##### 2.1.1 Energy loss of particle

Ion beam radiotherapy utilizes accelerated charged particles to irradiate the cancer cells. It has more advantages than conventional radiotherapy because of its inverted depth-dose profile. When charged particles are absorbed in matter or target such as human body, the charged particles ionize matter by transferring some of their kinetic energy into matter. The amount of energy transferred or the energy loss per unit path length  $dE/dx$  in matter (mass stopping power) can be expressed by Bethe-Bloch equation (Bethe, 1930; Bloch, 1933a; Bloch, 1933b),

$$-\left\langle \frac{dE}{dx} \right\rangle = K \rho \frac{Z_t Z_p^2}{A_t \beta^2} \left[ \frac{1}{2} \ln \frac{2m_e c^2 \beta^2 \gamma^2 T_{\max}}{I^2} - \beta^2 - \frac{\delta(\beta\gamma)}{2} \right] \quad (2.1)$$

where  $K = 4\pi N_A r_e^2 m_e c^2$ ,  $N_A$  is Avogadro's constant,  $r_e$  is classical electron radius,  $\rho$  is the mass density of target,  $Z_p$  is the atomic number of projectile,  $Z_t$  is the atomic number of target,  $A_t$  is the atomic weight of target,  $m_e$  is the mass of electron,  $c$  is speed of light,  $\beta = \frac{v}{c}$  where  $v$  is the velocity of projectile,  $\gamma = (1 - \beta^2)^{-1/2}$ ,  $I$  is the mean ionization potential  $\hbar \langle \nu \rangle$ ,  $T_{\max}$  is the maximum energy transfer in a single collision, and  $\delta$  is the density correction. The  $dE/dx$  has dimension  $\text{MeV/g cm}^{-2}$ .

When fast charged particles travel inside the matter, the energy loss increases along the way until particles lose all the energy and then stop traveling. Therefore, the energy loss of particles falls to zero after it reaches the maximum value near the end of the path and this maximum value of energy loss is known as Bragg peak (Tavernier, 2010). Figure 2.1 presents Bragg peaks at the same depth produced by carbon ions and protons with different



**Figure 2.1** Depth dose profile of carbon ions and protons. Carbon ions with energy of 156.38 MeV/u and protons with energy of 80.69 MeV yield Bragg peaks at depth of 50 mm.

energies.

The amount of energy deposited in matter caused by the particles traveling through matter in radiotherapy is known as LET and the unit of LET is keV/ $\mu$ m. Heavy ions such as carbon ions have a high LET value because carbon ions have a higher atomic number ( $Z_p$ ) compared to protons which are a lighter particle. LET will be proportional to the mass stopping power if the projectile undergoes little scattering so it travels along a straight line and becomes identical if the mass density of medium is equal to 1 (e.g. in water). The total path length of heavy charged projectiles in matter is similar to the mean range  $R$  because heavy ions are less scattered and travel nearly a straight line. The mean range of heavy ions traveling in matter can be calculated by integrating over the inverse of the linear energy transfer (Scharadt et al., 2010),

$$R = \int_0^{E_0} \left( \frac{dE}{dx} \right)^{-1} \cdot dE \quad (2.2)$$

with  $dE$  depends on initial energy where  $E_0$  is the initial energy.

### 2.1.2 Radiation dose

The amount of energy deposited in tissue is very important in radiotherapy and is quantified by absorbed dose. The absorbed dose  $D$  is the mean energy deposited by ionizing radiation per unit mass in matter or tissue (ICRU, 1993). For parallel particle beam with fluence  $F$  penetrating a medium with mass density  $\rho$ , the absorbed dose can be calculated by

$$D = \frac{dE}{dm} = \frac{\left(\frac{dE}{dx}\right) \cdot \Delta x \cdot N}{\rho \cdot A \cdot \Delta x} = \phi \cdot \frac{S}{\rho} \quad (2.3)$$

where  $\phi = \frac{N}{A}$  is the fluence,  $S$  is the stopping power, and  $\frac{S}{\rho} = \frac{1}{\rho} \cdot \frac{dE}{dx}$  is the mass stopping power. The absorbed dose is measured in the unit (SI system) called as Gray or Gy where 1 Gy is equal to 1 J/kg.

For a given target dose, carbon ions and protons have a low radiation dose in the entrance channel (because of Bragg peak) compared to electrons and photons. Thanks to Bragg peak, cancer cells located deep inside the body receive a maximum radiation dose while the healthy tissue receives a minimum radiation dose (figure 2.1). In case of large volume tumour, a spread-out Bragg peak (SOBP) is employed to irradiate the whole tumour. A simple spread-out Bragg peak consists of the multiple Bragg peaks produced e.g. by modulator wheel (Chu et al., 1993). Meanwhile at GSI, the active scan system has been utilized to combine different energy beams that stop in different tissue depths ("slices") in order to irradiate the whole target volume (Krämer et al., 2000).

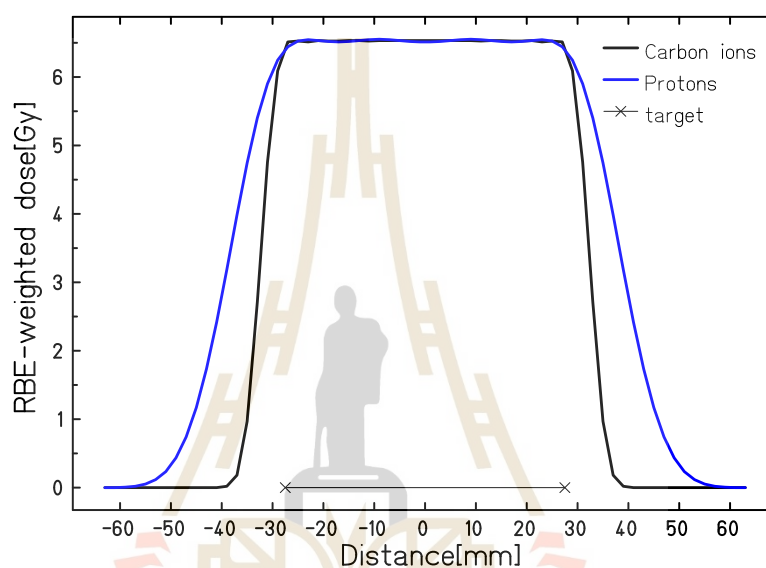
### 2.1.3 Lateral scattering

In ion beam radiotherapy, the elastic Coulomb interactions with nuclei of matter or multiple Coulomb scattering cause lateral scattering (Schardt et al., 2010). The scattering angle is described by Molière-Highland scattering theory (Molière, 1948; Highland, 1975)

$$(\theta)^2 = \left(\frac{13.6 \text{ MeV}}{\beta_{pc}} Z_p\right)^2 \frac{d}{L_0} \left(1 + 0.038 \log \frac{d}{L_0}\right)^2 \quad (2.4)$$



where  $p$  is particle momentum,  $d$  is thickness of target, and  $L_0$  is radiation length. Heavy ions such as carbon ions have smaller lateral deflection than protons which is good for irradiating cancer cells close to organ at risk (OAR). Figure 2.2 presents the comparison of lateral profile between carbon ions and protons in extended target at depth of 71 mm. According to lateral profiles, carbon beam has less lateral scattering than proton beam which is very good to spare the healthy tissue surrounding the target.



**Figure 2.2** Lateral profile of carbon beam in comparison to proton beam in extended target at depth of 71 mm.

#### 2.1.4 Fragmentation tail

When charged particles penetrating in matter, nuclear fragmentation produces lighter ions. Measurement of fragmentation produced by carbon ions with energy of 400 MeV/u penetrating in water has been performed and lighter ions such as proton, helium,  $^{10}\text{Li}$ ,  $^{10}\text{B}$ , and  $^{10}\text{Be}$  have been measured after Bragg peak (Haettner et al., 2006; Schardt et al., 2010). Since ions produced by nuclear reactions are lighter than primary ions, these lighter ions penetrate deeper resulting in a dose tail after Bragg peak. Meanwhile for protons, there is no nuclear fragmentation produced but there are target fragments produced, but with less significant contribution. Thus, there is no fragmentation tail produced

after Bragg peak for proton beam. Figure 2.1 presents the depth dose profile of carbon ions and protons. For carbon ions, fragmentation tail is observed following Bragg peak and it leads to a radiation dose "tail". In contrast to carbon ions, radiation dose for protons completely falls down after Bragg peak which is very good for irradiating target close to OAR or important organ.

## 2.2 Relative biological effectiveness

Different radiation modalities will cause different biological effect in human body. The dose ratio between sparsely ionizing radiation (X-rays, gamma rays) and densely ionizing radiation (protons, carbon ions, helium) which gives the same biological effect is described by relative biological effectiveness or RBE (Hall and Giaccia, 2012).

$$\text{RBE} = \frac{D_{\text{x-rays}}}{D_{\text{ions}}} \quad (2.5)$$

RBE plays an important role in ion beam radiotherapy as the value of RBE is increasing toward the Bragg peak resulting in more biological effect in target and less biological effect in entrance channel or healthy tissue (Weber and Kraft, 2009). RBE depends on types of ions, LET, energy, and radio-sensitivity of cells (Weyrather et al., 1999). RBE can be measured by comparing two survival curves of sparsely ionizing radiation, e.g. X-rays or electrons, and densely ionizing radiation (figure 2.3).

### 2.2.1 Cell survival curve

Survival curves describe the survival probability of a single cell after irradiated to the certain radiation dose (Hall and Giaccia, 2012). In order to obtain survival curve, the irradiated cells then are re-seeded and incubated for one or two weeks in order to let the cells forming colonies. After one or two weeks, the formed colonies are counted and considered as the surviving cells.

In survival curve experiments, the plating efficiency of cells needs to be considered when adjusting the number of cells re-seeded after the irradiation. The plating efficiency (PE) describes the percentage of cells that attach and grow into colonies. Every cell lines have different plating efficiency value and

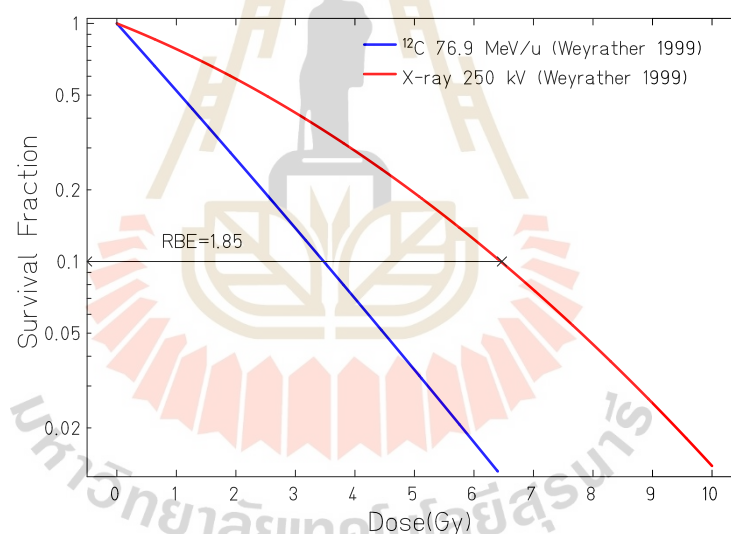
the plating efficiency can be expressed as

$$PE = \frac{\text{Number of colonies counted}}{\text{Number of cells seeded}} \quad (2.6)$$

Measured surviving cells are then plotted in logarithmic scale as a function of radiation dose. Different type of radiations gives a different shape of survival curves as shown in figure 2.3. The shape of survival curves is described by the linear-quadratic model and it is expressed by the formula

$$S = \exp(-\alpha D - \beta D^2) \quad (2.7)$$

where  $S$  is the fraction of surviving cells at dose  $D$  while  $\alpha$  and  $\beta$  are parameters that describe the radio-sensitivity of cell line.



**Figure 2.3** Survival curves of CHO-K1 cells irradiated by X-ray and carbon ions with energy of 76.9 MeV/u (Weyrather et al., 1999).

For producing a lethal event (DSB), there are two mechanisms. At low dose, one single electron can break two chromosome at the same time and its probability is proportional to the dose. At the high dose, two chromosome breaks caused by two different electrons and its probability is proportional to the dose square (Hall and Giaccia, 2012). The survival curve of sparsely ionizing radiation or X-rays starts with linear curve at lower dose which shows the

repairing ability of cells after the irradiation and this stage is corresponded by  $\alpha$  parameter. After that, the curve starts to bend because it is influenced by  $\beta$  parameter. If the  $\beta$  parameter is more dominant than  $\alpha$  parameter, then the curve will be more bent at the high dose. The survival curve of very densely ionizing radiation such as high-LET ion beams is described only by the  $\alpha$  parameter which makes it has a straight linear slope line. The survival curve of ion beams also can be predicted using the local effect model (LEM) (Scholz et al., 1997; Elsässer and Scholz, 2007; Elsässer et al., 2008).

### 2.3 TRiP98 treatment planning system

Before patient undergoes the radiotherapy treatment, treatment plan needs to be done in order to delineate cancer localization and optimize the absorbed dose distribution in target, healthy tissue and OAR. Treatment planning system is utilized to compute the treatment plan. TRiP98 (treatment planning for particles, 1998 edition) is a research treatment planning system developed at GSI (Krämer et al., 2000; Krämer and Scholz, 2000; Krämer, 2001). TRiP98 was utilized to make biological-optimized treatment plan for patients during GSI patient trial project which is started in 1997 and around 400 patients have been successfully treated using this approach at GSI over several years. TRiP98 has been designed to deliver the irradiation using 3D active scanning beam and control the beam position, size, energy and intensity for optimal irradiation. Furthermore, RBE can be used to optimize the treatment plan resulting the RBE-weighted dose (biologically effective dose) in target. Over decades, TRiP98 has been upgraded and improved to compute the treatment plan for mixed fields irradiation, multiple ions irradiation, hypoxic irradiation or complex treatment plan geometries (Krämer et al., 2000; Krämer and Scholz, 2000; Krämer and Durante, 2010; Krämer et al., 2014; Sokol et al., 2017; Sokol et al., 2019).

### 2.4 Gafchromic EBT3 film

Gafchromic film is a radiochromic film that has self-developing (darkening) ability due to polymerization. It is usually used as dosimetry and verification tools in intensity-modulated radiotherapy (IMRT). Gafchromic film consists of a 30  $\mu\text{m}$  active layer sandwiched between two matte-polyester layer with a thickness of

125  $\mu\text{m}$ , respectively (Ashland Advanced Materials, 2016). It has high spatial resolution and is water resistant because of its polyester surface. Gafchromic EBT3 film is used in this study because it has more advantages compared to the EBT2 film such as symmetry structure and no Newton's rings interference pattern occurred (Lewis et al., 2012). Gafchromic film physically reacts chemically to the radiation and changes its colors. This transformation can be described by the net optical density or net OD. The net optical density is the darkening degree of the Gafchromic film caused by the irradiation after eliminating the optical density of background (unexposed film). The net OD value is given by

$$\text{netOD} = \text{OD}_{\text{exp}} - \text{OD}_{\text{bg}} = \log_{10} \left( \frac{I_0}{I_{\text{exp}}} \right) - \log_{10} \left( \frac{I_0}{I_{\text{bg}}} \right) \quad (2.8)$$

with  $I_0$  is the maximum intensity which can be measured by a scanner,  $I_{\text{bg}}$  is the transmitted intensity of background while  $I_{\text{exp}}$  is the transmitted intensity of the exposed film.

The longtime development of the EBT films irradiated by carbon ions of energy 250 MeV/u was analyzed for more than five months (Martišiková and Jäkel, 2010). The darkening degree of EBT film irradiated by carbon ions in the peak and in the plateau was compared to the ones irradiated by photons ( $^{60}\text{Co}$ ) at the dose of 1 Gy. The netOD value has increased around 3-4% within 20 days for both in the peak and in the plateau region due to the slow development of EBT film and the different between those two curves is 1%. A preliminary study on field homogeneity of 24-well plates by employing the Gafchromic film has been performed (Kartini, 2018). The 24-well plates were irradiated by oxygen beams with energies of 30 MeV/u and 50 MeV/u. The netOD of irradiated Gafchromic film inside well plate and outside well plate showed a good agreement indicating there is no any artifacts or reflection effects from the wall of 24-well plate were found.

## CHAPTER III

### CHO CELL CULTURE AND BASIC CELL TESTS

A comprehensive protocol for culturing cells as well as recovering cells from Matrigel inside 96-well plate are described in this chapter. The investigation of cell behavior inside Matrigel matrix including the measurement of cell numbers and the observation of cell shape inside Matrigel matrix has been performed. The shape of cells cultured in Matrigel has been compared to cells cultured in monolayer culture for evaluation. Besides that, the Matrigel recovery protocol has been investigated and number of cells obtained from different recovery methods are presented in this chapter. The oxygenation inside Matrigel matrix has also been investigated by measuring the oxygen level inside Matrigel using optical sensor.

#### 3.1 Cell culture setups

Chinese hamster ovary (CHO-K1) cell line has been chosen because it is easy in handling and CHO cells have been used in many radiation response studies. Cells have been maintained in standard monolayer culture inside T-25 tissue culture flask (TCF) filled with complete growth medium consisting of Ham's F-12 supplemented with 10% fetal bovine serum (FBS) and 1% penicillin/streptomycin (all from Biochrom). Cells were incubated at 37°C with 5% CO<sub>2</sub> and passaged to new culture flask every 3-4 days (or until cells reached 80-90% of cell confluency) without changing the medium. In this work, cells were cultured in three different culture setups for irradiation which are Matrigel, monolayer, and stack setup. All protocols are presented below.

##### 3.1.1 Matrigel setup

For Matrigel setup, cells were cultured in Matrigel matrix (Corning) as embedded culture inside 96-well plate. Matrigel is an extracellular matrix (ECM) extracted from the Engelbreth-Holm-Swarm mouse sarcoma which contains plentiful ECM proteins that provides structure for cells growing in 3D environment.

The protocol for cell culture in this setup was done according to the protocol suggested by Matrigel (Corning, 2017b) with some modifications conducted at GSI.

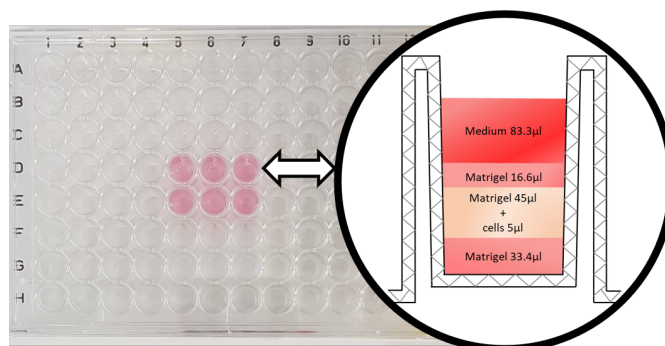
### Cell seeding

First, the protein concentration of Matrigel matrix used in this work was adjusted to 5 mg/ml by diluting Matrigel matrix with iced-cold culture medium according to the protocol in appendix A.1. Subsequently, the bottom of 96-well plate was pre-coated with 33.4  $\mu\text{l}$  of Matrigel matrix to restrain the cells from attaching to the bottom of 96-well plate and then the first layer of Matrigel was incubated for an hour or until the Matrigel become solid. Next, the cell suspension was prepared by trypsinizing and centrifugation at 300g for 5 minutes and cell concentration was adjusted to  $4 \times 10^6$  cells/ml. After that, 5  $\mu\text{l}$  of cell suspension was mixed with 45  $\mu\text{l}$  of Matrigel matrix, so the final cell number becomes  $2 \times 10^4$  cell/well. This mixture was then added on top of the first layer and incubated for an hour.

To prevent the Matrigel matrix got teared due to the cell proliferation process, the third layer of Matrigel matrix (16.6  $\mu\text{l}$ ) was added on top of the second layer giving more space for cells to proliferate. The well plate was then incubated for an hour to solidify the third layer of Matrigel matrix. Last, 83.3  $\mu\text{l}$  of medium was added to keep the moisture of Matrigel matrix and supply nutrients, then the well plate was incubated for 48 hours. Figure 3.1 displays the structure of Matrigel layers inside 96-well plate. Since Matrigel matrix will solidified at temperature above  $10^\circ\text{C}$ , it is recommended to use cold pipette tips and 96-well plates.

### Cell recovery

For recovering the cells from Matrigel matrix, dispase (Corning) was used to dissolve the Matrigel matrix as recommended by Corning (Corning, 2017a). Medium was taken out from 96-well plate immediately after the irradiation. Afterwards, dispase was added and well plate was incubated for an hour or until the Matrigel matrix was completely dissolved. The mixture of dissolved Matrigel and cell suspension from each well was then collected into a micro-tube. In this step, it is recommended to wash the wells a few times with 200  $\mu\text{l}$



**Figure 3.1** The final structure of Matrigel layers inside 96-well plate. Cells were cultured as embedded culture.

of medium to completely take out the leftover cells in the well. In order to separate the Matrigel matrix from the cells, the micro-tube was centrifuged at 2500 rpm for 5 minutes and the supernatant was discarded. Since cells in Matrigel tend to grow in groups, 300  $\mu\text{l}$  of trypsin (0.05% trypsin / 0.02% EDTA in PBS, from PAN Biotech) was added into the cells pellet and cells were incubated for 3 minutes in order to prevent the cell clumping and to obtain single cells. Afterwards, 900  $\mu\text{l}$  of medium were added to avoid cell damage by the trypsin. 200  $\mu\text{l}$  of cell suspension was taken and added to 10 ml of isotone solution for counting the cell number using Beckman Coulter counter machine (profile C with dilution 1:50).

An alternative cell recovering method based on the combination of cooling and centrifuge process was also performed in order to recover the cells in Matrigel (Corning, 2017a). Since dispase method requires an hour incubation step which allows the cells to start repairing the damage after irradiation, so the combination method was identified as an alternative method. First, the 96-well plate was placed in the 4°C fridge for 1-2 hours to liquify the Matrigel matrix. Next, the mixture of cell suspension and Matrigel matrix was collected to micro-tube then the micro-tube was centrifuged at 2500 rpm for 5 minutes to separate the cell suspension from the Matrigel matrix. After that, the supernatant was discarded and the remaining cell pellet was trypsinized to prevent the cell clumping and incubated for 3 minutes. Subsequently, 900  $\mu\text{l}$  of medium was added to the cell suspension and then 200  $\mu\text{l}$  of cell suspension was taken and added to 10 ml of isotone solution for counting the cell number using



Coulter counter machine (profile C).

### 3.1.2 Monolayer setup

For monolayer setup, cells were seeded in standard monolayers inside 96-well plate according to following protocol. First, cell suspension was counted and  $1.1 \times 10^4$  cells was seeded into each well of 96-well plate filled with  $250 \mu\text{l}$  of medium. After that, the well plate was incubated for 24 hours. To recover the cells, the medium was removed and  $50 \mu\text{l}$  of trypsin was added to detach the cells from the bottom of well plate. The well plate was incubated for 5 minutes then,  $150 \mu\text{l}$  of medium was added to stop the trypsin and the cell suspension was collected to a micro-tube. Last, 1 ml of medium was added to the micro-tube and  $200 \mu\text{l}$  of cell suspension was taken and added to 10 ml of isotone solution for counting the cell number using Coulter counter machine (profile C).

### 3.1.3 Stack setup

Stack setup consists of cell culture covered polystyrene slides imitating the bottom part of the  $25 \text{ cm}^2$  TCF and a  $9.5 \times 16 \times 9.5 \text{ cm}$  box made by polymethyl methacrylate (PMMA). The polystyrene slides was produced as special order from Greiner and the slides can be arranged at certain depth inside the PMMA box (figure 3.2). Stack phantom is usually used as standard method for performing treatment plan verification at GSI Stack phantom is usually used as standard method for performing treatment plan verification at GSI (Krämer et al., 2003; Gemmel et al., 2008; Krämer and Durante, 2010; Krämer et al., 2014; Sokol et al., 2017). Currently, the stack phantom is employed for cross-calibration experiment conducted by different participating institutions within the EU INSPIRE project.

The cell culture in stack setup was performed according to this following protocol. First, the cell culture treated polystyrene slides were placed in square bio-assay dishes. Next,  $5 \mu\text{l}$  of cell suspension containing  $5 \times 10^4$  cells was seeded at the center of slide in central plating manner and the dishes were incubated for 3–4 hours to let the cells attaching to the slides. Subsequently, culture medium was added into the dishes until all slides were covered and the dishes were incubated for 24 hours. Prior to the irradiation, the slides were



**Figure 3.2** Stack phantom consists of PMMA box and polystyrene slides: a) outside part and b) inside part where slides are arranged.

inserted to the PMMA box (phantom) and medium was added until all slides were covered.

To recover the cells in stack phantom, all slides were taken out from the phantom box and rinsed with 1 ml of phosphate buffered saline (PBS Dulbecco). Next, 1 ml of trypsin was added and slides were incubated for 4-5 minutes or until the cells were detaching from the slides. After that, cell suspensions were collected into a tube filled with 4 ml of medium. 1 ml of cell suspension was taken and added to 9 ml of isotone solution for counting the cell number using Coulter counter machine (profile B with dilution 1:10).

### 3.2 Clonogenic assay

The fraction of surviving cell was determined by clonogenic assay or colony formation assay. A single cell able to grow into a colony will be considered as a survived cell. At least 50 cells are required to become a colony. The clonogenic assay is performed according to following protocol. Cells were recovered following the irradiation using protocol described in section 3.1. Next, the cell suspensions were counted using Beckman Coulter Counting machine to obtain the cell number in each sample. Subsequently, cells were re-seeded into triplicates for each sample in T-25 flask filled with 5 ml of culture

medium. In order to have enough statistic with minimal overlaps between each colonies, the cells were re-seeded to achieve 100 colonies by adjusting cell number to the expected plating efficiency in the flask and the expected survival. After that, cells were incubated for one week to allow the cells to grow into colonies. Finally, the colonies were stained with methylene blue staining solution and colonies consisting of at least 50 cells were considered as viable and were considered as one survived (original) cell.

### 3.3 Cell growth test

For cell growth test, 70.000 cells have been seeded into 20 flasks T-25 (Falcon) and incubated at 37°C. After 4 hours, two flask were trypsinized by discarding the medium and adding 1 ml of trypsin to the flasks. Next, cells were incubated for 5 minutes and 3 ml of medium was added post-incubation. Cell number was then counted using Coulter counting machine (Profile B). After that, flasks were trypsinized and cell numbers were counted every morning and afternoon until all flasks were finished. The obtained cell numbers were plotted over the time to obtain the cell growth curve.

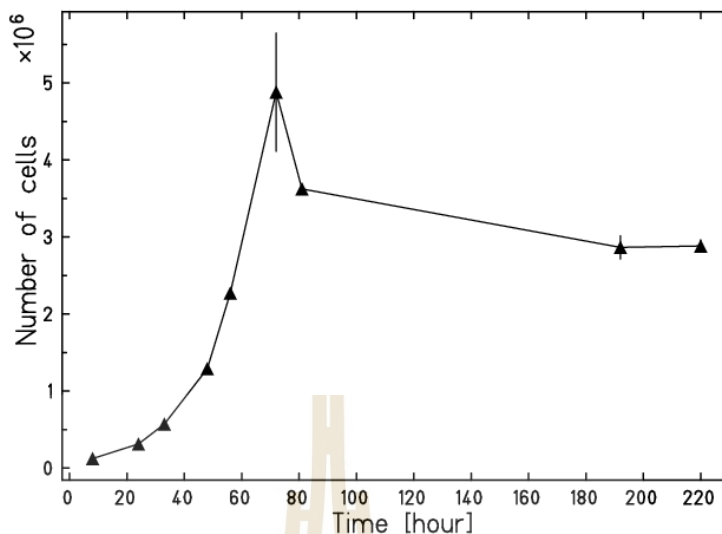
#### 3.3.1 Cell growth curve

The cell proliferation of CHO cells has been observed for nine days and the obtained cell growth curve is shown in figure 3.3. In the first 4 hours, cells started attaching to the flask and they were adapting to the culture environment so they didn't proliferate yet, this phase known as "lag phase".

Next, cells started to actively proliferate and an exponential increase in cell density arises, this phase known as 'logarithmic phase' or log phase. Each cell line will show different cell proliferation kinetics during the log phase and it is therefore the optimal phase for determining the population doubling time. In order to obtain the doubling time of CHO cells, the number of cells in log phase were plotted against incubation time and fitted using exponential function as below

$$N(t) = N_0 \exp(gr \cdot t) \quad (3.1)$$

where  $N(t)$  is the number of cells at  $t$  hours,  $N_0$  is the initial number of

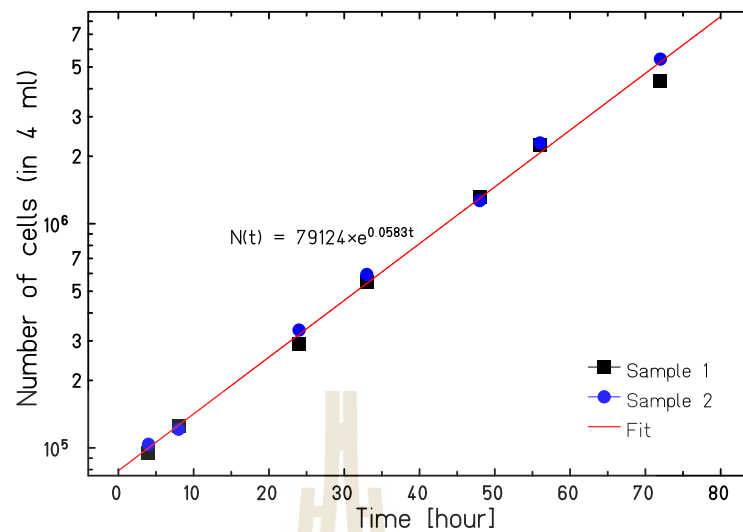


**Figure 3.3** Cell growth curve of CHO cells. Number of cells are obtained from 4 ml of cell suspension and the error bars represent the standard deviation of two independent repetitions.

cells seeded,  $g_r$  is the growth rate of cells, and  $t$  is incubation time (hour). The slope in figure 3.4 is the specific growth rate of the organism, which is a measure of the number of divisions per cell per unit time. From equation 3.1, the doubling time of cells could be calculated using equation 3.2 and the doubling time of CHO cells was obtained after 11.89 hours of incubation.

$$\text{doubling time} = \frac{\ln 2}{g_r} \quad (3.2)$$

After 72 hours of incubation, cellular proliferation has slowed down due to the cell population becoming confluent. The number of cells in the active cell cycle has decreased to 0–10% and the cells are most susceptible to injury, this phase known as plateau or 'stationary phase' (Hall and Giaccia, 2012). Following 80 hours of incubation, a sharp decrease was observed. Cells started to detached and cells apoptosis have occurred, this phase called as death phase.



**Figure 3.4** The doubling time of CHO cells. Number of cells were plotted in logarithmic scale and all data points were fitted using exponential function.

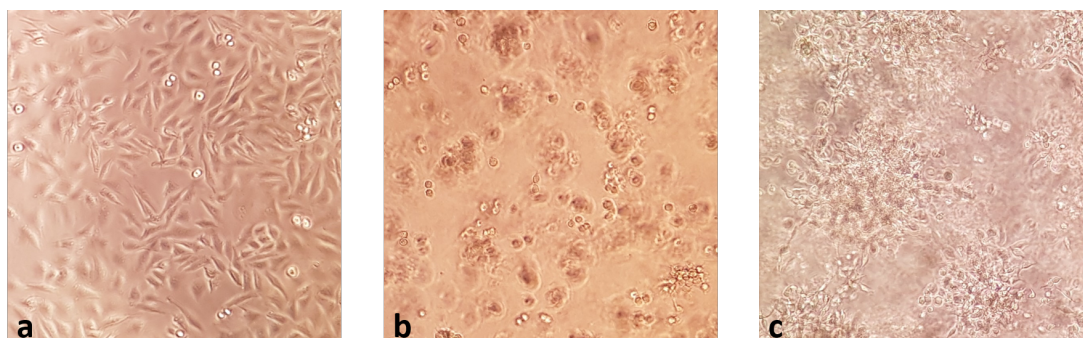
### 3.4 Cell proliferation test

To compare total cell number achievable in one well of 96-well plate ( $\phi = 6.6$  mm), cells were cultured in Matrigel and monolayer setups as per protocols in section 3.1.1 and 3.1.2. After 24 hours of incubation, the shape of cells in monolayer setup were observed and after that cells were recovered and cell numbers were counted. Meanwhile for Matrigel setup, cells in Matrigel has been incubated longer as cells need more time to fully interact with ECM and grow in 3D environment. After 48 hours of incubation, the shape of cells were observed and cells were recovered using dispase and combination method, cell numbers were counted afterwards. The obtained cell numbers from monolayer and Matrigel setups were then compared for evaluation.

#### 3.4.1 The shape of cells cultured in Matrigel

In order to observe the interaction between cells and Matrigel matrix, at first cells have been cultured in Matrigel setup and incubated for 24 hours. The shape of cells inside Matrigel matrix were observed under inverted compound microscope. As for comparison, cells cultured in monolayer setup has been

prepared and incubated for the same time.



**Figure 3.5** The shape of CHO cells cultured in different setup and incubation time: (a) monolayer setup after 24 hours of incubation, (b) Matrigel setup after 24 hours of incubation, and (c) Matrigel setup after 48 hours of incubation.

After 24 hours of incubation, cells in monolayer setup showed a flat and elongated shape (figure 3.5a) while cells in Matrigel showed a spherical shape similar to the shape of cells in suspension as shown in figure 3.5b. Since no interaction of cells with ECM was evident yet, cells were re-cultured in Matrigel and incubated for 48 hours. In case of monolayer culture, it could be seen from the normal passage that cells could not develop different shape even though cells were incubated for more than 5 days. After 48 hours in Matrigel culture, cells were more elongated and stretched out to any directions due to the cell interaction with ECM where cells attached to ECM similar to a 3D scaffold (figure 3.5c). However, huge cell clumpings are spotted as cells tend to grow close to each other.

### 3.4.2 Proliferation of cells cultured in Matrigel

To observe the proliferation of cells cultured in Matrigel setup and to find out the most efficient method to recover cells from Matrigel matrix, cells cultured in Matrigel have been recovered after 48 hours of incubation using four different methods: cooling, centrifugation, combination and dispase. The first attempt has been done by cooling the Matrigel matrix inside 4°C fridge for one hour as Matrigel matrix will dissolve in low temperature. The second attempt has been done by centrifugate the Matrigel matrix. The number of cells

obtained from both methods gave poor and inconsistent cell numbers. Because of this, the recovery method has been improved by combining the cooling and centrifugation methods which is also recommended by Corning (Corning, 2017a).

The combination of cooling and centrifugation method has been performed according to this following protocol. Twenty four samples in Matrigel setup inside 96-well plate have been prepared. Well plate was cooled down in 4°C fridge for one hour and afterwards the Matrigel matrix was collected to micro-tube and centrifuge for 5 minutes at 2500 rpm. Next, 300  $\mu\text{l}$  of trypsin was added to break the cell clumps and incubate for 3 minutes. Afterwards, 900  $\mu\text{l}$  of medium was added to stop the trypsin and cell numbers were counted. The last attempt has been done using dispase solution from Corning to dissolve the Matrigel matrix, 24 samples in Matrigel setup inside 96-well plate have been recovered using Dispase solution. The detailed protocol for dispase method is explained in section 3.1.1. For evaluation, cells were also cultured in monolayer setup inside 96-well plate and 22 samples were recovered using trypsin.

**Table 3.1** Number of CHO cells in Matrigel setup in comparison to monolayer setup. The standard deviations are presented in percentage uncertainty.

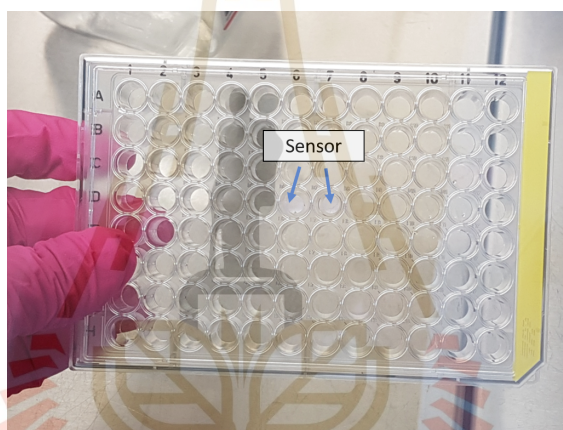
Culture setups	Recovery methods	24 hours	48 hours
Monolayer	Trypsin	32 596 $\pm$ 17%	-
Matrigel	Dispase	-	158 517 $\pm$ 8.7%
Matrigel	Cooling + centrifugation	-	62 256 $\pm$ 50%

Table 3.1 shows the comparison of cell numbers obtained from Matrigel and monolayer setups using different recovery methods. Matrigel setup with dispase recovery method yields the highest number of cells with percentage uncertainty less than 10%. In contrast to dispase method, the combination method of cooling and centrifugation yields a lower number of cells with inconsistent cell numbers resulting in a large uncertainty of 50%. Cell clumping is one of factor that affect the counting process resulting the cell number is not counted properly. From the evidence above, it has been verified that dispase could dissolve the Matrigel matrix very well and break the cell clumping to obtain single cells with reliable counting number (lowest uncertainty) compared

to other method.

### 3.5 Oxygen level measurement inside Matrigel matrix

In order to investigate the oxygen saturation inside Matrigel matrix, the oxygen measurement has been performed using optical sensor device. A "self-adhesive" sensor spot (SP-PSt3-NAU-D5-OIW-SA from PreSens) with the diameter of 5 mm was inserted on the bottom of 96-well plate as shown in figure 3.6. The purpose of placing the spot sensor on the bottom of well plate is to enable the probe to measure the oxygen rate without breaking and contaminating the Matrigel layers which is not possible done using needle sensor.

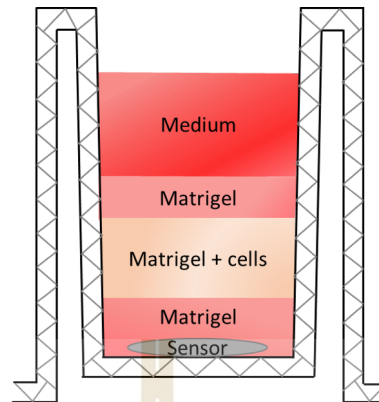


**Figure 3.6** Oxygen spot sensor placed inside the bottom part of 96-well plate.

Next, Matrigel matrix was added above the sensor according to protocol in section 3.1.1. Figure 3.7 presents the final structure of Matrigel culture with spot sensor inside 96-well plate. Two wells filled with CHO cells and sensors were prepared and incubated for 48 hours. During incubation, the oxygen level inside Matrigel was measured using an oxygen meter (OXY-1 SMA-trace-RS232-AO from PreSens) by optically exciting the chemical compound (fluorophore) inside the sensor spot with a laser. The molecular oxygen present in the sample will quench this excitation so that the fluorescence emitted by the sensor spot when relaxing to its ground state depends on the local oxygenation. This fluorescence is measured by the sensor device. Therefore, the oxygen level in either dissolved, liquid or gaseous environment can be measured online with

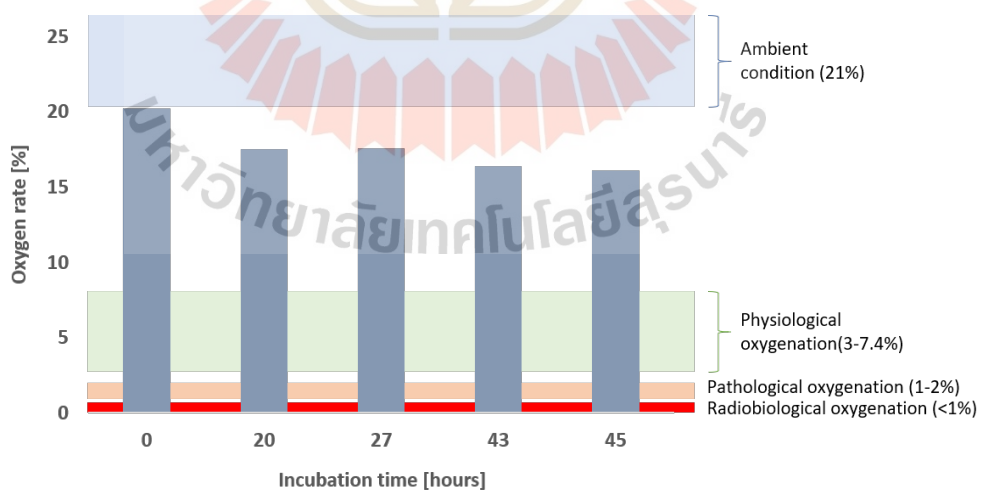


the range of measurement from 0–100%.



**Figure 3.7** Final structure of sensor placed inside Matrigel layers.

During incubation, the oxygen rate inside Matrigel was measured using an optical sensor device at five different times: 0, 20, 27, 43, and 45 hours. A decrease in oxygen level was observed, but it is not significant (figure 3.8). Even after 45 hours of incubation, the oxygen rate has dropped to 16% and this amount of oxygen is still considered as normoxic condition where there is enough oxygen inside Matrigel to be consumed by cells (McKeown, 2014).



**Figure 3.8** Cell oxygenation inside Matrigel matrix within 48 hours of incubation. The level of oxygen percentage in tissue is also presented in different colors (McKeown, 2014)

In order to ensure the oxygen consumption by cells in Matrigel, the cells were recovered from Matrigel after the oxygen measurement has been carried out. Cells were recovered using Dispase and counted using Beckman Coulter counter. The averaged cell number was 34 250 cells/ml with uncertainty of 8.3%. This number of cells is very low compared to the amount of cell number obtained in cell proliferation test (table 3.1). There is a possibility that the presence of a sensor spot inside the Matrigel culture interrupts cell proliferation. Since the number of cells inside Matrigel is inadequate and therefore resulting in less oxygen consumption. However, there is still a big margin in oxygen level despite we have more cell numbers in Matrigel, the oxygenation measured will be far above critical level (radiobiological hypoxia).

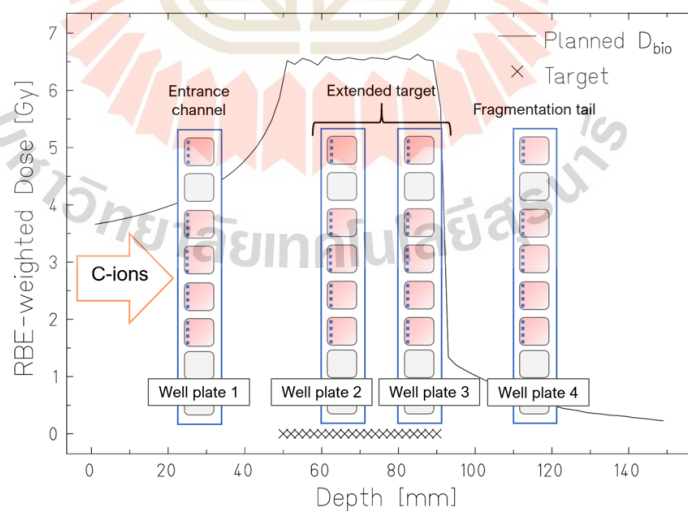
### 3.6 Summary

Basic cell test consisting of cell growth curve and cell proliferation as well as the shape of cells in different culture setup have been investigated. The evolution of CHO cells has been observed and the cell cycle of CHO cells is 11 hours. In contrast to cells in monolayer culture which exhibit flat shape, cells in Matrigel exhibit an elongated shape which stretched to different direction after 48 hours of incubation due to cells attaching to ECM 3D scaffold. Based on the cell proliferation test, cell recovery utilizing dispase is confirmed to produce higher and more reliable cell numbers with convenient procedures. The oxygen saturation in Matrigel matrix has been measured as well to examine the possibility of cells being in hypoxic condition. According to the result, the oxygen rate measured is still considered as normoxic condition, however, the cell proliferation observed is deficient in cell number resulting in fewer cells consuming the oxygen.

## CHAPTER IV

### RADIOBIOLOGICAL VERIFICATION OF SIMPLE TREATMENT PLAN USING 3D BIO-PHANTOM

In this chapter, the response of cells cultured in Matrigel to irradiations has been investigated by obtaining the reference (X-rays) and carbon ion survival curves. The shape of survival curves obtained from Matrigel setup were observed and the  $\alpha$  and  $\beta$  parameters according to the linear-quadratic model (Hall and Giaccia, 2012) from Matrigel curve have been calculated as well in order to obtain a customized RBE table for cells in Matrigel. Afterwards, the radiobiological verification for a simple treatment plan employing 3D bio-phantom consisting of cells cultured in Matrigel matrix inside 96-well plate has been performed. Four well plates filled with cells were placed vertically at different positions and irradiated by active scanning carbon ion beam as shown by figure 4.1. The investigation on field homogeneity of 96-well plate inside Matrigel matrix are also described in this chapter.

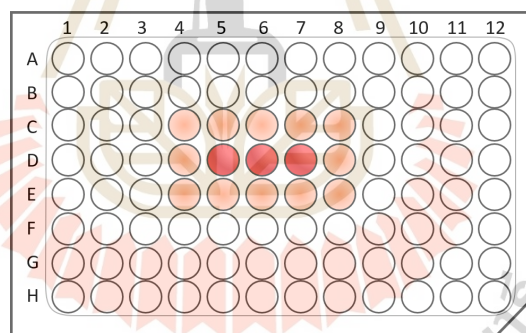


**Figure 4.1** Well plate arrangement for radiobiological verification irradiation. Four 96-well plates were placed in vertical position at entrance channel, extended target and fragmentation tail.

## 4.1 Survival irradiation setup

### 4.1.1 X-rays survival experiment

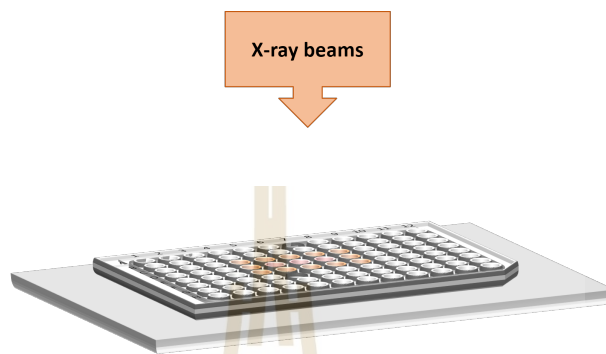
In survival experiment, cells have been cultured in Matrigel setup only. Eight 96-well plates have been prepared for irradiation including the control well plate. Cells with cell number of 20 000 cell/well were seeded in three wells and incubated for 48 hours (figure 4.2). After that, cells were irradiated by X-rays beams from Isovolt DS1 X-rays machine with a peak voltage of 250 kV and dose rate of 2.2 Gy/min at GSI. Cells were irradiated from the top of well plate (figure 4.3) with radiation doses ranging from 0–11 Gy. The dosimetry for X-rays irradiation was done using Farmer-type ionization chamber which placed directly below the 96-well plate. The dosimetry was performed before the cells irradiation and dose rate was measured at this point. After that, the expected dose was set into the control system. The control system will turn off the irradiation automatically once the desired dose has been delivered.



**Figure 4.2** Cells were cultured in Matrigel in three wells (red color) and irradiated with same dose. The surrounding wells and the space between wells have been filled with culture medium (orange color) in order to have a homogeneous field with lateral build-up.

Post-irradiation, cells were recovered immediately using dispase protocol in section 3.1.1 and cells were then re-seeded and incubated in order to obtain survived colonies according to the clonogenic assay protocol in section 3.2. To obtain the survival curve, the survived colonies were then plotted in semi-logarithmic scale and fitted to linear-quadratic equation  $S(D) = \exp(-\alpha D -$

$\beta D^2$ ) where  $S$  is the survival fraction and  $D$  is the radiation dose. For evaluation, the Matrigel survival curve was compared to the reference survival curve obtained from standard monolayer in T-25 culture flask (Sokol et al., 2017).

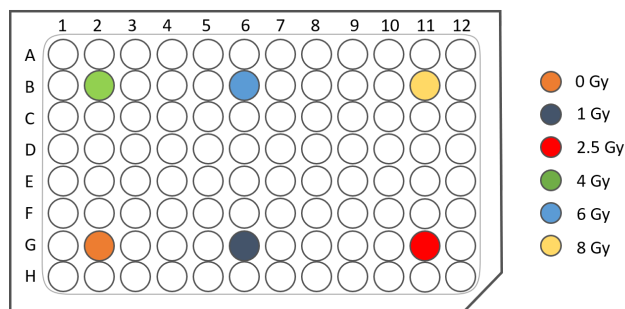


**Figure 4.3** Experimental setup for X-rays irradiation. 96-well plate filled with cells and Matrigel was placed horizontally and irradiated from above.

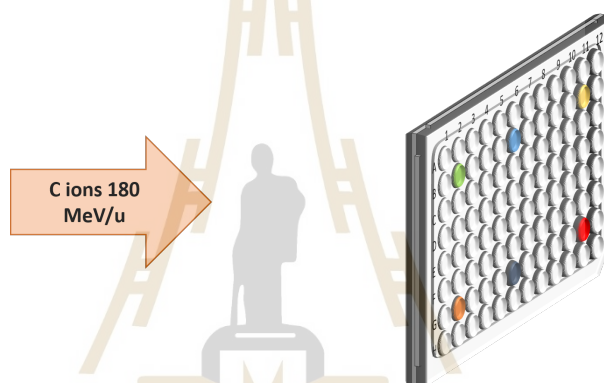
#### 4.1.2 Carbon ion survival experiment

To investigate the cells response to ion beam irradiation, cells have been cultured in Matrigel and monolayer setups and irradiated by monoenergetic carbon ion. For both setups, cells were seeded in six wells where each well receives different dose as shown in figure 4.4. All wells with cells were filled with culture medium completely and the well plates were also sealed by micro-plate sealing film. For carbon ion irradiation, it is not necessary to fill up the surrounding wells and the space between wells as the pencil beam of carbon ions is very precise and without lateral scattering. Two independent 96-well plates were placed vertically on treatment couch and irradiated at the same time in vertical position (figure 4.5). After that, cells were irradiated by monoenergetic carbon ion with energy of 180 MeV/u and dose ranging from 0–8 Gy at Marburg Ion-Beam Therapy Centre (MIT), Marburg.

The dose plan for survival experiment with carbon ion was computed using TRiP98. The dosimetry was done using Farmer-type ionization chamber placed in the entrance channel and only one dose was measured in one field. Next, this absorbed dose was obtained and used as correction factor



**Figure 4.4** Cells in Matrigel and monolayer setup were irradiated by monoenergetic carbon ion beams with different dose according to respective colors.

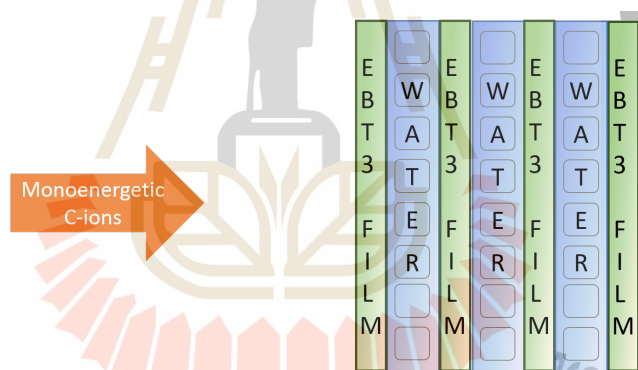


**Figure 4.5** Experimental setup for monoenergetic carbon ion irradiation. Cells in Matrigel and monolayer setup were placed vertically and irradiated from behind (bottom of well plate).

for the remaining dose. Post-irradiation, cells in Matrigel were recovered using dispase protocol in section 3.1.1, while cells in monolayer were recovered using protocol in section 3.1.2. After that, cells were re-seeded and incubated in order to obtain survived colonies according to the clonogenic assay protocol in section 3.2. To obtain the survival curve, the survived colonies were then plotted in semi-logarithmic scale and fitted to linear-quadratic equation  $S(D) = \exp(-\alpha D - \beta D^2)$ .

## 4.2 EBT3 film irradiation setup

In order to investigate the influence of 96-well plate to the radiation field homogeneity, Gafchromic EBT3 film has been cut into size of 96-well plate and placed before, in between and after 96-well plates as shown in figure 4.6. All well plates were completely filled with water and sealed with micro-well plate sealing film in order to have homogeneous field. Next, films were irradiated to monoenergetic carbon ion beam at MIT, Marburg with energy of 145 and 195 MeV/u and dose range of 1.4 Gy and 5 Gy depending on the beam energy and film depth. In addition to assess the possibility of artefacts caused by the well of 96-well plate, EBT3 film was cut into size of well with diameter of 6 mm using a punch. Those circular films were inserted into the well and filled with water, then irradiated in the similar irradiation setups as the large films above.



**Figure 4.6** EBT3 film irradiation setup where films were placed before, in between and after 96-well plate.

After that, the irradiated films were scanned after 24 hours post-irradiation using flat-bed film scanner (Perfection V800 Photo from Epson) in portrait orientation. In order to have an optimum scanning process, the color mode was arranged to 48-bit rgb, image resolution was adjusted to 200 dpi and all image enhancement features was deactivated. The pixel values of irradiated films from red color channel were analyzed using ImageJ, image processing program developed by National Institutes of Health (NIH) and the standard deviations of respective films were investigated as well. The film

profiles corresponding to each film position were then plotted to observe any artefacts caused by the structure of 96-well plate. Furthermore, the standard deviations of film profile were observed as well.

### 4.3 Treatment planning system

TRIP98, a GSI in-house treatment planning system, has been used to compute the dose distribution and simulate the cell survival rate for all treatment plans. The target volume has been adjusted according to the phantom setup. For treatment plan with 3D bio-phantom (Matrigel setup), the target volume had lateral dimension of  $60 \times 40 \text{ mm}^2$  while target volume in treatment plan with stack phantom had lateral dimension of  $40 \times 80 \text{ mm}^2$  and the target depth for both treatment plans was ranging from 55 mm to 85 mm in order to have an optimal coverage of samples.

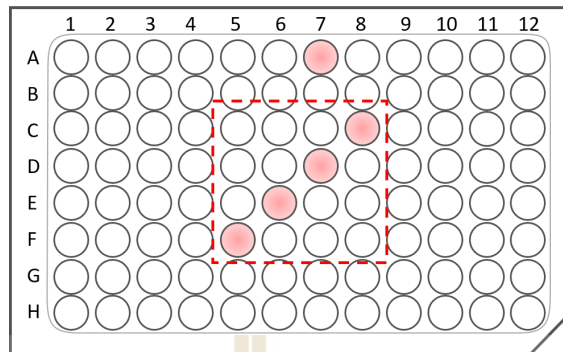
All treatment plans were optimized for a uniform RBE-weighted dose of 6.5 Gy in target region which is resulting in a flat survival rate of  $\sim 10\%$  in the target region. In order to compute the expected cell survival distribution, the standard CHO RBE table has been used for treatment plan with stack phantom (Sokol et al., 2017) and new CHO Matrigel RBE table has been used for treatment plan with Matrigel setup. The CHO Matrigel RBE table was calculated using LEMIV (Elsässer et al., 2010; Friedrich et al., 2012; Scholz et al., 2020) by employing the new  $\alpha$  and  $\beta$  parameters obtained from X-rays survival curve (Matrigel setup) in section 4.6.1.

### 4.4 Sample preparation

In this work, cells were cultured in two different setups: Matrigel setup and stack setup. For Matrigel setup, cells have been cultured according to the protocol in section 3.1.1. Cells were seeded in five wells with the arrangement as follow: four wells in the target region and one well outside the target region (represents as healthy tissue) as shown in figure 4.7. Four 96-well plates have been prepared for irradiation. After that, cells were incubated for 48 hours prior to irradiation. Meanwhile for stack setup, cells have been cultured in stack phantom according to the protocol in section 3.1.3. Cells were seeded in standard monolayer culture in four slides. After that, cells were incubated for



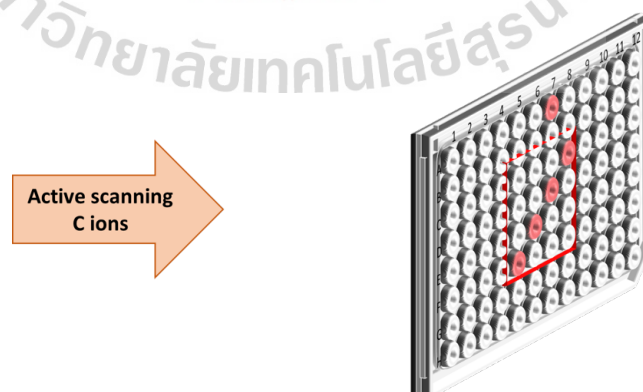
24 hours prior to irradiation.



**Figure 4.7** Wells arrangement for radiobiological verification irradiation. Four wells inside the red dashed-line box represent as target (cancer cells) while one well outside represents as healthy tissue.

#### 4.5 In-vitro irradiation setup

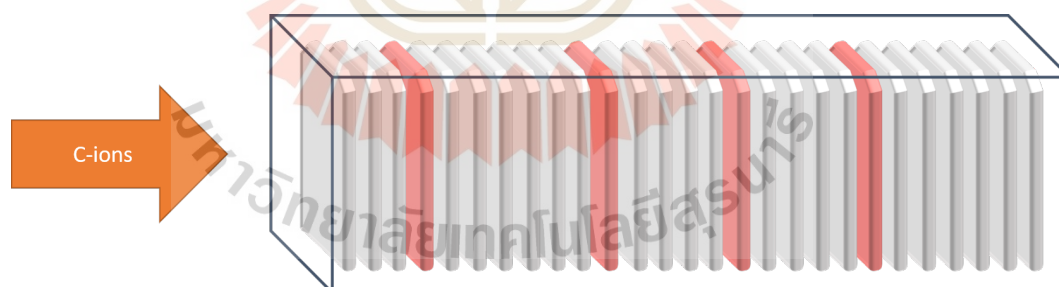
The irradiation setup for treatment plan verification using 3D bio-phantom was arranged according as follows. After 48 hours of incubation, wells filled with cells were completely filled with culture medium and sealed with micro-plate sealing film. Next, all 96-well plates were stacked up in vertical position and placed in different positions individually (figure 4.1).



**Figure 4.8** Irradiation setup for radiobiological verification using Matrigel setup. Well plate was placed in vertical position and irradiated from behind.

Well plate 1 was placed in the entrance channel at a depth of 26.8 mm where well plate was positioned after a 23.8 mm WET of PMMA. Next, well plate 2 was placed in proximal part of extended target at a depth of 62.5 mm after additional 59.5 mm of PMMA. In distal part of extended target, well plate 3 has been placed at a depth of 86.3 mm after additional of two PMMA blocks (with total thickness (WET) of 83.3 mm). At the last position (fragmentation tail), well plate 4 was placed at a depth of 113.9 mm after additional of two PMMA blocks and two well plates filled with water. After that, all well plates were irradiated from behind in standing position by active scanning carbon ion beam with energy range of 156.34–211.54 MeV and dose ranging from 0–6.5 Gy at MIT, Marburg (figure 4.8). Two independent well plates were irradiated at the same time for each corresponding position.

Meanwhile for treatment plan verification using stack phantom, four slides filled with cells were arranged in different position inside stack phantom as shown in figure 4.9. Slide 1 was placed at a depth of 26.5 mm which represents the entrance channel. Slide 2 and 3 were placed in the proximal and distal part of extended target at depth of 61.5 mm and 86.5 mm, respectively. Last, slide 4 was placed at a depth of 111.5 mm which represents fragmentation tail. Two stack phantoms were prepared and irradiated independently.

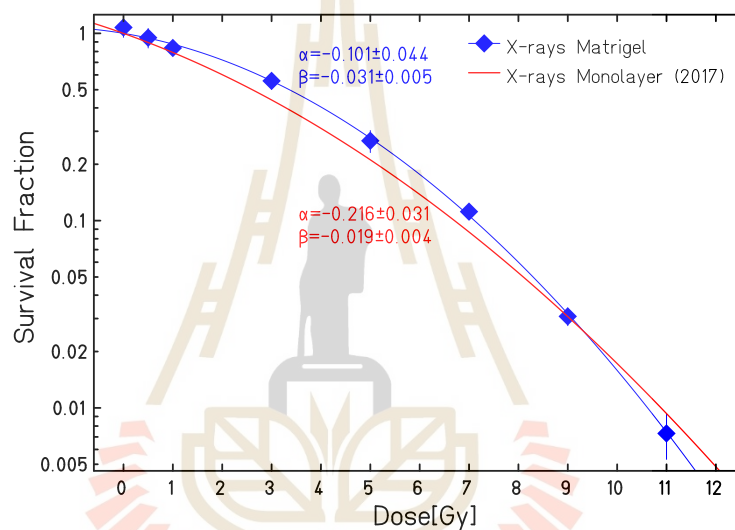


**Figure 4.9** Experimental setup for radiobiological verification using stack phantom. Four slides were arranged at different position which correspond to entrance channel, extended target (SOBP), and fragmentation tail.

## 4.6 Results and discussion

### 4.6.1 Response of cells cultured in Matrigel-based phantom to irradiations

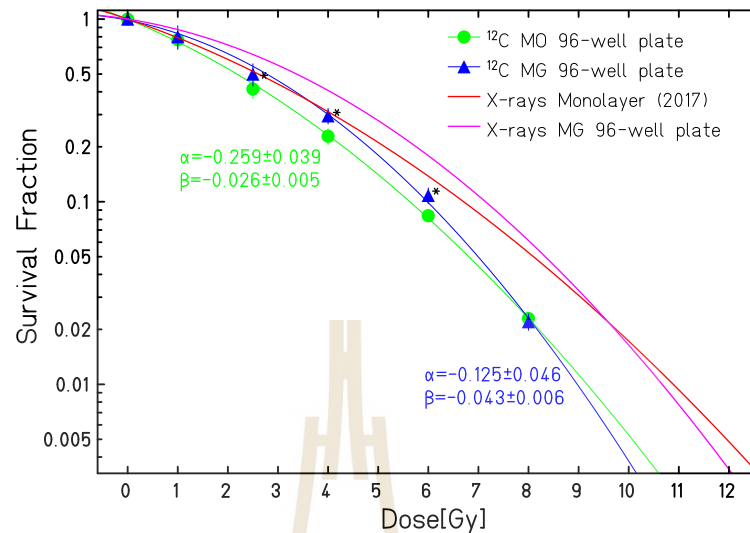
The response of cells in Matrigel to X-ray irradiation is presented by figure 4.10. Matrigel curve shows more bend compared to monolayer curve. At lower dose, Matrigel curve exhibits a shoulder curve and then more pronounced decline happened at higher dose which implies cells in Matrigel are less sensitive to low dose radiation and more sensitive to high dose radiation. Since Matrigel



**Figure 4.10** Survival curve of CHO cells cultured in Matrigel setup after irradiation with X-ray beams. Blue data points represent the average survival fraction of cells in Matrigel while the red line represents the reference survival curve of cells in standard monolayer culture (Sokol et al., 2017). Error bars represent the standard deviations of nine samples. Measured data points were fitted using linear quadratic equation.

curve shows a bent curve, new  $\alpha$  and  $\beta$  parameters have been extracted as shown in figure 4.10 and the obtained  $\alpha/\beta$  ratio is 3.221 which implies cells in Matrigel give a late response to radiation. New RBE table dedicated for cells in Matrigel has been computed using the new  $\alpha$  and  $\beta$  parameters together with LEMIV (Elsässer et al., 2008; Friedrich et al., 2012; Scholz et al., 2020) to calculate the TRiP98 simulation for treatment planning verification with 3D

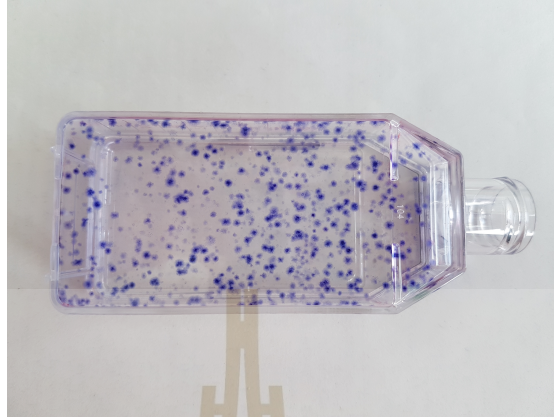
bio-phantom.



**Figure 4.11** Survival curve of CHO cells cultured in Matrigel and monolayer setups after irradiation with 180 MeV/u monoenergetic carbon ion beams. Blue and green data points represent the average survival fraction of cells in Matrigel and monolayer setup, respectively. Red and purple lines represent survival curves of cells in standard monolayer culture and Matrigel setup after irradiation with X-rays, respectively. Symbols \* represent the significant differences ( $p \leq 0.05$ ) between Matrigel and monolayer survival curves after irradiation with monoenergetic carbon ion. Error bars represent the standard deviations of six samples. All data points were fitted using linear quadratic equation.

For carbon ion irradiation, figure 4.11 shows the response of cells in Matrigel and monolayer setup after irradiation with monoenergetic carbon ion. Matrigel curve (blue line) shows a slightly raised curve in contrast to monolayer curve (green line) especially at lower dose region. Matrigel curve also shows a shoulder curve at low dose region which indicates cells radio-resistant to low dose irradiation. According to the statistic analysis done using t-test for two-sample equal variance, the survival fractions at dose of 2.5, 4, and 6 Gy show significant differences ( $p \leq 0.05$ ). At high dose region, the curve shows a downward inclination, especially at dose of 8 Gy. The obtained colonies at dose of 8 Gy for both Matrigel and monolayer setups exhibit numerous colonies as shown in figure 4.12. The colonies were overlap with each other and it is

difficult to identify a single colony which caused unreliable results and therefore, it was considered as lower limit of survived colonies.



**Figure 4.12** Excessive number of colonies was obtained after irradiated by monoenergetic carbon ion with dose of 8 Gy in Matrigel setup.

**Table 4.1** List of  $\alpha$  and  $\beta$  parameters of CHO cells cultured in Matrigel and monolayer setups after irradiated to X-rays and monoenergetic carbon ion. The  $\alpha$  and  $\beta$  parameter of monolayer X-rays curve is obtained from standard monolayer culture (Sokol et al., 2017). The ratio of  $\alpha$  to  $\beta$  is also presented.

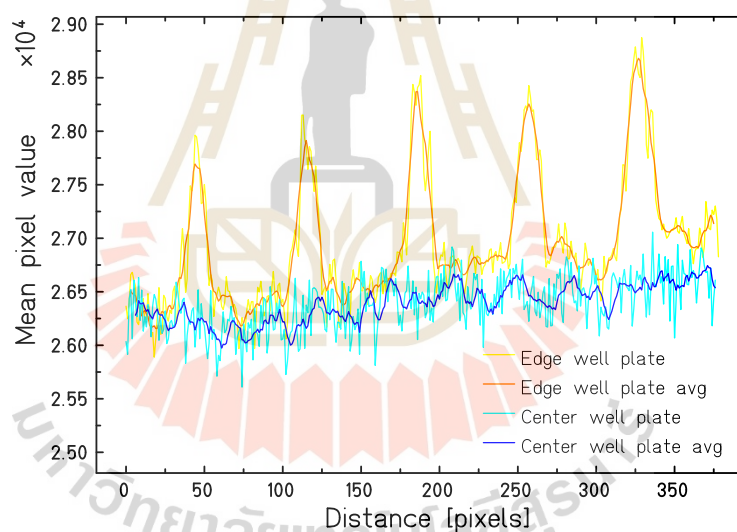
Beam	Culture setup	$\alpha$ (Gy <sup>-1</sup> )	$\beta$ (Gy <sup>-2</sup> )	$\alpha/\beta$ (Gy)
X-rays	Standard monolayer	$-0.216 \pm 0.031$	$-0.019 \pm 0.004$	11.11
	Matrigel setup	$-0.101 \pm 0.044$	$-0.031 \pm 0.005$	3.221
carbon ion	Monolayer setup	$-0.259 \pm 0.039$	$-0.026 \pm 0.005$	9.791
	Matrigel setup	$-0.125 \pm 0.046$	$-0.043 \pm 0.006$	2.894

From figure 4.11, it could be observed that the way of Matrigel curve lifted at low dose region is similar to the X-ray Matrigel curve which means both Matrigel curves are in good agreement. The  $\alpha$  and  $\beta$  parameters obtained from both Matrigel and monolayer setup is presented by table 4.1. Both monolayer culture irradiated to X-rays and monoenergetic carbon ion present  $\alpha/\beta$  ratio more than 9 Gy which indicates cells in monolayer culture give early response to irradiation. In contrast to monolayer culture, the Matrigel culture irradiated with X-rays and monoenergetic carbon ion present a smaller  $\alpha/\beta$  ratio of

2–3 Gy. These small  $\alpha/\beta$  ratio might indicate that cells cultured in Matrigel culture exhibit late response to irradiation.

#### 4.6.2 Radiation field homogeneity of stacked 96-well plate with Gafchromic EBT3 film

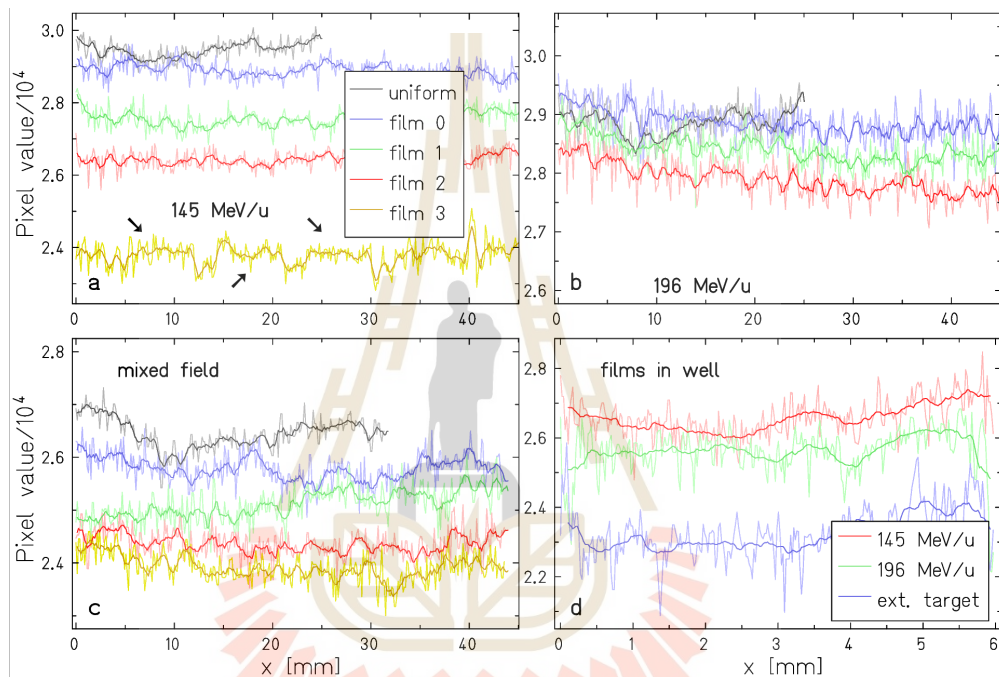
To investigate the influence of the 96-well plate to radiation field homogeneity, the lateral profiles of the irradiated EBT3 films at different position have been analyzed. First, lateral profiles of film placed after one well plate at the edge and center of well plate have been analyzed by plotting the mean value from the red channel across the length of ROI (region of interest). To reduce the noise, group of seven mean values were averaged and plotted as shown by figure 4.13.



**Figure 4.13** Comparison of film profiles at the edge and center part of 96-well plate. Yellow lines represent the film profiles at the edge of well plate while blue lines represent the profiles at the center of well plate.

Yellow lines represent profiles at the edge of well plate where the field is not uniform due to the presence of a flat polystyrene rim which cannot be filled. Blue lines represent profiles at the center of well plate where samples are located and at this region, the whole wells and the space between wells are completely filled with medium. Profiles at the edge region

present significant peaks corresponding to the outer part of well plate which is lacking of medium and the percentage uncertainty of mean value was 2.24%. These peaks demonstrate the spacing between wells and the appearance of real artefacts if the irradiation field was done in the border of well plate. In contrast, the profiles at the center region show a flat curve with uncertainty of 0.94% indicating the field at center region where samples are located is homogeneous and there is no artefact caused by the wall of well plate.



**Figure 4.14** Field homogeneity assessment using Gafchromic EBT3 film placed before, in between, and after 96-well plates. Lateral profiles along the center of 96-well plate irradiated in two monoenergetic carbon ion fields (a) 145 MeV/u and (b) 195 MeV/u; and (c) one mixed field. (d) Profiles of small films placed inside the well of 96-well plate and irradiated to monoenergetic and active scanning carbon ion beams. The profile of films placed after “ $n$ ” number of well plate is represented by “film  $n$ ” while profile of film irradiated to uniform field without any well plate is represented by “uniform”. Arrows in figure (a) indicate the artefact pattern obtained from film placed after 3 well plates.

Next, film profiles placed before well plate as well as following one, two and three stacked well plates are presented by figure 4.14. For evaluation,

the obtained film profiles were compared to the profile of film irradiated in uniform field without well plate (replaced by 2 mm of PMMA instead for build-up) with similar dose. There are no artefacts detected from film profiles placed after two well plates. However, after three well plates in irradiation field with 145 MeV/u, artefacts were spotted every 9 mm interval as pointed by arrows in figure 4.14a. Those artefacts represent the space between each wells in 96-well plate.

**Table 4.2** Standard deviation of Gafchromic EBT3 film profile presented in percentage uncertainties.

Films	Irradiation setups		
	145 MeV/u	196 MeV/u	Mixed field
Uniform	0.93%	0.88%	1.16%
Film 0	0.90%	1.05%	1.08%
Film 1	0.94%	1.00%	1.26%
Film 2	0.92%	1.12%	1.05%
Film 3	1.40%	-	1.18%

Figure 4.14d presents the profiles of small placed inside the well of 96-well plate. The obtained profiles displayed flat profiles without significant peaks but higher noise was observed due to the sensitivity of the active layer of EBT3 film to the high resolution scanner. However, there is an issue to reproduce the experiment with small film particularly in cutting the EBT3 film into small circular film using a punch. The edge of film was slightly peeled during the cutting process resulting in a ring pattern in the center of film which causing unreliable film profile. All the standard deviation of film profiles irradiated to carbon ion in different irradiation setup and different number of well plate is presented in table 4.2.

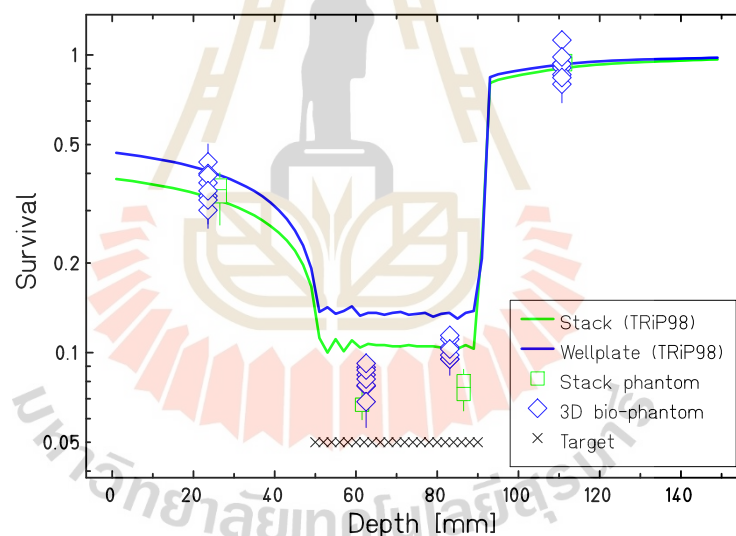
#### 4.6.3 Treatment plan verification

In order to verify the feasibility of 3D bio-phantom for radiobiology verification, cells have been cultured in Matrigel setup and irradiated to active scanning carbon ion beam. Four 96-well plates filled with cells have been irradiated at different position (see section 4.5) in order to observe the practica-



bility of 3D bio-phantom for radiobiology verification of more complex treatment plans. To ensure the accuracy of measurement, the obtained cell survival was compared to the cell survival obtained from GSI's standard radiobiology verification tool which is stack phantom (stack setup).

Figure 4.15 shows the cell survival rate of cells in Matrigel and stack setup after irradiated to active scanning carbon ion beam. TRiP98 calculation for both treatment plans were also presented in figure 4.15. Well plate plan for Matrigel setup (blue line) showed an elevated curve at the entrance channel and extended target regions compared to stack plan (green line). In section 4.6.1, it was shown that cells in Matrigel setup exhibited an increased radio-resistance after irradiated to X-rays and new Matrigel RBE table was used for computing the well plate treatment plan causing the differences between well plate plan and stack plan.



**Figure 4.15** Cell survival rate after being irradiated to active scanning carbon ion beam along z-direction (depth). Lines represent the TRiP98 treatment plan for stack phantom (green) and 3D bio-phantom (blue). Diamond data points represent the measured survival of cells in Matrigel setup while square data points represent the measured survival of cells in stack phantom. All data were plotted in semi-logarithmic scale.

In the extended target region, the average cell survival measured for Matrigel setup is 0.0919 and for stack setup is 0.0716. Both setups show more

consistent data points with uncertainties of 8–14%. In contrast, the measured cell survival from Matrigel setup at the entrance channel and fragmentation tail shows spread data points with average cell survivals of 0.364 and 0.922, respectively, with uncertainties of 11–12%. For stack setup, the obtained average cell survival at the same region shows more consistent results of  $0.350 \pm 5.9\%$  and  $0.942 \pm 1.8\%$ , respectively. The spread data points in Matrigel setup might be caused by cell clumping during the cell counting before the reseeding process. In contrast to cells in target region, cells in low-dose region have a higher possibility to survive and grow into colonies, therefore the cell clumping might affect more to the cells survival level.

#### 4.6.4 Adaptation to 384-well plate

To achieve the radiobiological verification with higher spatial resolution, an attempt to culture CHO cells in Matrigel inside flat-bottom 384-well polystyrene (PS) plate has been carried out. The Matrigel culture in 384-well plate has been performed according to following protocol equivalent to the protocol with 96-well plate.  $11.49 \mu\text{l}$  of Matrigel matrix was added to the bottom of 384-well plate and incubated for an hour. Next, the cell suspension with cell concentration of  $4 \times 10^6$  cell/ml was prepared and then  $2.5 \mu\text{l}$  of cell suspension was taken out and mixed with  $22.5 \mu\text{l}$  of Matrigel matrix resulting the final cell concentration of  $2 \times 10^4$  cell/well. This mixture was then added on top the first layer and incubated for an hour. After that,  $5.75 \mu\text{l}$  of Matrigel matrix was added on top of the second layer and incubated for an hour to solidify the third layer of Matrigel matrix. Finally,  $28.74 \mu\text{l}$  of medium was added as final layer and well plate was incubated for 48 hours.

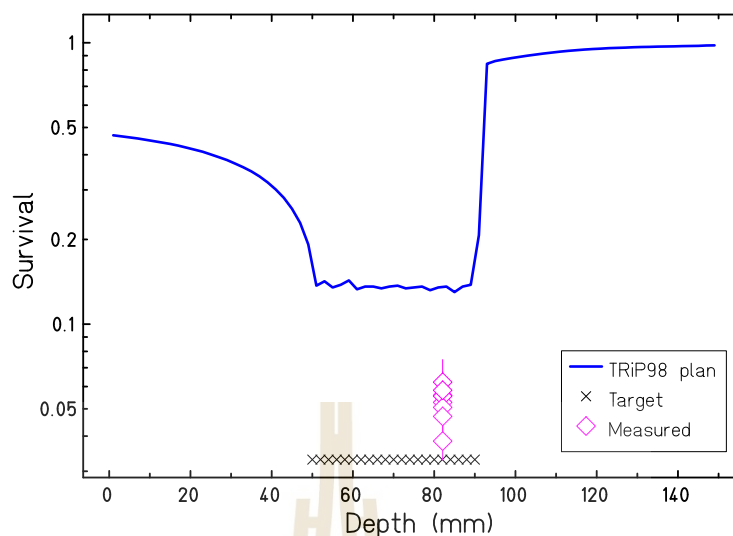
Two 384-well plates with five wells filled with cells were prepared for irradiation. After 48 hours, all well plates were completely filled with medium and sealed with micro-plate sealing film. Well plates were placed in vertical (standing) position at depth of 86.3 mm which is in distal part of extended target (see in section 4.5) and irradiated with active scanning carbon ion beams. Post-irradiation, cells were recovered using dispase method as mentioned in see section 3.1.1 with some modification to match the surface area of 384-well plate.  $22 \mu\text{l}$  of dispase was added to the 384-well plate instead of  $64 \mu\text{l}$  and incubated for an hour to dissolve the Matrigel matrix. After that, the cells were

**Table 4.3** Number of CHO cells in Matrigel setup inside F-bottom 384-well plate after 48 hours of incubation. Cell numbers are counted in 1 ml of isoton solution.

Sample	Cell number/ml
1	65 000
2	58 400
3	62 800
4	56 600
5	43 600
6	73 500
7	64 300
8	68 100
9	67 500
10	56 300
Averaged	61 610 $\pm$ 13.5%

centrifuged and trypsinized in the same methods of cell recover with 96-well plate. Cell numbers recovered from 384-well plate were varying compared to cells recovered from 96-well plate which have more uniform cell number (table 4.3).

Next, the recovered cells were adjusted to the plating efficiency (0.7) and the expected survival (0.1) then re-seeded into T-25 flasks and incubated for one week. After one week, the colonies were then stained using methylene blue staining solution and colonies with more than 50 cells were counted as survival cells. The measured survival of cells cultured in 384-well plate was 0.0573 with uncertainty of 14% which is in disagreement to the expected survival (0.1 or 10%). Figure 4.16 shows the measured cell survivals in comparison to the same Matrigel treatment plan in section and all data points were spread and much lower than expected. This might happened due to the irregular samples obtained during cell recovery from 384-well plate.



**Figure 4.16** Survival fractions of CHO cells cultured in Matrigel inside 384-well plate after irradiated to active scanning carbon ion beam at distal part of extended target region (diamond data points). Blue line corresponds to the TRiP98 prediction using well plate treatment plan.

#### 4.7 Summary

The investigation of the cells response to irradiation and the application of 3D bio-phantom as new verification tool has been conducted in this study. The response of CHO cells cultured in Matrigel and monolayer setups to X-rays and carbon ion irradiation have been performed by obtaining the survival curve of CHO cells. The shape of survival curve from both setups have also been observed as well. In contrast to monolayer survival curve, the Matrigel survival curve showed a shouldered curve at low dose and an inclined slope at high dose which indicating cells cultured in Matrigel matrix are less sensitive to irradiation but they become more sensitive after irradiated to higher dose. The field homogeneity of stacked 96-well plates have been analyzed utilizing Gafchromic EBT3 films which placed following 96-well plates. Based on the obtained result, there are no significant artefacts found in film profiles placed after two well plates, indicating it is possible to irradiate two stacked up well plates at the same time in the entrance channel. Finally, the verification of biological optimized treatment plan has been conducted utilizing the new

verification tool, 3D-bio phantom consisting cells cultured in Matrigel matrix inside 96-well plate. Measured survival cells at entrance channel, extended target and fragmentation tail shows a good agreement with the reference method which concludes the 3D-bio phantom as a convenient verification tool for validating different treatment planning techniques.



# CHAPTER V

## ADAPTATION TO XRS-5 CELLS AND OUT-OF-FIELD RADIOBIOLOGICAL VERIFICATION

After refining the cell culture protocols and attaining the first successful applications with CHO-K1 cell line, the experiments have been extended to xrs-5 cell line. In addition, in order to advance towards higher spatial resolution, feasibility tests including cell growth in Matrigel matrix inside 384-well polystyrene (PS) and polypropylene (PP) plate and cell response to irradiation have been observed as well. Finally, the radiobiological verification at out-of-field region experiments have been performed using xrs-5 cells cultured in Matrigel inside 384-well PP plate.

### 5.1 Matrigel cell culture with xrs-5 cell

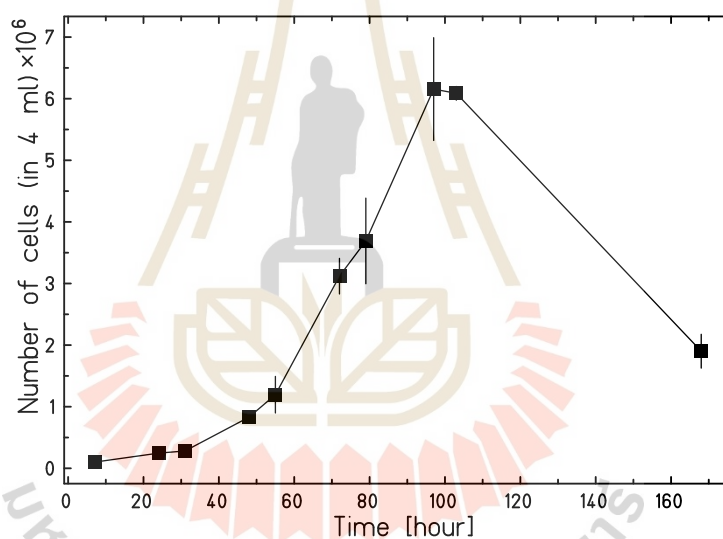
xrs-5 cell line is a mutant version of CHO-K1 cell line and sensitive to irradiation due to its incapacity of DSB repair which is causing cell death (Costa and Bryant, 1988; Taccioli et al., 1994; Weyrather et al., 1999; Hromčíková et al., 2006). This cell line is suitable for investigating the cell survival in low-dose region. Cells were maintained in standard monolayer culture inside T-25 flask filled with complete growth medium  $\alpha$ MEM (minimum essential medium, from Gibco) supplemented with 10% of FBS (Gibco) and penicillin/streptomycin. Cells were incubated in standard condition at 37°C with 5% CO<sub>2</sub> and passaged to the new culture flask every 4 days without additional medium change in between.

In order to observe the growth of xrs-5 cells, some basic cell tests including the cell growth, plating efficiency and cell proliferation in Matrigel have been performed by applying the CHO protocol that has been modified to fit the characteristic of xrs-5 cells.

#### 5.1.1 Cell growth curve

Cells were seeded in monolayer culture inside T-25 culture flask filled with 5 ml of culture medium with cell concentration of 100 000 cells/flask.

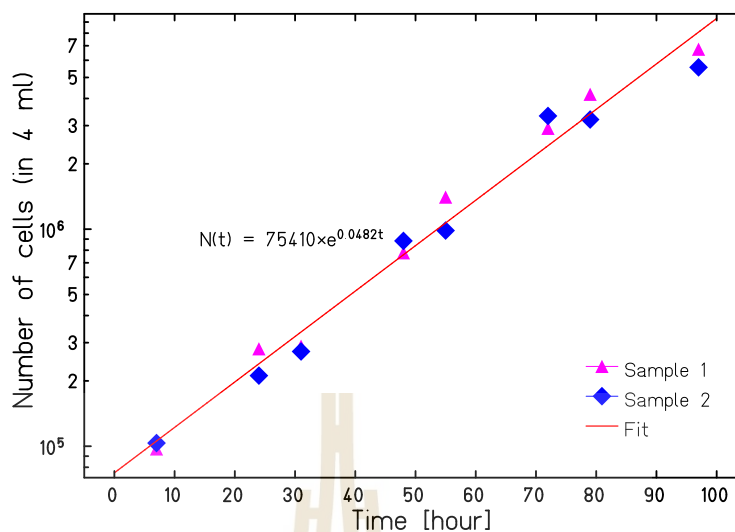
Twenty flasks were prepared and incubated at 37°C. Two flasks were trypsinized with 1 ml of trypsin-EDTA at fixed time (every morning and late afternoon) and cells were counted using Coulter counter machine (Profile B). To obtain the cell growth curve, number of cells were plotted against time of incubation. Figure 5.1 presents the cell growth curve of xrs-5 cells. The doubling time of xrs-5 cells was obtained by plotting the cell numbers from log phase in logarithmic scale. The data points were then fitted using exponential function (see equation 3.1) in order to obtain the cell growth rate which is represented by the slope as shown in figure 5.2. After the growth rate is obtained, the doubling time of xrs-5 cells was calculated using equation 3.2 and the doubling time was obtained to be 14.38 hours.



**Figure 5.1** Cell growth curve of xrs-5 cells. Number of cells are obtained from 4 ml of cell suspension and the error bars represent the standard deviation of two independent repetitions.

### 5.1.2 Plating efficiency

In order to measure the ability of xrs-5 cells to grow into a colony, plating efficiency test has been performed. Approximately 100 cells were seeded in monolayer culture inside T-25 culture flask filled with 5 ml culture medium, eight flasks were prepared. Since the doubling time of xrs-5 cells is 14 hours,



**Figure 5.2** The doubling time of xrs-5 cells. Number of cells were plotted in logarithmic scale and all data points were fitted using exponential function.

all cells were incubated for eight days to allow cells growing into colonies. After eight days, colonies were stained with methylene blue staining solution and colony consisting of at least 50 cells was scored as surviving cell. Table 5.1 presents the number of colonies after 8 days of incubation and the average number of colonies counted was 50 colonies. The plating efficiency of xrs-5 cells obtained was 0.5 with uncertainty of 13.9% which means 50% of cells will attach and proliferate into colonies after eight days of incubation.

### 5.1.3 Cell proliferation in Matrigel

The protocol for conducting cell proliferation of xrs-5 cells in Matrigel has been performed equivalent to CHO Matrigel protocol in section 3.1.1. Cells were cultured in Matrigel matrix inside 96-well plate and six wells filled with cells were prepared. Cells were recovered after 48 hours of incubation using dispase method (see section 3.1.1). The number of cells recovered was counted using Beckman Coulter counter machine (profile C). Table 5.2 presents the number of cells obtained after 48 hours of incubation. The cell numbers were consistent with low uncertainty meaning xrs-5 cells are well grown in 3D cell culture.



**Table 5.1** Number of colonies obtained after 8 days of incubation.

Samples	Number of colonies
1	49
2	50
3	41
4	41
5	61
6	52
7	49
8	57
Average	50 $\pm$ 13.9%

**Table 5.2** Number of xrs-5 cells in Matrigel setup inside 96-well plate after 48 hours of incubation. Cell numbers are counted in 1 ml of isoton solution.

Samples	Cell number/ml
1	125 550
2	120 550
3	123 550
4	119 600
5	124 550
6	118 100
Average	121 983 $\pm$ 2.45%

As previously mentioned in section 4.6.4, an attempt to achieve higher spatial resolution has been performed, however, there are some practical issues while working with 384-well plate due to the limitation of working area of 384-well plate. This includes for example issues with applying the Matrigel matrix to the wells and recovering the cells from the well plate. These practical issues might contribute in resulting the irregular samples and results (see table 4.3). To overcome those issues, another test has been made by using V-bottom 384-well PP plate to culture the cells (Kartini, 2021). In contrast to the flat-bottom plate, the PP well plate has a V-shape bottom area which is convenient for recovering the cells (cells are not attached to the corner of well). However,

the cells cultured inside well plate could not be observed under microscope due to the material of PP well plate which is not optically clear. Therefore, cell proliferation test in V-bottom 384-well PP plate has been performed using CHO cells.

CHO cells were cultured in Matrigel inside 384-well PP plate following to the protocol in appendix A.10. Table 5.3 shows the obtained cell numbers of CHO cells cultured in V-bottom 384-well PP plate after 48 hours of incubation. Cells were recovered using dispase method which has been modified to adapt the size of 384-well plate, the detailed protocol is presented in appendix A.9. Average cell number obtained from V-bottom 384-well plate was 69 850 cells/ml with uncertainty of 5.97%. This indicating the 384-well PP plate could be used to culture cells in Matrigel matrix.

**Table 5.3** Number of CHO cells in Matrigel setup inside V-bottom 384-well PP plate after 48 hours of incubation. Cell numbers are counted in 1 ml of isoton solution.

Sample	Cell number/ml
1	68 100
2	76 850
3	70 350
4	66 350
5	67 600
Average	69 850 $\pm$ 5.97%

Next, xrs-5 cells have been cultured in Matrigel inside 384-well PP plate and cell proliferation test has been performed as well. However in this test, new type of trypsin has been introduced for optimizing the cell recovery process (Kartini, 2021). As recommended by ATCC for recovery of xrs-5 cells, trypsin-EDTA containing of 0.25% Trypsin and 0.02% EDTA in Hank's Balanced Salt Solution (Sigma) has been used in cell recovery method (ATCC, 2021). Ten wells filled with different cell concentration have been prepared: five wells with 10 000 cells/well (C1) and another five wells with 15 000 cells/well (C2).

After 48 hours of incubation, cells were immediately recovered using dispase and trypsinized using the new trypsin. The results show samples with less

initial cell concentration (C1) yields more cells number of 62 540 cells/ml with uncertainty of 11.5% compared to samples with more initial cell concentration (see table 5.4). This concludes xrs-5 cells are able to grow in 384-well PP plate very well and the new trypsin is suitable for recovering xrs-5 cells. For Matrigel setup with 384-well PP plate, the 'standard' cell concentration (10 000 cells/well) will be used for in-vitro irradiation.

**Table 5.4** Number of xrs-5 cells recovered from Matrigel in 384-well PP plate following the change of trypsin. Number of cells were counted per 1 ml and the standard deviation of the cell counting is given by percentage uncertainty.

Sample	C1	C2
1	61 800	41 550
2	66 800	22 350
3	71 000	55 400
4	61 200	42 450
5	51 900	33 600
Average	62 540 $\pm$ 11.5%	39 070 $\pm$ 31.2%

## 5.2 Response of xrs-5 cells cultured in Matrigel to irradiation

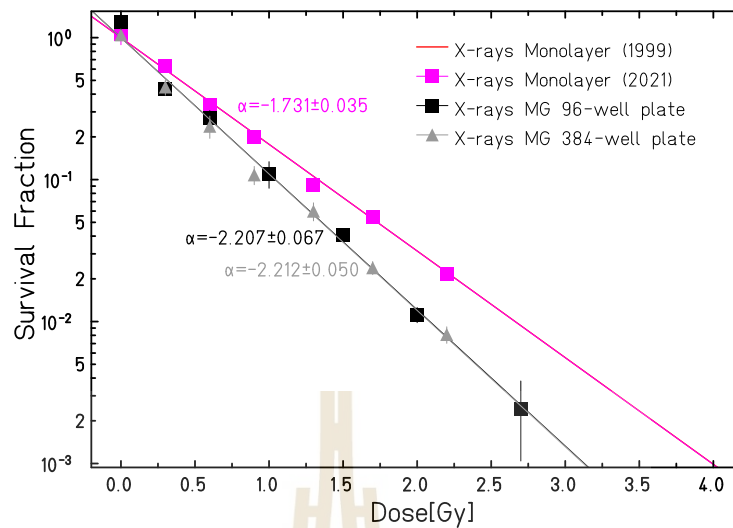
### 5.2.1 X-rays survival curve

To investigate the cells response to X-rays irradiation, xrs-5 cells have been cultured in three different setups. Approximately  $2 \times 10^5$  cells were seeded in standard monolayer inside T-25 flask, 20 000 cells were seeded in Matrigel inside 96-well plate, and 10 000 cells were seeded in Matrigel inside 384-well PP plate. For Matrigel setup, two samples each have been prepared in both types of well plate and incubated 48 hours before irradiation. Seven well plates including the control well plate have been prepared for irradiation. Wells filled with cells, surrounding wells, and space in between wells (where applicable) were completely filled with medium to achieve a homogeneous build-up. Meanwhile for monolayer setup, 15 flasks including control samples have been prepared and incubated 24 hours before irradiation.

Next, cells were irradiated by X-ray beams generated from Isovolt DS1 X-rays machine with a peak voltage of 250 kV at GSI. Samples in monolayer setup, 96-well plate, and 384-well plate were irradiated with a dose rate of 2.5 Gy/min, 2.6 Gy/min, and 3 Gy/min, respectively. The irradiation was performed from above (see section 4.1.1) with radiation dose ranging from 0–2.7 Gy. Two duplicate samples received the same doses for all setups. The dosimetry for X-rays irradiation has been performed using Farmer-type ionization chamber which is connected to the control system and turned off automatically once the dose has been delivered. The ionization chamber was placed under the well plate, exactly where cells were located. Post-irradiation, cells in Matrigel setup were recovered immediately using dispase protocol in section 3.1.1 and cells in monolayer setup were trypsinized using trypsin-EDTA (0.25% Trypsin - 0.02% EDTA). Recovered cells were immediately re-seeded into triplicates inside T-25 flask and incubated for 8 days. Colonies containing at least 50 cells were considered as survived cells. Next, the survival colonies were then plotted in semi-logarithmic scale and fitted to the exponential equation  $S(D) = \exp(-\alpha D)$ .

Figure 5.3 presents the survival curves of xrs-5 cells cultured in Matrigel setup and standard monolayer after irradiation with X-rays. All curves have been normalized to the measured cell plating efficiency. Black and gray line represent the survival curve of xrs-5 cells cultured in Matrigel setup inside 96-well plate and V-bottom 384-well plate, respectively. Meanwhile, purple line represent measured survival curve of xrs-5 cells cultured in standard monolayer. All curves demonstrate linear curves with consistent data points, especially 384-well plate setup. Both Matrigel survival curves are in good agreement and exhibit lower survival fractions compared to monolayer survival curve indicating cells in Matrigel are more sensitive to X-rays. Since the shape of all measured curves have straight linear slope line, only  $\alpha$  parameter could be extracted. List of  $\alpha$  parameter extracted from all measured X-rays survival curves is presented in table 5.5.

Figure 5.4 shows the comparison of measured survival curves of xrs-5 cells with survival curves from different research groups (Weyrather et al., 1999; Genet et al., 2012; Cartwright et al., 2015). Measured survival curve of xrs-5 cells in standard monolayer is compatible with reference curve (red line) from published literature (Weyrather et al., 1999). This indicates the survival curve of

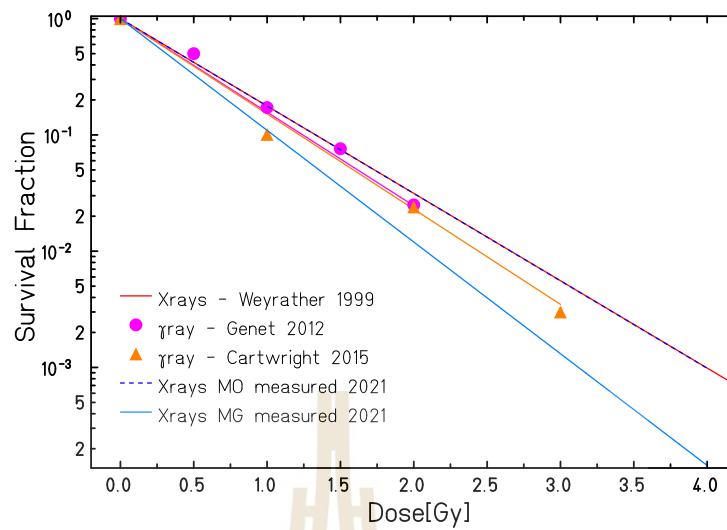


**Figure 5.3** Measured xrs-5 cell survival curves after irradiation with X-ray beams. Black and gray data points represent the average survival fractions of cells cultured in Matrigel inside 96-well PS plate and 384-well PP plate, respectively. Meanwhile, purple data points represent the average survival fractions of cells cultured in standard monolayer. Red line represents the reference survival curve in standard monolayer (Weyrather et al., 1999). All measured data points were fitted using exponential equation  $S(D) = \exp(-\alpha D)$ . Error bars represent the standard deviations of six or nine samples.

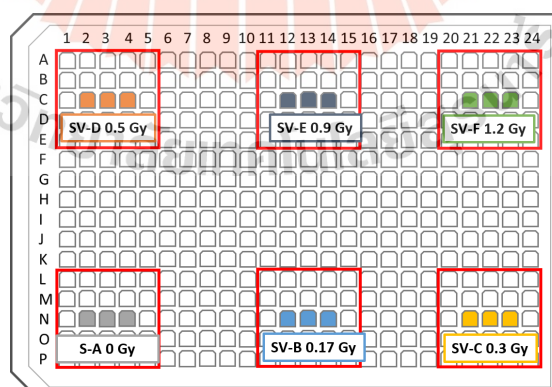
cells cultured in standard monolayer could be reproduced precisely. For xrs-5 cells cultured in Matrigel setup, the survival curve shows an increased of cell sensitivity in contrast to all existing curves.

### 5.2.2 Carbon ion survival curve

For carbon ion irradiation, xrs-5 cells were cultured in standard monolayer and Matrigel matrix inside 384-well plates. Approximately  $1.5 \times 10^5$  cells were cultured in standard monolayer inside T-25 flask and incubated 24 hours before irradiation. 14 flasks including control samples have been prepared. For Matrigel setup, 10 000 cells were cultured in Matrigel and incubated 48 hours before irradiation. Cells were seeded at different location in 384-well plate corresponding to each radiation doses as shown in figure 5.5. Two samples were



**Figure 5.4** Measured X-rays survival curves of xrs-5 cells in comparison with existing X-rays survival curves. Red line corresponds to the reference survival curve of xrs-5 cells in standard monolayer after irradiation with X-rays (Weyrather et al., 1999). Purple and orange lines correspond to the curves of xrs-5 cells in standard monolayer after irradiation with  $\gamma$ -rays from  $\text{Cs}^{137}$  (Genet et al., 2012; Cartwright et al., 2015). Blue and light blue lines correspond to measured survival curves of xrs-5 cells in standard monolayer and Matrigel setup with V-bottom 384-well plate after irradiation with X-rays.



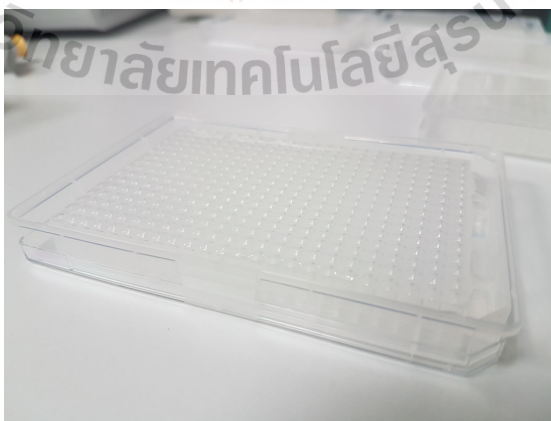
**Figure 5.5** Samples arrangement for survival experiment with carbon ions at MIT. Cells were cultured in Matrigel inside V-bottom 384-well plate.

**Table 5.5** List of xrs-5  $\alpha$  parameter extracted from X-rays survival curves in different culture setups.

Culture setup	$\alpha$ ( $\text{Gy}^{-1}$ )
Standard monolayer (2021)	$-1.731 \pm 0.035$
Matrigel 96-well PS plate	$-2.207 \pm 0.067$
Matrigel 384-well PP plate	$-2.212 \pm 0.050$

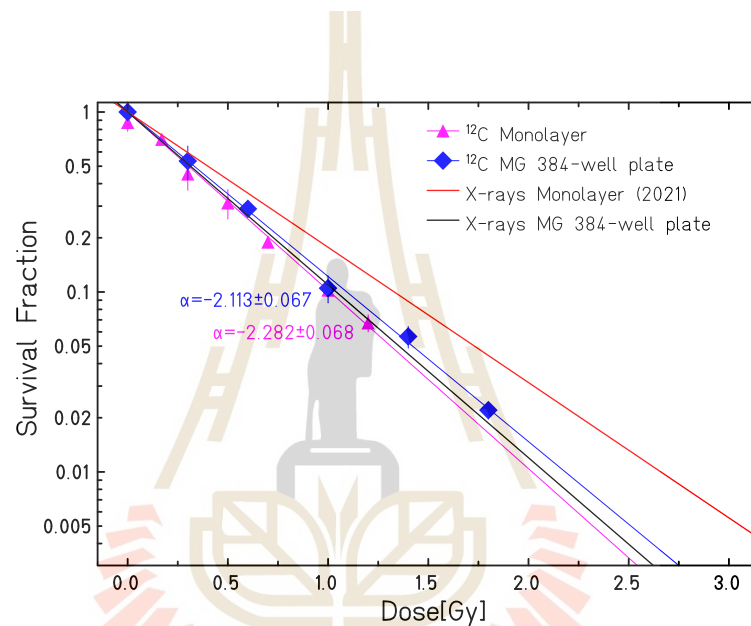
prepared for each dose. Only wells filled with cells were completely filled with medium and after that, the well plate was sealed with micro-well plate sealing film.

Next, cells were irradiated by monoenergetic carbon ions with energy of 110 MeV/u at MIT, Marburg. Well plate was placed in standing position and cells were irradiated from the bottom of well plate with radiation dose ranging from 0–1.2 Gy. The bottom part of 384-well plates have been covered with agarose to achieve a flat bottom. Two samples were irradiated at the same time. Post-irradiation, cells in Matrigel were recovered using Dispase method immediately (see appendix A.8). Recovered cells were reseeded in T-25 flask filled with 5 ml of medium, triplicate were prepared, and then cells were incubated for eight days. After eight days, colonies were stained and colonies fixation was done using methylene blue solution. Colonies consisting of at least 50 cells were counted as survivors.



**Figure 5.6** The bottom part of 384-well plate was covered by agarose layer.

Figure 5.7 presents measured survival curves of xrs-5 after irradiation with monoenergetic carbon ions in comparison to X-ray survival curves. All measured data points were normalized to the corresponding control samples. Matrigel (blue line) and monolayer (purple line) survival curves show linear survival curve, and both survival curves are comparable. Besides that, cells in Matrigel setup irradiated to X-rays exhibit the same sensitivity as cells irradiated to carbon ions (in both Matrigel and monolayer setups). Table 5.6 presents the  $\alpha$  parameters of xrs-5 cells extracted from measured carbon ion survival curves.



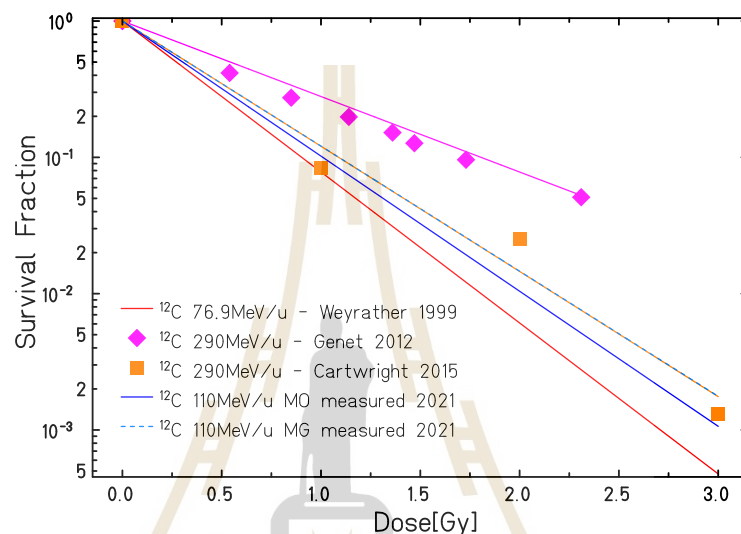
**Figure 5.7** Measured xrs-5 cell survival curves after irradiation with monoenergetic carbon ions in comparison to X-ray survival curves. Purple and blue data points represent the average survival fractions of cells cultured in standard monolayer and Matrigel, respectively, after irradiated using 110 MeV/u monoenergetic carbon ions. Red and black lines represent the X-rays survival curves of cells cultured in standard monolayer and Matrigel, respectively. All measured data points were fitted using exponential equation  $S(D) = \exp(-\alpha D)$ . Error bars represent the standard deviations of six sample.

Figure 5.8 shows the comparison between measured xrs-5 survival curves after irradiation with 110 MeV/u monoenergetic carbon ion with previously measured survival curves from different research groups (Weyrather et al., 1999; Genet et al., 2012; Cartwright et al., 2015). Both measured survival curves



**Table 5.6** List of xrs-5  $\alpha$  parameter extracted from carbon ion survival curves in different culture setups.

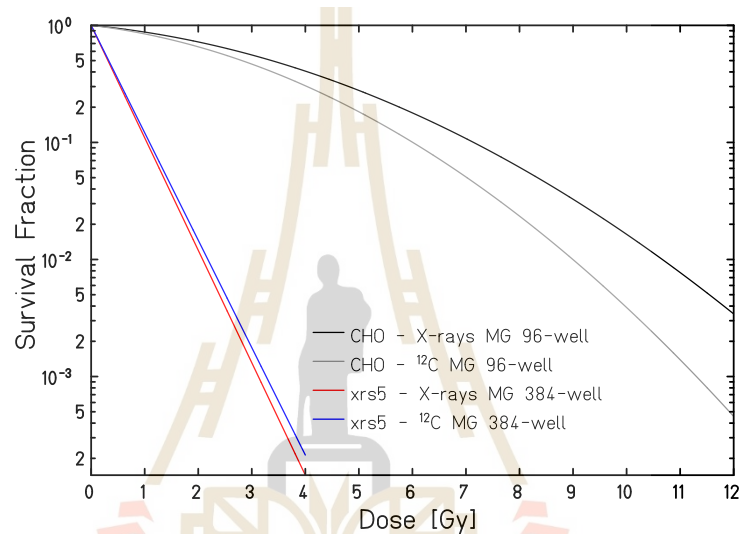
Culture setup	$\alpha$ ( $\text{Gy}^{-1}$ )
Standard monolayer	$-2.282 \pm 0.068$
Matrigel 384-well PP plate	$-2.113 \pm 0.067$



**Figure 5.8** Measured carbon ion survival curves of xrs-5 cells in comparison to existing carbon ion survival curves. Red line corresponds to the reference survival curve of xrs-5 cells in standard monolayer after irradiation with 76.9 MeV/u monoenergetic carbon ion (Weyrather et al., 1999). Purple and orange lines correspond to the curves of xrs-5 cells in standard monolayer after irradiation with 290 MeV/u carbon ion beam at SOBP (Genet et al., 2012; Cartwright et al., 2015). Blue and light blue lines correspond to measured survival curves of xrs-5 cells in standard monolayer and Matrigel setup with V-bottom 384-well plate after irradiation with 110 MeV/u monoenergetic carbon ion.

are compatible with curve from published literature (Cartwright et al., 2015) where xrs-5 cells were irradiated using 290 MeV/u carbon ion beams. According to measured X-ray and carbon ion survival curves of xrs-5 cells, all survival curves show a straight linear-shaped curve (figure 5.7). This is because xrs-5 cells are repair-deficient cells (Ku80-deficient) making cells incapable of repairing

the DNA damage after irradiation and most of the cells could not survive from irradiation (Weyrather et al., 1999; Genet et al., 2012; Cartwright et al., 2015). Figure 5.9 presents the comparison between CHO-K1 survival curves and xrs-5 survival curves. CHO cells have shouldered survival curve indicating cells are more resistant to irradiation. In contrast, xrs-5 cells which only lack one repair protein which is Ku80 compared to CHO cells, show sharp linear survival curves which are represented by red and blue lines.



**Figure 5.9** Survival curves of CHO-K1 and xrs-5 cells cultured in Matrigel after irradiation with carbon ions and X-rays. CHO and xrs-5 cells were irradiated using monoenergetic carbon ions with energy of 180 MeV/u and 110 MeV/u, respectively.

Since all measured xrs-5 survival curves are linear, the RBE value for xrs-5 cells could be obtained from the ratio of  $\alpha$  parameters extracted from X-rays and carbon ion survival curves as follows,

$$\text{RBE} = \frac{D_{\text{x-rays}}}{D_{\text{carbon ion}}} = \frac{\alpha_{\text{carbon ion}}}{\alpha_{\text{x-rays}}} \quad (5.1)$$

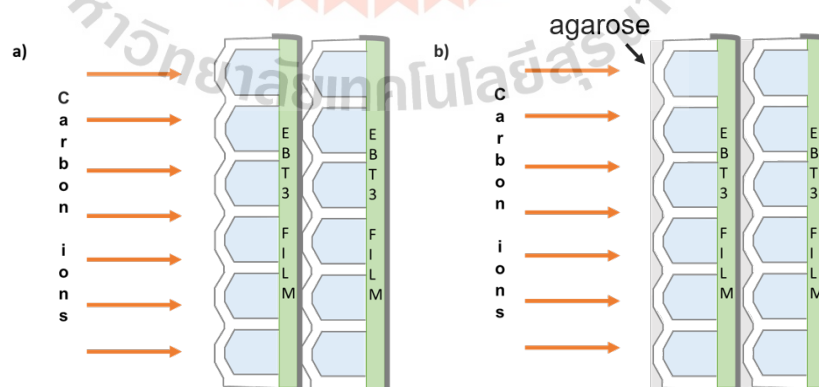
According to the equation above, RBE of xrs-5 cells in monolayer is 1.32 and RBE for xrs-5 cells in Matrigel is  $\sim 1$ . The low RBE of xrs-5 cells comes from the repair deficiency of xrs-5 cells, which implies that even single events

(secondary electrons) can cause lethal damage easily. This greatly enhances the radiosensitivity to X-rays and means that there is almost no room for improvement when using carbon ions. Because of this, xrs-5 cells will give the same response or sensitivity to any radiation regardless the type of radiation and there seems to be no LET dependence for xrs-5 cells.

### 5.3 Field homogeneity of V-bottom 384-well plate using Gafchromic EBT3 film

#### 5.3.1 Film dosimetry setup

In order to investigate the field homogeneity of V-bottom 384-well PP plate, Gafchromic EBT3 films placed after 384-well plates have been irradiated using active scanning carbon ions. Prior to irradiation, the bottom of 384-well plates have been coated with agarose layer to obtain a flat bottom surface (figure 5.6). Normal 384-well plates without agarose coating were also prepared for irradiation as for comparison. After that, all well plates were completely filled with water and sealed using micro-well plate sealing film. EBT3 film which has been cut into size of well plate were placed following one and two 384-well plates as shown in figure 5.10. Well plates and films were placed following a slab of PMMA with thickness of 4.5 cm thus films were exactly placed in the extended target and received a flat physical dose of 6.5 Gy.



**Figure 5.10** Film dosimetry setup using Gafchromic EBT3 film. EBT3 films were placed following one and two 384-well plate: a) without agarose layer and b) coated with agarose layer.

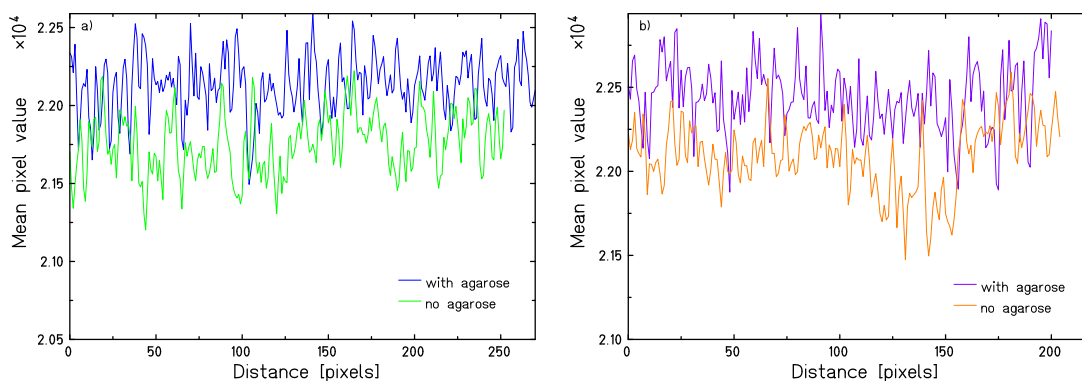
Twenty-four hours after irradiation, irradiated films were scanned using a flat-bed film scanner (Perfection V800 Photo, from Epson) in portrait orientation. In order to optimize the image scanning process, all image enhancement features were deactivated and the image resolution was adjusted to 200 dpi with color mode fixed to 48-bit rgb. The pixel values extracted from red color channel were analyzed using image processing program ImageJ (NIH). Film profiles were plotted in order to observe the field homogeneity and the possible artefact caused by different areal density of material in different part of the plate. The standard deviation of each EBT3 films were investigated as well.

### 5.3.2 Response of Gafchromic EBT3 film

Profiles of EBT3 films following 384-well plates with and without agarose layer are presented by figure 5.11. Film profiles following one well plate show a flatter profile, especially well plate coated with agarose layer where the profile is smoother and less fluctuated (figure 5.11a). In contrast, film profiles following two well plates either with and without agarose layer show fluctuating profile where some spikes are spotted along the profile as shown in (figure 5.11b). Standard deviation of ROI in irradiated EBT3 films were analyzed and summarized in table 5.7. Setup consisting of one 384-well plate coated with agarose layer (film 1) shows a standard deviation of 0.84% compared to other setups (film 2-4) with standard deviation values of 0.91%–0.97%.

**Table 5.7** Standard deviations of EBT3 films in different 384-well plate setups.

Films	Setups	Standard deviation	Stdev (%)
Film 1	1 well plate with agarose	186	0.84%
Film 2	1 well plate no agarose	209	0.93%
Film 3	2 well plate with agarose	199	0.91%
Film 4	2 well plate no agarose	215	0.97%



**Figure 5.11** Profiles of EBT3 films after irradiation with active scanning carbon ion beams. EBT3 films were placed following: a) one 384-well plate and b) two 384-well plates with and without agarose layer. Films' pixel values were plotted along x-axis.

## 5.4 Out-of-field radiobiological verification using 3D bio-phantom

### 5.4.1 Treatment planning system

All treatment plans have been computed using TRiP98 treatment planning system to calculate the dose distribution and simulate the cell surviving fraction. The target volume has been adjusted to the size of 384-well PP plate with lateral dimension of  $55 \times 46 \text{ mm}^2$  while the target depth was ranging from 50 mm to 90 mm in order to have an optimal coverage of samples. Treatment plan was optimized for a uniform RBE-weighted dose of 6.5 Gy in target region which is resulting the flat survival rate of  $\sim 10\%$  in the target region (figure 5.12d).

In order to compute the expected cell survival distribution, CHO Matrigel RBE table has been used to optimize the treatment plan and obtain the physical dose distribution (Kartini et al., 2020) because there is no complete RBE table for xrs-5 cells. However, according to supporting data and radiation qualities studied, the RBE of xrs-5 seems equal to 1 thus yields the same survival curve (Weyrather et al., 1999). After that, the xrs-5 alpha parameter is used to

compute the expected cell survival using the following equation,

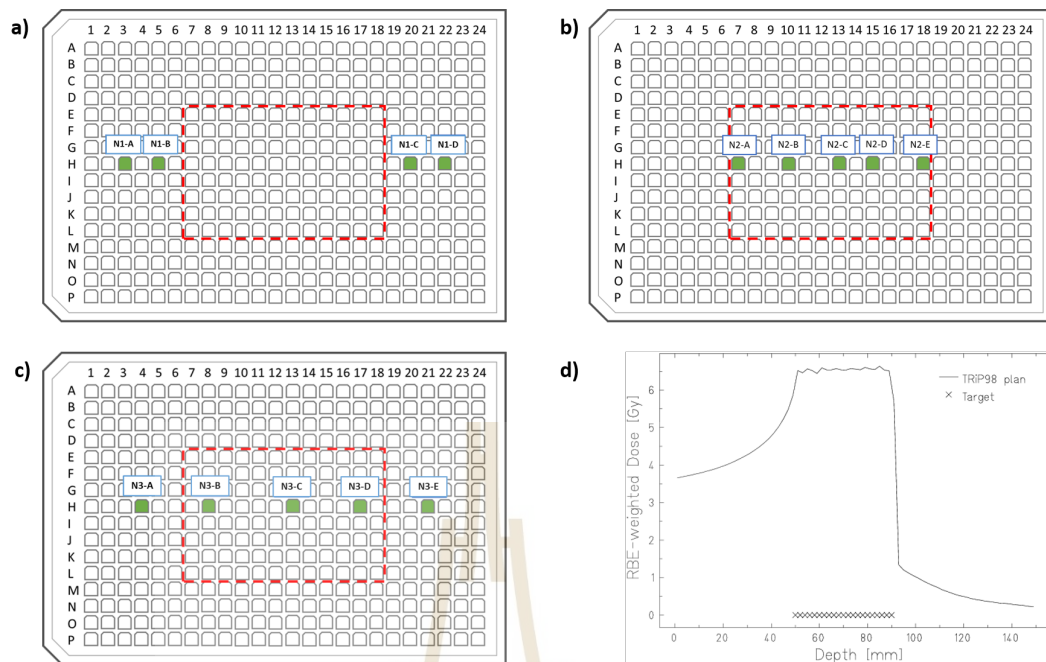
$$s(D) = \exp(-\alpha_{xrs-5} D_{phys}) \quad (5.2)$$

where  $S(D)$  is the cell survival at dose (D),  $\alpha_{xrs-5}$  is the  $\alpha$  parameter extracted from carbon ion Matrigel survival curve and  $D_{phys}$  is the physical dose obtained from TRiP98.

#### 5.4.2 In-vitro irradiation setup

To observe the cell survival in the out-of-field region, xrs-5 cells have been cultured in Matrigel inside 384-well PP plate 48 hours prior to irradiation. Cells were seeded at different wells location corresponding to each irradiation setup as shown in figure 5.12. For irradiation at extended target, cells were seeded in four wells outside the target field (figure 5.12a). Approximately 40 mm after extended target, cells have been seeded in five wells inside target field (figure 5.12b). In order to observe the lateral scattering at the end of fragmentation tail, cells have been seeded in five wells: two well outside target and three wells inside target field (figure 5.12c).

Wells filled with cells were completely filled with medium, and all well plates were sealed with micro-plate sealing film. In extended target, well plates were placed at a depth of 68.8 mm following a water-equivalent PMMA of 64.1 mm. For samples in fragmentation tail regions, well plates were placed at depth of 109.5 mm and 138.7 mm following PMMA with WET thickness of 104.8 mm and 134 mm, respectively (figure 5.12d). All well plates were irradiated in vertical position using active scanning carbon ion beam with energy range 156.34–211.54 MeV/u. Two well plates were irradiated at the same position shortly after each other. Post-irradiation, cells were immediately recovered using Dispase method and re-seeded into T-25 TCF filled with 5 ml of medium, triplicate were prepared for each sample. Next, cells were incubated for eight days in order to let cells grow into colonies. After that, colonies were stained using methylene blue staining solution and a colony consisting of at least 50 cells was scored as surviving cell.

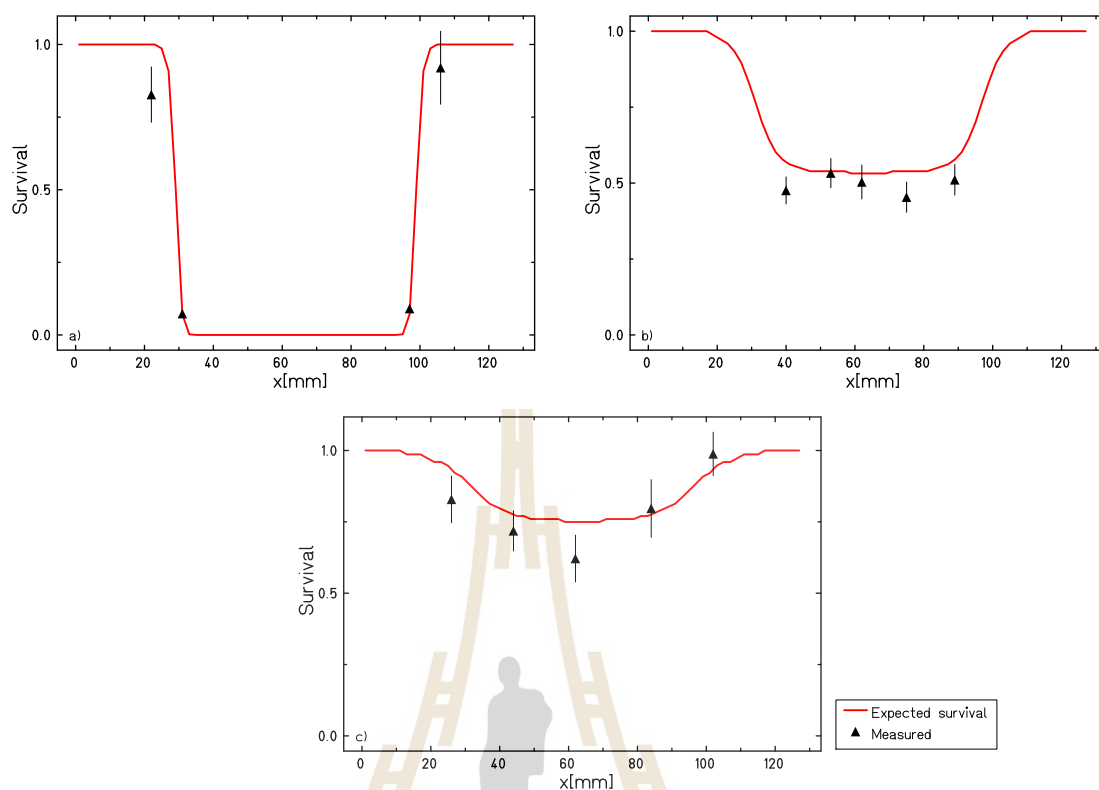


**Figure 5.12** Sample arrangement for out-of-field radiobiological irradiation at: a) extended target, b) fragmentation tail, and c) distal part of fragmentation tail. d) Depth dose profile computed using TRiP98 for out-of-field verification.

### 5.4.3 Out-of-field treatment plan verification

Radiobiological verification of treatment plan outside target field has been performed utilizing xrs-5 cells cultured in refined 3D bio-phantom in order to measure the cell survival at low-dose region. In the first experiment, measured cell survivals were lower than the expected survival due to the bad control samples and bad cell counting number (Kartini, 2021). Because of this, the experiment was repeated using new trypsin with higher trypsin concentration to recover the cells from Matrigel (see section 5.1.3) and the irradiation setup has been modified to obtain a better precision.

Figure 5.13 presents measured cell survival distributions in lateral cuts at three different depths obtained from the repeated experiment. All data points are normalized to the average control samples with survival fraction of  $S = 0.4864$ . Measured survival fractions show a good agreement with the expected survival, especially samples at the extended target where samples received different dose (figure 5.13a). For samples at 40 mm after SOBP (fragmentation tail) where



**Figure 5.13** Survival fraction of xrs-5 cells in lateral cuts at extended target (a) and fragmentation tail regions (b-c). Black data points and error bars are corresponding to the average survival fraction and the standard deviation of three or six samples. Red line is corresponding to the expected survival.

samples received similar dose, most of the data points show similar survival rate and the uncertainty bars of measured cell survival still cover the prediction. This means the measured survival fractions are in good agreement with the expected survival (figure 5.13b). In distal part of fragmentation tail, the survival fractions are compatible with the expected survival and the data points suggest the same profile shape than the prediction (figure 5.13c). In conclusion, there is no significant difference observed between measured cell survival with the expected survival indicating the cell survival prediction is accurate and work very well.



## 5.5 Summary

The adaptation of Matrigel-based phantom to xrs-5 cells has been investigated in this chapter. Cell proliferation in Matrigel inside V-bottom 384-well plate have been observed and cell number recovered using high trypsin concentration is sufficient for irradiation and colony forming assay. Dose response curves irradiated to X-rays and monoenergetic carbon ions in both standard monolayer and Matrigel setup have been obtained as well. All survival curves exhibit a straight linear curve and cells in Matrigel show the same sensitivity after irradiation with both X-rays and carbon ions. The field homogeneity of 384-well plate coated with agarose layer has been investigated and there is no significant artefact found in the film profile. Finally, out-of-field treatment plan verification using refined 3D bio-phantom has been performed and cell survivals measured at different depth show a good agreement with the expected survival. This implies 3D bio-phantom with V-bottom 384-well plate could be used as verification tool and the TRiP98 prediction is well-suited for predicting the cell survival in the normal tissue few cm from the target. Furthermore, for a specific cell line with straight LET-independent dose-response curves, an accurate biological deviation caused by mixed field in the tail would be almost impossible to detect.

## CHAPTER VI

### SUMMARY AND CONCLUSION

Radiotherapy utilizing charged particles has gained big interest due to its physical characteristics enabling the tumour to receive a maximum dose while sparing the normal tissue and OAR surrounding tumor. Before the radiotherapy treatment will be delivered to patients, treatment plan needs to be computed using treatment planning system in order to calculate the dose distribution and predict the cell survival in target and its surrounding tissue. However, it is still a challenge to conduct biological measurement to verify the treatment plan especially measure the cell survival at different area of treatment plan with high spatial resolution.

In this thesis, the investigation on a new verification setup consisting of cells cultured in Matrigel inside micro-well plate (3D bio-phantom) has been conducted. In Chapter 2, feasibility tests including cell proliferation and cell shape in Matrigel matrix inside 96-well plate have been conducted. According to cell number measured, Matrigel setup produced high cell number which is suitable for irradiation. The survival experiments have been performed and described in Chapter 3. Dose response curves of cells in Matrigel setup after irradiation with X-rays and carbon ions have been compared to the reference curves which cells were cultured in monolayer setup. Cells in Matrigel setup were observed to be more resistant at lower doses to irradiation compared to cells in monolayer setup. Next, Chapter 4 describes the radiobiological verification of rectangular treatment plan utilizing 3D bio-phantom. Cell survival at entrance channel, extended target regions and fragmentation tail have been analyzed and the obtained results present the measured cell survivals are in good agreement with the reference stack phantom. In addition, the field homogeneity of 96-well plate has been performed by irradiating EBT3 film following 96-well plate filled with water. There is no artefact and well plate pattern found in the film profile.

Adaptation to higher spatial resolution and radio-sensitive cell line have been conducted in Chapter 5. In order to solve the practical problems with flat-bottom 384-well plate, V-bottom 384-well PP plate has been chosen as

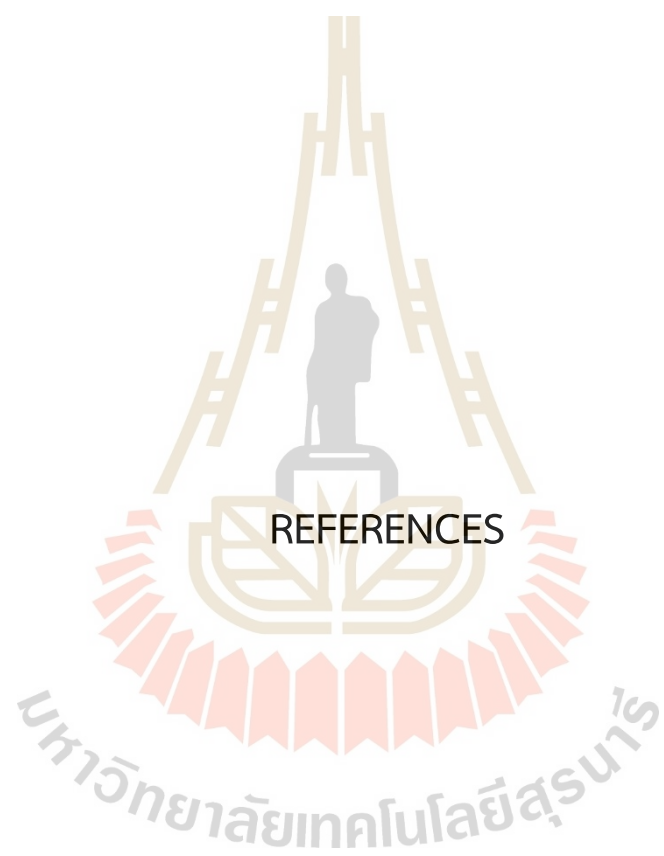
culture lab-ware. xrs-5 cells have been cultured in Matrigel matrix inside V-bottom 384-well plate and cell number recovered after 48 hours of incubation was sufficient for performing colony formation assay. Dose response curves of xrs-5 cells in Matrigel setup after irradiation with X-rays and carbon ions have been conducted and the measured survival curves have been compared to the standard monolayer curves. xrs-5 cells in Matrigel setup show the same sensitivity regardless the irradiation modalities. Due to the irregular bottom structure of 384-well plate, film dosimetry utilizing EBT3 film has been performed and the obtained results show well plate setup consisting of one 384-well plate coated with agarose layer yields a homogeneous field. Finally, the refined 3D bio-phantom consisting xrs-5 cells in Matrigel inside V-bottom 384-well plate has been used to verify the treatment plan outside the target volume. Measured cell survival in lateral cut at extended target and fragmentation tail show a good agreement with the expected survival.

To obtain more precise survival measurement, CHO 51D1 cells can be alternative option to investigate the survival fraction at fragmentation tail. CHO 51D1 cell line is CHO cells that lack of homologous recombination (HR) DNA repair (Hinz et al., 2006; Wilson et al., 2010). 51D1 cells have less sensitivity to radiation compared to xrs-5 cells (Genet et al., 2012; Cartwright et al., 2015). Thus, it has RBE effect but more sensitive than normal CHO cells which is suitable to investigate the cell survival at fragmentation tail where the survival fraction is close to 100%.

Furthermore, based on the agreement between Matrigel setup and TRiP98 prediction, it can be concluded that refined 3D bio-phantom works very well and is suitable to measure the survival fraction at area which is close to or few cm to the target region. It could also be used to verify treatment plans utilizing other ions beam such as protons. There is a possibility of using this system for performing biological measurements at low cell survival, for example at high doses where the linear-quadratic-linear model is better used or in FLASH condition. For the case of low cell survival, high cell number is required for colony forming assay which can be obtained by culturing the cells in Matrigel. The cell number in Matrigel culture could be still increased by increasing the cell-embedded layer thickness. Therefore, by embedding the cells in ECM, the environment becomes radiation chemically much closer to tissue

than a monolayer culture in growth medium. Beside that, this system has also been used to measure the oxygen consumption under irradiation which provides better insights about phenomenon occurring during irradiation inside tissue.





REFERENCES

## REFERENCES

- Ashland Advanced Materials (2016). EBT3 Specifications and user guide. [http://www.gafchromic.com/documents/EBT3\\_Specifications.pdf](http://www.gafchromic.com/documents/EBT3_Specifications.pdf). Accessed on 02-01-2019.
- ATCC (2021). xrs5 (ATCC CRL-2348). <https://www.atcc.org/products/crl-2348>. Accessed on 14-08-2020.
- Bethe, H. (1930). Zur Theorie des Durchgangs schneller Korpuskularstrahlen durch Materie. *Annalen der Physik*, 397(3), 325–400.
- Bloch, F. (1933a). Bremsvermögen von Atomen mit mehreren Elektronen. *Zeitschrift für Physik A Hadrons and Nuclei*, 81(5), 363–376.
- Bloch, F. (1933b). Zur Bremsung rasch bewegter Teilchen beim Durchgang durch Materie. *Annalen der Physik*, 408(3), 285–320.
- Buglewicz, D. J., Banks, A. B., Hirakawa, H., Fujimori, A., and Kato, T. A. (2019). Monoenergetic 290 MeV/n carbon-ion beam biological lethal dose distribution surrounding the Bragg peak. *Scientific Reports*, 9(1), 1–9.
- Cartwright, I. M., Bell, J. J., Maeda, J., Genet, M. D., Romero, A., Fujii, Y., Fujimori, A., Kitamuta, H., Kamada, T., Chen, D. J., and Kato, T. A. (2015). Effects of targeted phosphorylation site mutations in the DNA-PKcs phosphorylation domain on low and high LET radiation sensitivity. *Oncology Letters*, 9(4), 1621–1627.
- Chu, W., Ludewigt, B., and Renner, T. (1993). Instrumentation for treatment of cancer using proton and light-ion beams. *Review of Scientific Instruments*, 64(8), 2055–2122.
- Corning (2017a). Corning Matrigel Matrix Frequently Asked Questions. <https://www.corning.com/catalog/cls/documents/faqs/CLS-DL-CC-026.pdf>. Accessed on 08-04-2019.

- Corning (2017b). Matrigel Matrix 3D In Vitro Protocol. [https://www.corning.com/catalog/cls/documents/application-notes/Application\\_Note\\_CLS-DL-AN-414\\_Matrigel\\_Matrix\\_3D\\_In\\_Vitro\\_Protocol.pdf](https://www.corning.com/catalog/cls/documents/application-notes/Application_Note_CLS-DL-AN-414_Matrigel_Matrix_3D_In_Vitro_Protocol.pdf). Accessed on 31-10-2018.
- Costa, N. D. and Bryant, P. E. (1988). Repair of DNA single-strand and double-strand breaks in the Chinese hamster xrs 5 mutant cell line as determined by DNA unwinding. *Mutation Research/DNA Repair Reports*, 194(2), 93–99.
- Elsässer, T., Krämer, M., and Scholz, M. (2008). Accuracy of the local effect model for the prediction of biologic effects of carbon ion beams in vitro and in vivo. *International Journal of Radiation Oncology, Biology, Physics*, 71(3), 866–872.
- Elsässer, T. and Scholz, M. (2007). Cluster effects within the local effect model. *Radiation Research*, 167(3), 319–329.
- Elsässer, T., Weyrather, W. K., Friedrich, T., Durante, M., Iancu, G., Krämer, M., Kragl, G., Brons, S., Winter, M., Weber, K.-J., and Scholz, M. (2010). Quantification of the relative biological effectiveness for ion beam radiotherapy: direct experimental comparison of proton and carbon ion beams and a novel approach for treatment planning. *International Journal of Radiation Oncology, Biology, Physics*, 78(4), 1177–1183.
- Friedrich, T., Scholz, U., Elsässer, T., Durante, M., and Scholz, M. (2012). Calculation of the biological effects of ion beams based on the microscopic spatial damage distribution pattern. *International Journal of Radiation Biology*, 88(1-2), 103–107.
- Gemmel, A., Bert, C., Saito, N., Von Neubeck, C., Iancu, G., Kraft-Weyrather, W., Durante, M., and Rietzel, E. (2010). Development and performance evaluation of a dynamic phantom for biological dosimetry of moving targets. *Physics in Medicine and Biology*, 55(11), 2997.
- Gemmel, A., Hasch, B., Ellerbrock, M., Weyrather, W. K., and Krämer, M. (2008). Biological dose optimization with multiple ion fields. *Physics in Medicine and Biology*, 53, 6991–7012.

- Gemmel, A., Rietzel, E., Kraft, G., Durante, M., and Bert, C. (2011). Calculation and experimental verification of the RBE-weighted dose for scanned ion beams in the presence of target motion. *Physics in Medicine and Biology*, 56(23), 7337.
- Genet, S. C., Maeda, J., Fujisawa, H., Yurkon, C. R., Fujii, Y., Romero, A. M., Genik, P. C., Fujimori, A., Kitamura, H., and Kato, T. A. (2012). Comparison of cellular lethality in DNA repair-proficient or-deficient cell lines resulting from exposure to 70 MeV/n protons or 290 MeV/n carbon ions. *Oncology Reports*, 28(5), 1591–1596.
- Greiner Bio-One (2011). Customer Drawing 384 Well Microplate, PP, V-Bottom. <https://shop.gbo.com/en/thailand/products/bioscience/microplates/384-well-microplates/384-well-polypropylene-microplates/781281.html>. Accessed on 02-11-2020.
- Greiner Bio-One (2021). Customer Drawing 384 Well Microplate, PS, F-Bottom. <https://shop.gbo.com/en/thailand/products/bioscience/microplates/384-well-microplates/384-well-polystyrene-microplates-clear/781185.html>. Accessed on 23-05-2021.
- Haettner, E., Iwase, H., and Schardt, D. (2006). Experimental fragmentation studies with <sup>12</sup>C therapy beams. *Radiation Protection Dosimetry*, 122(1-4), 485–487.
- Hall, E. and Giaccia, A. (2012). *Radiobiology for the Radiologist*. Radiobiology for the Radiologist. Wolters Kluwer Health/Lippincott Williams & Wilkins.
- Highland, V. L. (1975). Some practical remarks on multiple scattering. *Nuclear Instruments and Methods*, 129(2), 497–499.
- Hinz, J. M., Tebbs, R. S., Wilson, P. F., Nham, P. B., Salazar, E. P., Nagasawa, H., Urbin, S. S., Bedford, J. S., and Thompson, L. H. (2006). Repression of mutagenesis by Rad51D-mediated homologous recombination. *Nucleic Acids Research*, 34(5), 1358–1368.
- Hromčíková, H., Kunderát, P., and Lokajíček, M. (2006). Detailed analysis of the response of different cell lines to carbon irradiation. *Radiation Protection Dosimetry*, 122(1-4), 121–123.



- ICRU (1993). *ICRU Report 51, Quantities and Units in Radiation Protection Dosimetry*. International Commission on Radiation Units.
- Kartini, Dea, A. (2018). *Imaging and radiobiological applications for ion beam therapy*. GET INvolved Internship and Training Project Report GI18-TH-001, Fair and GSI Darmstadt.
- Kartini, Dea, A. (2021). *Radiobiological verification of complex patient treatment plan using a pseudo-3D gel phantom*. GET INvolved Internship and Training Project Report GI-20215K-TH-PDE, Fair and GSI Darmstadt.
- Kartini, D. A., Sokol, O., Wiedemann, J., Tinganelli, W., Witt, M., Camazzola, G., Krämer, M., Talabnin, C., Kobdaj, C., and Fuss, M. C. (2020). Validation of a pseudo-3D phantom for radiobiological treatment plan verifications. *Physics in Medicine and Biology*, 65(22), 225039.
- Klein, C., Dokic, I., Mairani, A., Mein, S., Brons, S., Häring, P., Haberer, T., Jäkel, O., Zimmermann, A., Zenke, F., Blaukat, A., Debus, J., and Abdollahi, A. (2017). Overcoming hypoxia-induced tumor radioresistance in non-small cell lung cancer by targeting DNA-dependent protein kinase in combination with carbon ion irradiation. *Radiation Oncology*, 12(1), 208.
- Krämer, M. (2001). Treatment planning for heavy-ion radiotherapy: biological optimization of multiple beam ports. *Journal of Radiation Research*, 42(1), 39–46.
- Krämer, M. and Durante, M. (2010). Ion beam transport calculations and treatment plans in particle therapy. *European Physics Journal D*, 60, 195.
- Krämer, M., Jäkel, O., Haberer, T., Kraft, G., Schardt, D., and Weber, U. (2000). Treatment planning for heavy-ion radiotherapy: physical beam model and dose optimization. *Physics in Medicine and Biology*, 45(11), 3299.
- Krämer, M. and Scholz, M. (2000). Treatment planning for heavy-ion radiotherapy: calculation and optimization of biologically effective dose. *Physics in Medicine and Biology*, 45(11), 3319.

- Krämer, M., Scifoni, E., Schmitz, F., Sokol, O., and Durante, M. (2014). Overview of recent advances in treatment planning for ion beam radiotherapy: ion beam transport calculations and treatment plans in particle therapy. *European Physics Journal D*, 68, 306.
- Krämer, M., Wang, J., and Weyrather, W. (2003). Biological dosimetry of complex ion radiation fields. *Physics in Medicine and Biology*, 48(14), 2063.
- Lewis, D., Micke, A., Yu, X., and Chan, M. F. (2012). An efficient protocol for radiochromic film dosimetry combining calibration and measurement in a single scan. *Medical Physics*, 39(10), 6339–6350.
- Marburger Ionenstrahl-Therapiezentrum (2021). Technische Details. <https://www.mit-marburg.de/fuer-forscher/technische-details.html>. Accessed on 18-09-2021.
- Martišiková, M. and Jäkel, O. (2010). Dosimetric properties of gafchromic® EBT films in monoenergetic medical ion beams. *Physics in Medicine and Biology*, 55(13), 3741.
- McKeown, S. R. (2014). Defining normoxia, physoxia and hypoxia in tumours—implications for treatment response. *The British Journal of Radiology*, 87(1035), 20130676.
- Mein, S., Dokic, I., Klein, C., Tessonier, T., Böhlen, T. T., Magro, G., Bauer, J., Ferrari, A., Parodi, K., Haberer, T., Debus, J., Abdollahi, A., and Mairani, A. (2019). Biophysical modeling and experimental validation of relative biological effectiveness (RBE) for 4 He ion beam therapy. *Radiation Oncology*, 14(1), 123.
- Molière, G. (1948). Theorie der Streuung schneller geladener Teilchen II Mehrfach- und Vielfachstreuung. *Zeitschrift für Naturforschung A*, 3(2), 78–97.
- Pardee, A. B. and Stein, G. S. (2011). *The biology and treatment of cancer: Understanding cancer*. John Wiley & Sons.
- Patel, D., Bronk, L., Guan, F., Peeler, C. R., Brons, S., Dokic, I., Abdollahi, A., Rittmüller, C., Jäkel, O., Grosshans, D., Mohan, R., and Titt, U. (2017). Optimization of Monte Carlo particle transport parameters and validation of a

novel high throughput experimental setup to measure the biological effects of particle beams. *Medical Physics*, 44(11), 6061–6073.

Peroni, G. (2018). *Survival curve study for 3D cell culture and TRiP98 simulation of the experimental setup*. GSI Summer School Program Report, GSI Darmstadt.

Schardt, D., Elsässer, T., and Schulz-Ertner, D. (2010). Heavy-ion tumor therapy: Physical and radiobiological benefits. *Reviews of Modern Physics*, 82(1), 383.

Scheeler, U., Haberer, T., Krantz, C., Sievers, S., Strohmeier, M., Cee, R., Feldmeier, E., Galonska, M., Höppner, K., Mosthaf, J., Scheloske, S., Schömers, C., Winkelmann, T., and Peters, A. (2016). Recommissioning of the Marburg Ion-Beam Therapy Centre (MIT) Accelerator Facility. In *Proc. 7th Intl. Particle Accelerator Conf.(IPAC'16)*, pages 1908–1910.

Scholz, M., Friedrich, T., Magrin, G., Colautti, P., Ristić-Fira, A., and Petrović, I. (2020). Characterizing radiation effectiveness in ion beam therapy part I: Introduction and biophysical modeling of RBE using the LEMIV. *Frontiers in Physics*, 8, 272.

Scholz, M., Kellerer, A., Kraft-Weyrather, W., and Kraft, G. (1997). Computation of cell survival in heavy ion beams for therapy. *Radiation and Environmental Biophysics*, 36(1), 59–66.

Sokol, O., Krämer, M., Hild, S., Durante, M., and Scifoni, E. (2019). Kill painting of hypoxic tumors with multiple ion beams. *Physics in Medicine and Biology*, 64, 045008.

Sokol, O., Scifoni, E., Tinganelli, W., Kraft-Weyrather, W., Wiedemann, J., Maier, A., Boscolo, D., Friedrich, T., Brons, S., Durante, M., and Krämer, M. (2017). Oxygen beams for therapy: advanced biological treatment planning and experimental verification. *Physics in Medicine and Biology*, 62, 7798–7813.

Taccioli, G. E., Gottlieb, T. M., Blunt, T., Priestley, A., Demengeot, J., Mizuta, R., Lehmann, A. R., Alt, F. W., Jackson, S. P., and Jeggo, P. A. (1994). Ku80: product of the XRCC5 gene and its role in DNA repair and V (D) J recombination. *Science*, 265(5177), 1442–1445.

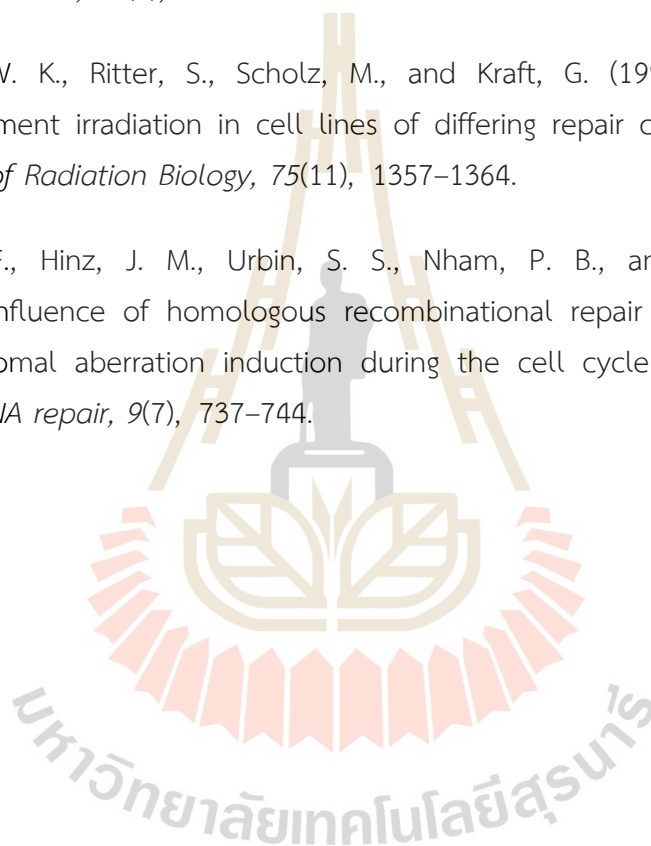
Tavernier, S. (2010). *Experimental techniques in nuclear and particle physics*. Springer Science & Business Media.

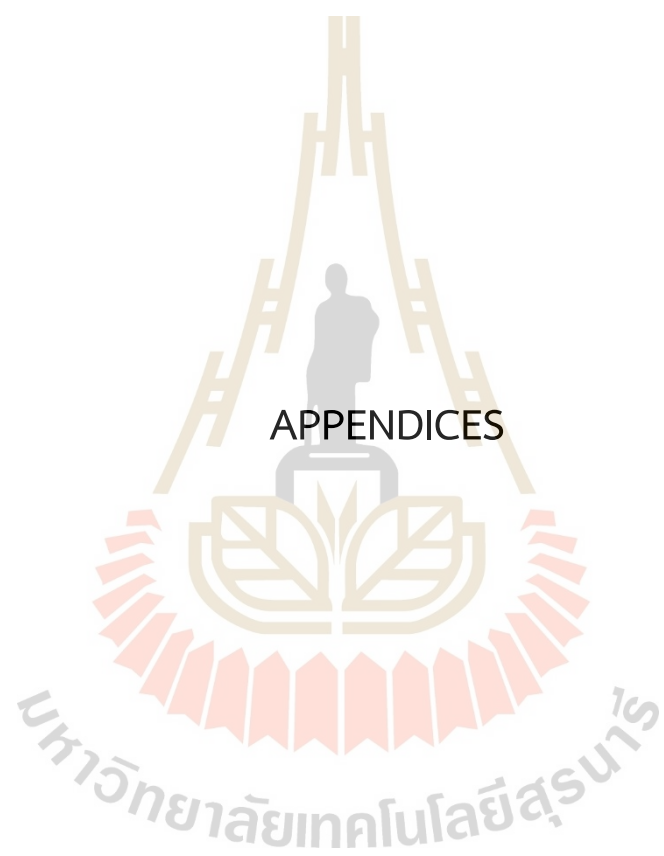
TPP Techno Plastic Product (2020). Measurements TPP Tissue Culture Test Plate. [https://www.tpp.ch/page/produkte/09\\_zellkultur\\_testplatte.php](https://www.tpp.ch/page/produkte/09_zellkultur_testplatte.php). Accessed on 08-06-2021.

Weber, U. and Kraft, G. (2009). Comparison of carbon ions versus protons. *The Cancer Journal*, 15(4), 325–332.

Weyrather, W. K., Ritter, S., Scholz, M., and Kraft, G. (1999). RBE for carbon track-segment irradiation in cell lines of differing repair capacity. *International Journal of Radiation Biology*, 75(11), 1357–1364.

Wilson, P. F., Hinz, J. M., Urbin, S. S., Nham, P. B., and Thompson, L. H. (2010). Influence of homologous recombinational repair on cell survival and chromosomal aberration induction during the cell cycle in  $\gamma$ -irradiated CHO cells. *DNA repair*, 9(7), 737–744.





APPENDICES

## APPENDIX A

### CELL CULTURES PROTOCOL

#### A.1 Matrigel dilution

To obtain the estimated concentration of Matrigel, it can be done by diluting Matrigel matrix with ice-cold medium using the following ratio calculation: If we have 600  $\mu\text{l}$  of undiluted Matrigel with a concentration of 11.7 mg/ml and we need 5 mg/ml diluted Matrigel.

$$V_p = V_{MG,ND} \times C_0$$
$$V_p = 0.6 \text{ ml} \times 11.7 \text{ mg/ml} = 7.02 \text{ mg}$$

The new concentration is 5 mg/ml, so,

$$V_p = V_{MG,D} \times C_1$$
$$7.02 \text{ mg} = V_{MG,D} \times 5 \text{ mg/ml}$$
$$V_{MG,D} = \frac{7.02 \text{ mg}}{5 \text{ mg/ml}} = 1.404 \text{ ml}$$

The volume of diluted Matrigel is 1.404 ml, so the required volume of medium will be

$$V_{MG,D} = V_{MG,ND} + V_M$$
$$V_M = 1.404 \text{ ml} - 0.6 \text{ ml} = 0.804 \text{ ml}$$

#### A.2 Matrigel cell seeding protocol in 96-well plate

1. Thaw the Matrigel on ice in the 4°C fridge overnight.
2. Dilute the Matrigel with ice-cold medium to a concentration of 5 mg/ml while keeping all the ingredients and tools on ice.
3. Pre-coating: put 33.4  $\mu\text{l}$  of diluted Matrigel, spread evenly in the well of 96-well plate. Incubate for 30 - 45 minutes.

4. Cell suspension preparation: trypsinite the cells, centrifuge them for 5 minutes at 300g and 21°C. Adjust the density to  $4 \times 10^6$  cell/ml.
5. Cell seeding: mix 5  $\mu\text{l}$  of cell solution with 45  $\mu\text{l}$  of diluted Matrigel so the final concentration of cells seeded is  $2 \times 10^4$  cell/well. Mix them very well and then put them on top the first Matrigel layer. Incubate for 30 - 45 minutes.
6. Add 16.6  $\mu\text{l}$  of diluted Matrigel. Incubate for another 30 - 45 minutes.
7. Gently add 83.3  $\mu\text{l}$  of medium. Incubate the cells for 48 hours.

### A.3 Matrigel cell recovering protocol in 96-well plate - Dispase protocol

1. Defrost the Dispase solution.
2. Remove the medium from the well without damaging the Matrigel matrix.
3. Prepare the Dispase: per each  $\text{cm}^2$  of the well surface 10 units are needed. For 96-well plate, the surface area is  $0.32 \text{ cm}^2$ , then
 
$$0.32 \text{ cm}^2 \times 10 \text{ U} = 3.2 \text{ U}$$

$$V_{\text{bottle}} = 100 \text{ ml} \approx 5000 \text{ U}$$

$$100 \text{ ml} : 5000 \text{ U} = V : 3.2 \text{ U}$$

$$V = 0.064 \text{ ml} = 64 \mu\text{l}$$
4. Add 64  $\mu\text{l}$  of Dispase to each well then incubate the plate for 1 - 2 hours until the gel is dissolved.
5. Pipette up and down to mix the Matrigel and collect everything in to micro-tubes. Wash the remaining cell in the well with 200  $\mu\text{l}$  of medium and put into micro-tubes.(Wash the well multiple times if necessary).
6. Add medium until the cell suspension reach 1 ml and then centrifuge them (5 minutes at 2500 rpm)
7. Remove the leftover medium and gel, add 300  $\mu\text{l}$  of trypsin and mix it well. Incubate for 3 minutes to get rid of the cell clumps. Add 900  $\mu\text{l}$  of medium to stop the trypsin and mix well.

8. Take 200  $\mu\text{l}$  of cell solution to isotone cup filled with 10 ml of isotone solution then count the cells using profile C.

#### A.4 Matrigel cell recovering protocol in 96-well plate - Cooling protocol

1. Put the 96-well plate inside 4°C fridge for one hour.
2. Pipette up all the matrigel layer. Add some medium to take out all the cell/matrigel inside the well.
3. Put the cell solution into micro-tubes and add more medium until all solution reach 1 ml. Mix well.
4. Take 200  $\mu\text{l}$  of cell solution and put in 10 ml of isotone then count the cells using profile C. Reseed them into T-25 TCF (4.2 ml of medium and 800  $\mu\text{l}$  of cell solution).

#### A.5 Matrigel cell recovering protocol in 96-well plate - Centrifuge protocol

1. Take out the 96 well-plate from the incubator.
2. Pipette up all the matrigel layer. Add 200  $\mu\text{l}$  of medium to wash and take out all the cell and matrigel inside the well. Wash the well multiple times if necessary.
3. Put the cell solution into micro-tubes and add more medium until all solution reach 1 ml.
4. Centrifuge the cell solution at 600g for 5 minutes.
5. Take 200  $\mu\text{l}$  of cell solution and put in 10 ml of isotone then count the cells using profile C. Reseed them into T-25 TCF (4.2 ml of medium and 800  $\mu\text{l}$  of cell solution).



## A.6 Matrigel cell recovering protocol in 96-well plate - Cooling and centrifuge protocol

1. Put the 96-well plate in the 4°C fridge for 1 - 2 hours.
2. Mix the Matrigel very well by pipetting up and down. Collect everything into micro-tubes and wash the left over with medium.
3. Add medium into micro-tubes until all solution reach 1 ml. Centrifuge for 5 minutes at 2500 rpm.
4. Remove the medium and add 300  $\mu\text{l}$  of trypsin. Incubate for 3 minutes to get rid of the cell clumps. Add 900  $\mu\text{l}$  of medium to stop the trypsin and mix well.
5. Shortly vortex the micro-tubes so that the medium will better penetrate into the cell pellet.
6. Take 200  $\mu\text{l}$  of cell solution to isotone cup filled with 10 ml of isotone solution then count the cells using profile C.

## A.7 Matrigel cell seeding protocol in 384-well plate

1. Thaw the Matrigel on ice in the 4°C fridge overnight.
2. Dilute the Matrigel with ice-cold medium to 5 mg/ml while keeping all the ingredients and tools on ice.
3. Pre-coating: put 11.49  $\mu\text{l}$  of diluted Matrigel, spread evenly in the well of 384-well plate. Incubate for 30 - 45 minutes.
4. Cell suspension preparation: trypsinite the cells, centrifuge them for 5 minutes at 300g and 21°C. Adjust the density to  $4 \times 10^6$  cells/ml.
5. Cell seeding: mix 2.5  $\mu\text{l}$  of cell solution with 22.5  $\mu\text{l}$  of diluted Matrigel. Mix them very well and then put them on top the first Matrigel layer. Incubate for 30 - 45 minutes.
6. Add 5.75  $\mu\text{l}$  of diluted Matrigel. Incubate for another 30 - 45 minutes.

7. Gently add 28.74  $\mu\text{l}$  of medium. Incubate the cells for 48 hours.

#### A.8 Matrigel cell recovering protocol in 384-well plate

1. Defrost the Dispase solution.
2. Remove the medium from the well without damaging the Matrigel matrix.
3. Add 22  $\mu\text{l}$  of Dispase to each well then incubate the plate for 1 - 2 hours until the gel is dissolved.
4. Pipette up and down to mix the Matrigel and collect everything in to micro-tubes. Wash the remaining cell in the well with 200  $\mu\text{l}$  of medium and put into micro-tubes.(Wash the well multiple times if necessary)
5. Add medium until the cell suspension reach 1 ml and then centrifugate them (5 minutes at 2500 rpm)
6. Remove the leftover medium and gel, add 300  $\mu\text{l}$  of trypsin and mix it well. Incubate for 3 minutes to get rid of the cell clumps. Add 900  $\mu\text{l}$  of medium to stop the trypsin and mix well.
7. Take 200  $\mu\text{l}$  of cell solution to isotone cup filled with 10 ml of isotone solution then count the cells using profile C.

#### A.9 Matrigel cell seeding protocol in V-bottom 384-well PP plate

1. Thaw the Matrigel on ice in the 4°C fridge overnight.
2. Dilute the Matrigel with ice-cold culture medium to concentration of 5 mg/ml while keeping all the ingredients and tools on ice.
3. Pre-coating: put 30  $\mu\text{l}$  of diluted Matrigel, spread evenly in the well of 384-well plate. Incubate for one hour or until gel become dense.
4. Cell suspension preparation: trypsinite the cells, centrifuge them for 5 minutes at 300g and 21°C. Adjust the density to  $4 \times 10^6$  cells/ml.

5. Cell seeding: mix  $2.5 \mu\text{l}$  of cell solution with  $22.5 \mu\text{l}$  of diluted Matrigel. Mix them very well and then put them on top the first Matrigel layer. Incubate for one hour.
6. Add  $10 \mu\text{l}$  of diluted Matrigel. Incubate for another one hour.
7. Gently add  $28.74 \mu\text{l}$  of medium and finally incubate the cells for 48 hours before irradiation.

#### A.10 Matrigel cell recovery protocol in V-bottom 384-well PP plate

1. Defrost the Dispase solution.
2. Prepare the Dispase: per each  $\text{cm}^2$  of the well surface 10 units are needed. For 384-well plate, the surface area is  $0.11 \text{ cm}^2$ , then
 
$$0.11 \text{ cm}^2 \times 10 \text{ U} = 1.1 \text{ U}$$

$$V_{\text{bottle}} = 100 \text{ ml} \approx 5000 \text{ U}$$

$$100 \text{ ml} : 5000 \text{ U} = V : 1.1 \text{ U}$$

$$V = 0.022 \text{ ml} = 22 \mu\text{l}$$
3. Remove the medium from the well without damaging the Matrigel matrix.
4. Add  $22 \mu\text{l}$  of Dispase to each well then incubate the plate for 1 - 2 hours until the gel is dissolved.
5. Pipette up and down to mix the Matrigel and collect everything in to micro-tubes. Wash the remaining cell in the well with  $200 \mu\text{l}$  of medium and put into micro-tubes.(Wash the well multiple times if necessary)
6. Add medium until the cell suspension reach 1 ml and then centrifuge the cell suspension for 5 minutes with 2500 rpm at  $4^\circ\text{C}$ .
7. Remove the leftover medium and gel, only cell pellet remained. Add  $300 \mu\text{l}$  of trypsin, mix it very well and then incubate for 3 minutes to get rid of the cell clumps.
8. Add  $900 \mu\text{l}$  of medium to stop the trypsin and mix cell suspension very well.

9. Take 200  $\mu\text{l}$  of cell solution to isotone cup filled with 10 ml of isotone solution then count the cells using profile C.

#### A.11 Monolayer cell culture protocol in 96-well plate - Cell seeding

1. Take out all medium from TCF and add 3 ml of PBS then remove.
2. Add 1 ml of trypsin then incubate the cells for 5 minutes.
3. Add 3 ml of medium to stop the trypsin and take out all cell suspension to the tube.
4. Take 1 ml of cell suspension and count the cells number (Profile B).
5. Seed 11 000 cells into each well.
6. Add 250  $\mu\text{l}$  of medium and incubate the cells for 24 hours.

#### A.12 Monolayer cell culture protocol in 96-well plate - Cell recovering

1. Take out all medium from well and add 50  $\mu\text{l}$  of PBS then remove.
2. Add 50  $\mu\text{l}$  of trypsin then incubate the cells for 5 minutes.
3. Add 150  $\mu\text{l}$  of medium to stop the trypsin and take out all cell solution to the tube.
4. Add 1 ml of medium to the tube (in total we have 1.2 ml).
5. Take out 200  $\mu\text{l}$  of cell suspension to isotone cup filled with 10 ml of isotone solution for counting (Profile C).

### **A.13 Monolayer cell culture protocol in stack phantom - Cell seeding**

1. Place the polystyrene slides in the square bio-assay dishes.
2. Add 0.5 ml of cell suspension containing  $5 \times 10^4$  cells at the center of each slide (central plating).
3. Incubate the dishes filled with slides for 2-4 hours in order to let the cells attach to the slides.
4. Fill in the the dishes with medium until all slides were covered.
5. Put back the dishes into incubator for 24 hours.
6. After 24 hours or right before the irradiation, put all slides in phantom box and fill up the phantom box with medium.

### **A.14 Monolayer cell culture protocol in stack phantom - Cell recovering**

1. Take out all slides from the phantom box.
2. Rinse the surface of slides with 1 ml of PBS Dulbecco.
3. Add 1 ml of trypsin and incubate for 4-5 minutes.
4. Collect the cell suspension immediately into a tube filled with 4 ml of medium. Mix the cell suspension very well to avoid the cell clumping.
5. Take out 1 ml of cell suspension to isotone cup filled with 9 ml of isotone solution for counting (Profile B).

### **A.15 Monolayer cell culture protocol in T-25 TCF - Cell seeding**

1. Take out all medium from TCF and add 3 ml of PBS then remove.
2. Add 1 ml of trypsin then incubate the cells for 5 minutes.

3. Add 3 ml of medium to stop the trypsin and take out all cell suspension to the tube.
4. Take 1 ml of cell suspension and count the cells number (Profile B).
5. Prepare T-25 flasks and fill all flasks with 5 ml of medium.
6. Seed  $2 \times 10^5$  cells into each flask and incubate the cells for 24 hours.

#### **A.16 Monolayer cell culture protocol in T-25 TCF - Cell recovering**

1. Take out all medium from flasks and add 3 ml of PBS then remove.
2. Add 1 ml of trypsin then incubate the cells for 5 minutes.
3. Add 3 ml of medium to stop the trypsin and take out all cell suspension to the tube.
4. Take out 1 ml of cell suspension to isotone cup filled with 9 ml of isotone solution for counting (Profile B).

## APPENDIX B

### TRIP98 TREATMENT PLANS CODE

#### B.1 96-well plate plan

```
time / on
scancap / offh2o(2.890) rifi(3) bolus(0.0) minparticles(15000) path(uw2) xmax(120)
ymax(120) scannerxdistance(6521.9) scannerydistance(7223.5)
hlut "19990211.hlut" / read

sis * / delete
sis "/u/osokol/MIT/SIS/SIS-Marburg_12C.sis" / read

ddd * / delete
ddd "/d/bio/bio/TRiP98BEAM/1308/DATA/12C/RF3MM/12C*.ddd" / read
spc * / delete
spc "/d/bio/bio/TRiP98BEAM/1308/DATA/12C/RF3MM/12C*.spc" / read
dedx * / delete
dedx "/u/kraemer/TRiP98DATA/DATA/DEDX/201006xx.dedx" / read

makegeometry 96wp / shape(box(60,40,40)) ctdim(64,43,75) ctsteps(2,2,2)
cteqv(1) centre(64,43,70)
ct "96wp000" / read
voi "96wp000" / read

rbe "/u/mfuss/MIT3DBIO/CHO2019Matrigel.rbe" / read
rbe target / alias(cho19mg)
rbe residual / alias(cho19mg)

field 1 / new proj(12C) raster(3,3) zstep(3) fwhm(5) targ(64,43,70) dose-
ext(1.8) contourent(0.7) couch(-180.0)
```

```
plan / dose(6.5) targettissue(cho19mg) residualtissue(cho19mg)
opt / bio field(*) dosealg(msdb) optalg(gr) ctbased iter(500) bioalg(ld) eps(1e-3)
```

\*Output the generated particle numbers for the raster scanner:

```
field 1 / write file(C_bioplan-wellplate.rst) reverseorder
*field 1 / bev(*) file(C_bioplan-wellplate.bev.gd) alg(msdb)
```

```
dose / delete
```

```
dose "C_bioplan-wellplate." / alg(msdb) bio bioalg(ld) calc write field(*)
dose "C_bioplan-wellplate-z." / bio export(gd) wi(62.9,63.1,42.9,43.1,*,*)
dose "C_bioplan-wellplate-xy." / bio export(gd) wi(*,*,*,112.9,113.1)
dose "C_bioplan-wellplate-x." / bio export(gd) wi(*,*,42.9,43.1,62.9,63.1)
dose "C_bioplan-wellplate-x." / export(gd) wi(*,*,42.9,43.1,62.9,63.1)
```

```
dose /delete
```

```
dose "C_bioplan-wellplate." / alg(msdb) calc write field(*)
dose "C_bioplan-wellplate-z." / export(gd) wi(62.9,63.1,42.9,43.1,*,*)
```

```
quit
```

## B.2 Stack phantom plan

```
time / on
scancap / offh2o(2.890) rifi(3) bolus(0.0) minparticles(15000) path(uw2) xmax(120)
ymax(120) scannerxdistance(6521.9) scannerydistance(7223.5)
hlut "19990211.hlut" / read
```

```
sis * / delete
```

```
sis "/u/osokol/MIT/SIS/SIS-Marburg_12C.sis" / read
```

```
ddd * / delete
```

```
ddd "/d/bio/bio/TRiP98BEAM/1308/DATA/12C/RF3MM/12C*.ddd" / read
```

```
spc * / delete
```

```
spc "/d/bio/bio/TRiP98BEAM/1308/DATA/12C/RF3MM/12C*.spc" / read
```

```
dedx * / delete
```



```

dedx "/u/kraemer/TRiP98DATA/DATA/DEDX/201006xx.dedx" / read

makegeometry stackbox / shape(box(40,80,40)) ctdim(35,60,75) ctsteps(2,2,2)
cteqv(1) centre(35,42,70)
ct "stackbox000" / read
voi "stackbox000" / read

rbe "/u/osokol/RBE/cho2015.rbe" / read
rbe target / alias(cho2015full)
rbe residual / alias(cho2015full)

field 1 / new proj(12C) raster(3,3) zstep(2) fwhm(5) doseext(1.8) con-
tourext(0.7) couch(-180.0) targ(33,42,70)

plan / dose(6.5) targettissue(cho2015full) residuالتissue(cho2015full)
opt / bio field(*) dosealg(msdb) optalg(gr) ctbased iter(500) bioalg(ld) eps(1e-3)

*Output the generated particle numbers for the raster scanner:
field 1 / write file(C_bioplan-stackbox.rst) reverseorder
*field 1 / bev(*) file(C_bioplan-stackbox.bev.gd) alg(msdb)

dose / delete
dose "C_bioplan-stackbox." / alg(msdb) bio bioalg(ld) calc write field(*)
dose "C_bioplan-stackbox-z." / bio export(gd) wi(34.9,35.1,38.9,39.1,*,*)
dose "C_bioplan-stackbox-xy." / bio export(gd) wi(*,*,*,62.9,63.1)
dose "C_bioplan-stackbox-x." / bio export(gd) wi(*,*,38.9,39.1,62.9,63.1)
dose "C_bioplan-stackbox-x." / export(gd) wi(*,*,38.9,39.1,62.9,63.1)

dose / delete
dose "C_bioplan-stackbox." / alg(msdb) calc write field(*)
dose "C_bioplan-stackbox-z." / export(gd) wi(34.9,35.1,38.9,39.1,*,*)

quit

```

### B.3 Out-of-field plan for V-bottom 384-well plate

```

time / on
scancap / offh2o(2.890) rifi(3) bolus(0.0) minparticles(15000) path(uw2) xmax(120)
ymax(120) scannerxdistance(6521.9) scannerydistance(7223.5)
hlut "19990211.hlut" / read

sis * / delete
sis "/u/osokol/MIT/SIS/SIS-Marburg_12C.sis" / read

ddd * / delete
ddd "/d/bio/bio/TRiP98BEAM/1308/DATA/12C/RF3MM/12C*.ddd"/read
spc * / delete
spc "/d/bio/bio/TRiP98BEAM/1308/DATA/12C/RF3MM/12C*.spc"/read
dedx * / delete
dedx "/u/kraemer/TRiP98DATA/DATA/DEDX/201006xx.dedx"/read

makegeometry 384wp / shape(box(55,36,40)) ctdim(64,43,75) ctsteps(2,2,2)
cteqv(1) centre(64,43,70)
ct "384wp000" / read
voi "384wp000" / read

rbe "/u/mfuss/MIT3DBIO/CHO2019Matrigel.rbe" / read
rbe target / alias(cho19mg)
rbe residual / alias(cho19mg)

field 1 / new proj(12C) raster(3,3) zstep(3) fwhm(5) targ(64,43,70) dose-
ext(1.8) alg(msdb) contourent(0.7) couch(-180.0)

plan / dose(6.5) targettissue(cho19mg) residuالتissue(cho19mg)
opt / bio field(*) dosealg(msdb) optalg(gr) ctbased iter(500) bioalg(ld) eps(1e-3)

field 1 / write file(xrs5_bioplan-carbon.rst) reverseorder
field 1 / bev(*) file(xrs5_bioplan-carbon.bev.gd) alg(msdb)

```

dose / delete

dose "xrs5\_bioplan-carbon." / alg(msdb) bio bioalg(ld) calc write field(\*)

dose "xrs5\_bioplan-carbon-z." / bio export(gd) wi(62.9,63.1,42.9,43.1,\*,\*)

dose "xrs5\_bioplan-carbon-xz." / bio export(gd) wi(\*,\*,42.9,43.1,\*,\*)

dose "xrs5\_bioplan-carbon-xy." / bio export(gd) wi(\*,\*,\*,70.9,71.1)

dose "xrs5\_bioplan-carbon-x." / bio export(gd) wi(\*,\*,42.9,43.1,70.9,71.1)

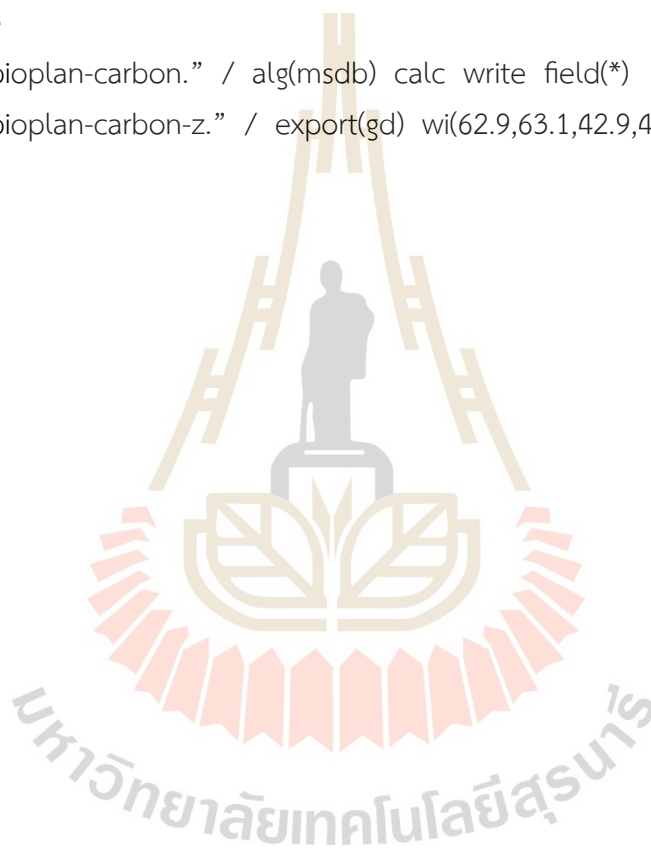
dose "xrs5\_bioplan-carbon-x." / export(gd) wi(\*,\*,42.9,43.1,70.9,71.1)

dose /delete

dose "xrs5\_bioplan-carbon." / alg(msdb) calc write field(\*)

dose "xrs5\_bioplan-carbon-z." / export(gd) wi(62.9,63.1,42.9,43.1,\*,\*)

quit



APPENDIX C  
MICRO-WELL PLATE DESIGN

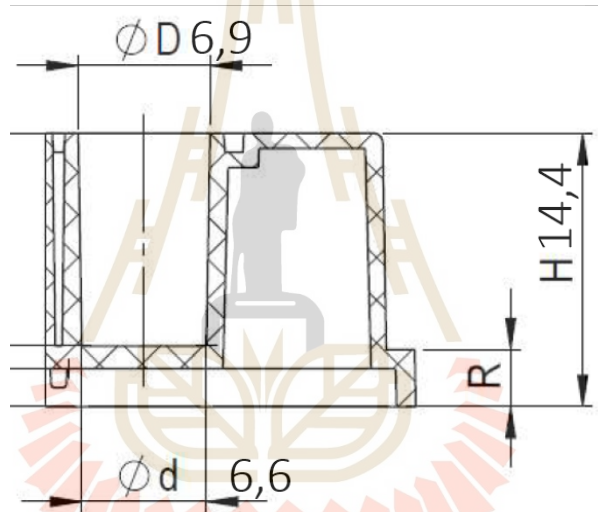
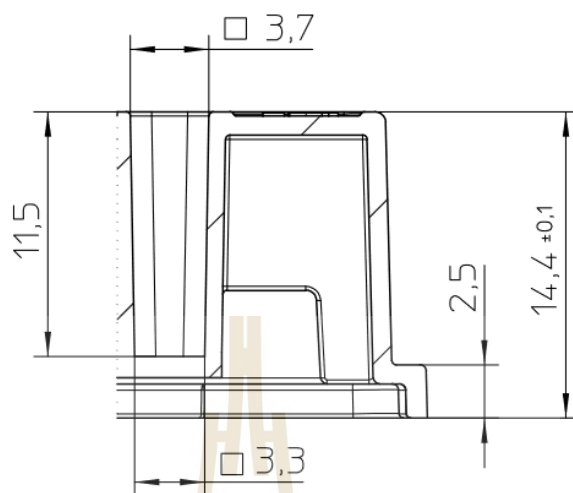
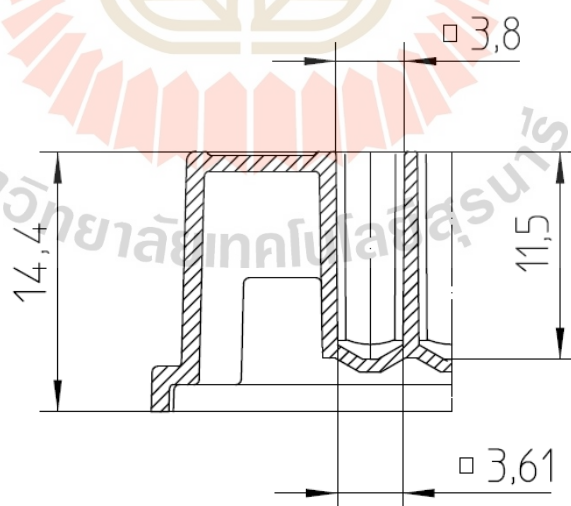


Figure C.1 Design of flat-bottom 96-well PS plate (TPP Techno Plastic Product, 2020). All measurements are in mm.



**Figure C.2** Design of flat-bottom 384-well PS plate (Greiner Bio-One, 2021). All measurements are in mm.

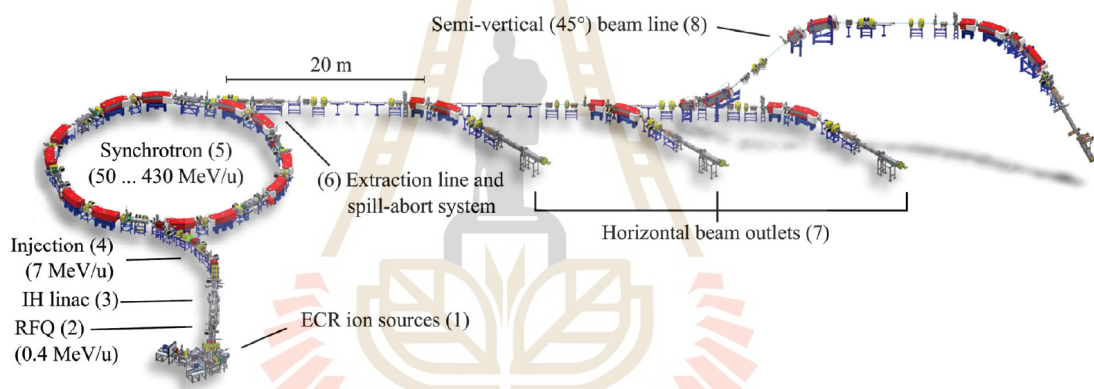


**Figure C.3** Design of V-bottom 384-well PP plate (Greiner Bio-One, 2011). All measurements are in mm.

## APPENDIX D

### MIT TECHNICAL DETAILS

Marburg Ion-Beam Therapy Centre (MIT) is a clinical ion beam facility located in Marburg, Germany. At MIT, protons and carbon ions beams are utilized for cancer treatment using raster scanning technique or active scanning beam. MIT accelerator is consisting of linear accelerator and synchrotron (Siemens Healthcare/Danfysik) to accelerate charged particles to desired energy (Scheeler et al., 2016; Marburger Ionenstrahl-Therapiezentrum, 2021).



**Figure D.1** Outline of accelerator at MIT and the position of beam outlets from (Scheeler et al., 2016).

The beam specifications of MIT accelerator are given as follows (Marburger Ionenstrahl-Therapiezentrum, 2021).

1. Beam energy:

- Protons = 48–221 MeV
- Carbon ions = 86–430 MeV/u

2. Intensity:

- Protons = up to  $1.9 \times 10^9$  ions/second

- Carbon ions =  $1.3 \times 10^6$  to  $6.5 \times 10^7$  ions/second

3. Beam size:

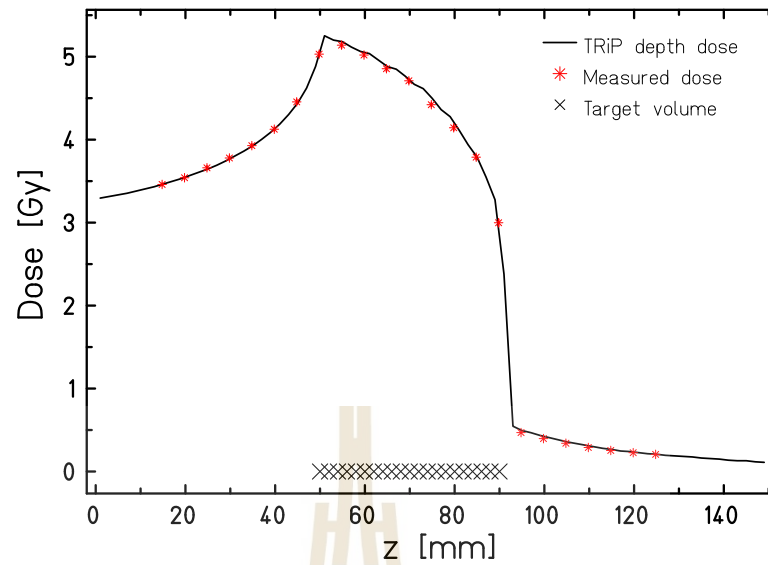
- Protons = 8.1–12.6 mm at lowest energy of 40.08 MeV and 32.5–32.7 mm at highest energy of 221.07 MeV
- Carbon ions = 9.9–13.5 mm at lowest energy of 86.22 MeV/u and 3.4–9.8 mm at highest energy of 430.12 MeV

4. Beam outlet: 3 horizontal beam lines and one semi-vertical ( $45^\circ$ ) beam line.

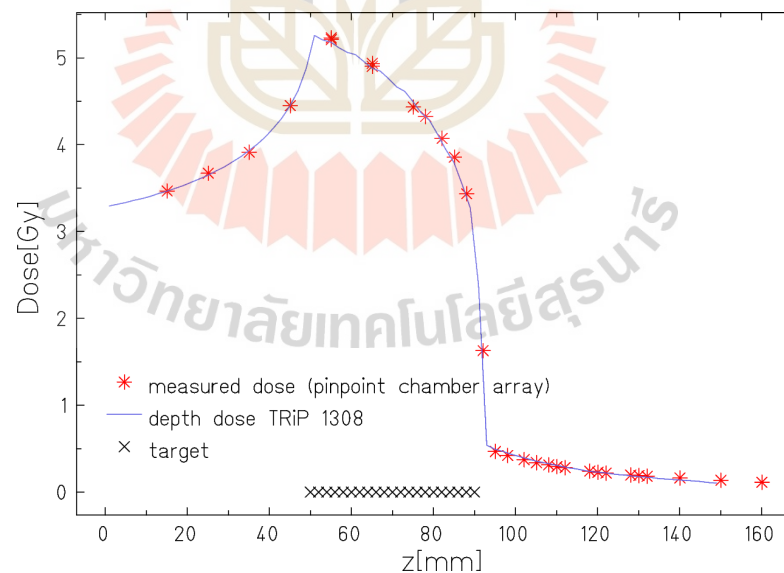
5. Irradiation time: depends on irradiation parameters such as volume of target, energies used, etc. For bio-experiment with target volume of  $18 \times 18 \times 1 \text{ cm}^3$ , it takes  $\approx 2$  minutes to deliver 1 Gy.

Physical dose measurement for irradiation utilizing active scanning carbon ion in the extended target was conducted using a pinpoint chamber (PTW type 31 015) array placed inside a water phantom in order to measure the depth dose distribution in center part. Figure D.2 shows the measured physical dose for RBE-weighted dose treatment plan utilizing CHO Matrigel RBE table for radiobiological verification of simple treatment planning with 3D bio-phantom (Kartini et al., 2020).

Figure D.3 shows the measured absorbed dose in depth distribution for treatment plan verification outside target field utilizing the refined 3D bio-phantom. The measurement of absorbed dose in lateral distribution at different depth was performed as well. Figure D.4 presents the measured absorbed dose in lateral distribution at extended target and fragmentation tail.

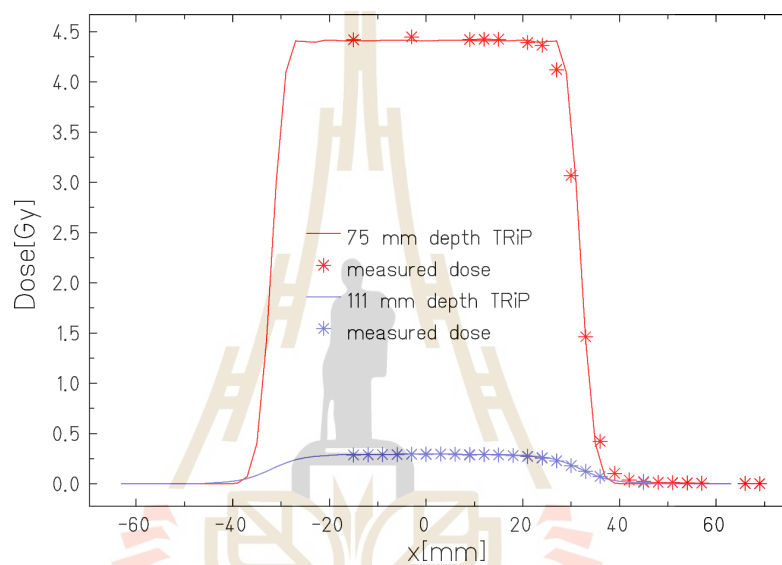


**Figure D.2** Measured absorbed dose in  $z$  distribution in water phantom for treatment plan optimized for uniform RBE-weighted dose in extended target for 3D bio-phantom setup (Kartini et al., 2020). Red data points correspond to the average of four pinpoint chamber measurements at a specific depth.



**Figure D.3** Measured absorbed dose in  $z$  distribution inside water phantom for out-of-field treatment plan optimized for uniform RBE-weighted dose in extended target for refined 3D bio-phantom setup. Red data points correspond to the average of four pinpoint chamber measurements at a specific depth.





**Figure D.4** Measured absorbed dose in lateral x-distribution inside water phantom for out-of-field treatment plan optimized for uniform RBE-weighted dose in extended target for refined 3D bio-phantom setup. Red data points correspond to the measured dose in the extended target at a depth of 75 mm and blue data points correspond to the measured dose in the fragmentation tail at depth of 111 mm.

## CURRICULUM VITAE

**Name** : Ms. Dea Aulia Kartini

**Date of Birth** : April 21, 1993

**Place of Birth** : Bogor, West Java, Indonesia

**Education** :

2011 - 2015 Bachelor of Science, Department of Physics, Faculty of Engineering and Science, Universitas Nasional, Indonesia

2016 -2021 Doctor of Philosophy, School of Physics, Institute of Science, Suranaree University of Technology, Thailand

**Publications** :

1. **Kartini, D. A.**, Sokol, O., Wiedemann, J., Tinganelli, W., Witt, M., Camazzola, G., Krämer, M., Talabnin, C., Kobdaj, C., and Fuss, M. C. (2020). Validation of a pseudo-3D phantom for radiobiological treatment plan verifications. *Physics in Medicine and Biology*, 65(22):225039
2. **Kartini, D. A.**, Malad, Y., Talabnin, C., and Kobdaj, C. (2020). Investigation of Cholangiocarcinoma cells cultured in Matrigel-based phantom. *SUT International Conference on Science and Technology, Nakhon Ratchasima, Thailand, 28 August.*